

**Dissertation zur Erlangung des Doktorgrades  
der Fakultät für Chemie und Pharmazie  
der Ludwig-Maximilians-Universität München**

**Generation of enhanced gene delivery vectors by  
directed evolution of adeno-associated virus**



**Jan Christof Endell  
aus  
Oberhausen**

**März 2006**

## **Erklärung**

Diese Dissertation wurde im Sinne von § 13 Abs. 3 bzw. 4 der Promotionsordnung vom 29. Januar 1998 von Herrn Prof. Dr. Michael Hallek betreut und von Herrn Prof. Dr. Horst Domdey vor der Fakultät für Chemie und Pharmazie vertreten.

## **Ehrenwörtliche Versicherung**

Diese Dissertation wurde selbständig, ohne unerlaubte Hilfe erarbeitet.

München, am 31.03.2006

Jan Endell

Dissertation eingereicht am:

1. Gutachter: Prof. Dr. Horst Domdey
2. Gutachter: Prof. Dr. Michael Hallek

Mündliche Prüfung am: 23.05.2006

## **DANKSAGUNG**

Ich danke...

Prof. Dr. Michael Hallek für die Gelegenheit, in dieser Arbeitsgruppe zu promovieren, die faszinierende Themenstellung, sowie die gewährten Freiräume während der gesamten Promotion.

Prof. Dr. Horst Domdey für die Möglichkeit, eine externe Promotion anzufertigen.

Prof. Dr. Patrick Cramer für die hervorragende Arbeitsatmosphäre im Genzentrum und den zur Verfügung gestellten Arbeitsplatz bis zum Abschluss der Promotion.

Dr. Hildegard Büning für die gute Labor-Organisation trotz des Umzuges, die vielen Grants, die mir die Sequenzierung von unglaublichen 5000 Klonen möglich gemacht haben, sowie Rat und Hilfe.

Dr. Luca Perabo für die engagierte Betreuung und Hilfe zu jeder Zeit, die vielen Ideen und besonders für das unermüdliche Korrekturlesen in der Schlussphase meiner Arbeit. Ein besonderer Dank auch für die allseits bekannten Haus-Mails, sowie für seinen maßgeblichen Beitrag zu einer Vielzahl von legendären Genzentrumsveranstaltungen, meist in Zusammenarbeit mit Dr. Karim Armache.

allen Mitgliedern des Arbeitskreises, besonders Kerstin Lux und Daniela Goldnau, für die freundschaftliche Atmosphäre, sowie die ständige Hilfsbereitschaft.

Dr. Heidi Feldmann für die viele und unersätzbliche Hilfe zu Beginn meiner Promotion.

Siegi Kastenmüller für die immer gut gelaunte Hilfe bei der Bewältigung ungezählter bürokratischer „last minute“-Angelegenheiten.

Melanie für die Geduld, die Ermutigung und alles andere und Matthias für seine Freundschaft.

meinen Eltern, die immer für mich da waren und mir soviel ermöglicht haben, und meiner Schwester.

Die vorliegende Arbeit wurde in der Zeit von Januar 2003 bis März 2006 am Institut für Biochemie der Ludwig-Maximilians-Universität München unter der Anleitung von Prof. Dr. Michael Hallek angefertigt.

Im Verlauf dieser Arbeit wurden folgende Veröffentlichungen angefertigt:

**Endell J** and Perabo L, King S, Lux K, Goldnau D, Hallek M, and Büning H (2006). Combinatorial engineering of a gene therapy vector: directed evolution of adeno-associated virus. *J Gene Med* 8: 155-162.

**Endell J** and Perabo L and Goldnau D and White K, Humme S, Work L, Janiki H, Hallek M, Baker A, and Büning H. HSPG binding properties of adeno-associated virus (AAV) retargeting mutants and consequences for their *in vivo* tropism. *J. Virol.* (in press).

Lux K, Goerlitz N, Schlemminger S, Perabo L, Goldnau D, **Endell J**, Leike K, Kofler D, Finke S, Hallek M, and Büning H (2005). Green Fluorescence Protein-Tagged Adeno-Associated Virus Particles Allow the Study of Cytosolic and Nuclear Trafficking. *J. Virol.* 79(18): 11776-11787.

*meinen Eltern und Mellie*

## Contents

|                  |   |            |
|------------------|---|------------|
| Chapter I        | Introduction .....  | <b>1</b>   |
| 1.1              | <i>Viral Gene Therapy: Chances and Risks</i> .....  | 2          |
| 1.2              | <i>Adeno-Associated Viruses</i> .....   | 3          |
| 1.3              | <i>Genome Organisation of AAV Type 2</i> .....  | 4          |
| 1.4              | <i>Infection Biology of AAV-2</i> .....   | 6          |
| 1.5              | <i>Structural and Functional Properties of AAV-2 and other Serotypes</i> .....  | 8          |
| 1.6              | <i>Production of Recombinant AAV Vectors</i> .....  | 11         |
| 1.7              | <i>AAV as a Vector for Gene Therapy</i> .....   | 12         |
| 1.8              | <i>Retargeting of AAV Vectors</i> .....   | 13         |
| 1.9              | <i>Humoral Immune Response against AAV</i> .....  | 15         |
| Chapter II       | Specific Goals of this Work (Summary).....  | <b>18</b>  |
| Chapter III      | Combinatorial Engineering of a Gene Therapy Vector:<br>Directed Evolution of Adeno-Associated Virus .....                               | <b>20</b>  |
| Chapter IV       | Improving Viral Phenotypes by DNA Shuffling and<br><i>Evolution Monitoring</i> .....  | <b>35</b>  |
| Chapter V        | HSPG Binding Properties of Adeno-Associated Virus<br>(AAV) Retargeting Mutants and their Consequence for <i>in vivo</i><br>Tropism..... | <b>62</b>  |
| Chapter VI       | Green Fluorescence Protein-Tagged Adeno-Associated<br>Virus Particles Allow the Study of Cytosolic and Nuclear<br>Trafficking.....      | <b>70</b>  |
| Chapter VII      | Conclusion and Outlook.....   | <b>94</b>  |
| Bibliography     | .....   | <b>98</b>  |
| Abbreviations    | .....   | <b>118</b> |
| Curriculum Vitae | .....   | <b>120</b> |

# **Chapter I**

## **Introduction**

## Viral Gene Therapy: Chances and Risks

Since the discovery of DNA as universal blueprint for living organisms, the idea of curing genetic diseases at their origin has evolved. In the past two decades considerable advances in molecular biology and medicine have given rise to a wide variety of gene therapy-based pre-clinical and clinical trials targeting both inherited and acquired diseases (Fig. 1A). In this context, several classes of viral and non-viral vectors are being used as transfer shuttles to deliver therapeutical genetic information into cells (Fig 1B). Since the first successful clinical trial in 1990 (Cluver *et al.*, 1991), 1145 clinical trials in the field of gene therapy have been approved world wide (Fig. 1C) and the number of approved trials has doubled since 2001. More than 70 % of these experiments employ viral vectors.

Viral vectors have the potential for high transduction efficiency and stable long-term expression of the therapeutic gene. Nevertheless, the complex viral biology is largely unknown, hampering the success of this approach.

In 1999, Jesse Gelsinger, an 18 years old patient, which suffered from a non-fatal Ornithine Transcarbamylase (OTC) deficiency, died after treatment with an adenoviral vector containing a functional copy of the OTC gene. The following investigation revealed a fatal multiple organ failure caused by a severe immune reaction to the administered vector. Accordingly, the host immune response to vector and transgene has become a major concern in gene therapy (Somia and Verma, 2000). In a similar way, the initially very successful clinical trial for fatal X-linked Severe Combined Immunodeficiency (SCID) showed both, blessing and risks of gene therapy. Administration of a retroviral vector containing the  $\gamma$ -chain for the cytokine receptors IL-2R, 4R, 7R, 9R and 15R resulted in a sustained restoration of the immune system in 15 patients (Cavazzana-Calvo *et al.*, 2005), which life expectancy was inferior to one year before treatment. However, 3 of the patients later developed T-cell leukaemia due to unspecific insertion of viral DNA in the chromosomes, which led to the death of one child until now. Almost five years after the treatment in 2001 the remaining 14 children are able to lead a life unaffected by SCID, although two are still fighting leukaemia. These examples demonstrate on one hand the enormous potential of gene therapy, while on the other hand remind the scientific community of associated risks and remark the need to develop a new generation of efficient and safe vectors.

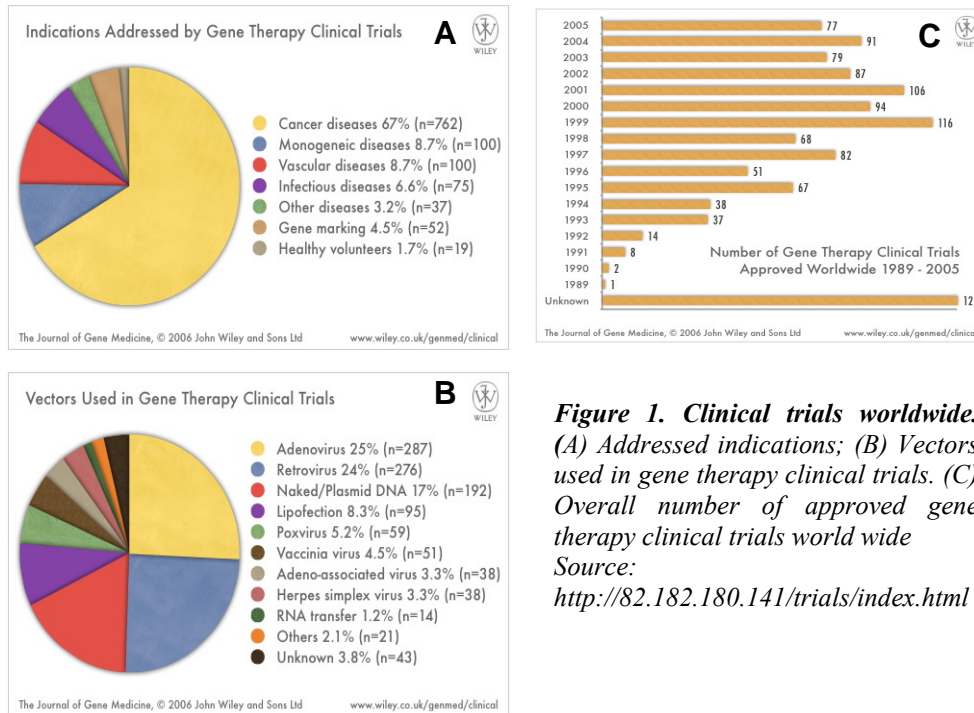


**Figure 1. Clinical trials worldwide.** (A) Addressed indications; (B) Vectors used in gene therapy clinical trials. (C) Overall number of approved gene therapy clinical trials world wide  
Source:  
<http://82.182.180.141/trials/index.html>

## Adeno-Associated Viruses

Initially, adeno-associated virus (AAV) was discovered as contaminant of adeno viral preparations, hence its name (Atchison *et al.*, 1965; Hoggan *et al.*, 1966). Due to its very small diameter of approx. 25 nm, it is classed to the family of *parvoviridae* (lat. *parvo*: small). This family groups viruses with a linear, single-stranded DNA genome of roughly 5 kb with a non-enveloped capsid of 18-30 nm in diameter (Siegel *et al.*, 1985). Parvoviridae are divided in two subfamilies: *Parvovirinae*, which infect vertebrates and *Densovirinae*, which infect insects. *Parvovirinae* consist of the genera of Parvoviruses, Erythroviruses and Dependoviruses, and AAV belongs to the latter. Except for the human Erythrovirus B19, which causes *erythema infectiosum*, *hydrops fetalis* and abortion (Brown, 2000), all other *parvovirinae* are non-pathogenic for humans (Vafaie and Schwartz, 2004; Berns and Linden, 1995). In addition, AAV has shown to convey cytotoxic influence on malignant cells (Raj *et al.*, 2001), as well as protective effects against bovine papillomavirus and against cellular transformation by adenovirus (Mayor *et al.*, 1973; de la Maza and Carter, 1981; Hermonat, 1989).

In contrast to other members of the parvovirus family (e.g. canine parvovirus and porcine parvovirus), AAV is not capable of autonomous replication, but instead requires exogenous factors for its replication. These factors can be provided by co-infection with unrelated helper

viruses, such as adenoviruses (Ad), herpesviruses (e.g. herpes simplex virus, Epstein-barr virus, varicella-zoster virus), human cytomegalovirus (HCMV), papillomavirus or general cellular stress factors, like UV- or  $\gamma$ -radiation, heat shock or carcinogenic compounds (Berns, 1990; McPherson *et al.*, 1985, Sanlioglu *et al.*, 1999; Schlehofer *et al.*, 1986; Thompson *et al.*, 1994; Walz *et al.*, 1997; Yakinoglu *et al.*, 1988; Yakobson *et al.*, 1987; Thompson *et al.*, 1991). In the absence of helper factors during infection, a latent infection is initialized by stable integration of viral DNA into the genome of the host cell (Berns and Linden, 1995). Following limited expression of viral regulatory proteins (Rep proteins) a site-specific insertion into the q-arm of chromosome 19 at the AAVS1 locus takes place (Kotin *et al.*, 1990; Kotin *et al.*, 1991; Samulski *et al.*, 1991; Weitzman *et al.*, 1994; Linden *et al.*, 1996a; Linden *et al.*, 1996b; Ponnazhagan *et al.*, 1997a;). When stress response genes are activated due to presence of helper factors, the lytic cycle is initiated and integrated AAV genomes are excised, leading to a productive infection (Berns *et al.*, 1975; Cheung *et al.*, 1980; McLaughlin *et al.*, 1988).

Since initial discovery of AAV, 11 serotypes sharing different levels of DNA sequence homology between 55 and 84 % have been found (Gao *et al.*, 2002; Gao *et al.*, 2004; Mori *et al.*, 2004). Differences in capsid composition between these serotypes result in different tropisms *in vitro* and *in vivo* (Lukashov and Goudsmit, 2001; Grimm and Kay, 2003). The first human adeno-associated virus discovered in 1966 has taken the name of adeno-associated virus of type 2 (AAV-2) and remains the best characterized serotype. However, other serotypes are receiving increasing attention due to peculiar advantages for certain gene therapy applications. Accordingly, a wide variety of therapeutically important tissues can be targeted using different AAV serotypes, including CNS, lung, liver, muscle and retina (Acland *et al.*, 2001; Huges *et al.*, 2002; Chao *et al.*, 2000; Halbert *et al.*, 2001; Xiao *et al.*, 1999).

## Genome organisation of AAV Type 2

The genome of AAV-2 consists of single-stranded DNA with a length of 4679 nucleotides and can be divided in three functional regions (Fig. 2). Two open reading frames (ORF), *rep* and *cap*, are flanked by *inverted terminal repeats* (ITR) (Carter and Samulski, 2000). The ITRs consist of 145 nucleotides and form two T-shaped structures on either side of the genome. Within these regions, a *Rep binding site* (RBS) and a specific cleavage site for bound

Rep protein (*terminal resolution site*, TRS) are located (Im and Muzyczka, 1990; McCarty *et al.*, 1994; Snyder *et al.*, 1990; Snyder *et al.*, 1993). These double stranded regions allow them to serve as *origin of replications (ori)* by priming DNA synthesis. In addition, they play a key role in the regulation of gene expression, site-specific integration of the genome during the latent phase, as well as in the subsequent rescue of viral DNA from the integrated state (Labow and Berns, 1988; McLaughlin *et al.*, 1988; Samulski *et al.*, 1987).

The 5'-located *rep* open reading frame encodes four multifunctional, non-structural proteins with regulatory roles. These genes are transcribed via two promoters, p5 and p19. p5 regulates the production of a 4.2 kb mRNA (that will give origin to a protein called Rep78) and its splicing variant, a 3.9 kb mRNA (protein Rep68). Promoter p19 regulates the production of a 3.6 kb mRNA and its splicing variant (3.3 kb) that will generate the proteins Rep52 and Rep40 respectively (Lusby and Berns, 1982; Marcus *et al.*, 1981). Biochemical activities of Rep79 and Rep68 include DNA binding, DNA ligase, ATPase, DNA helicase, as well as strand- and site-specific endonuclease activity. They are involved in AAV DNA replication, transcriptional control and integration. Rep 52 and 40 possess ATPase and helicase activities and play a role in accumulation and encapsidation of AAV genomes into preformed capsids (Chejanovsky and Carter, 1989; Dubielzig *et al.*, 1999; King *et al.*, 2001; Smith and Kotin, 1998). Finally, Rep proteins can act as repressors of AAV transcription in absence of helper virus by repressing p5 and p19 transcription (Kyostio *et al.*, 1994).

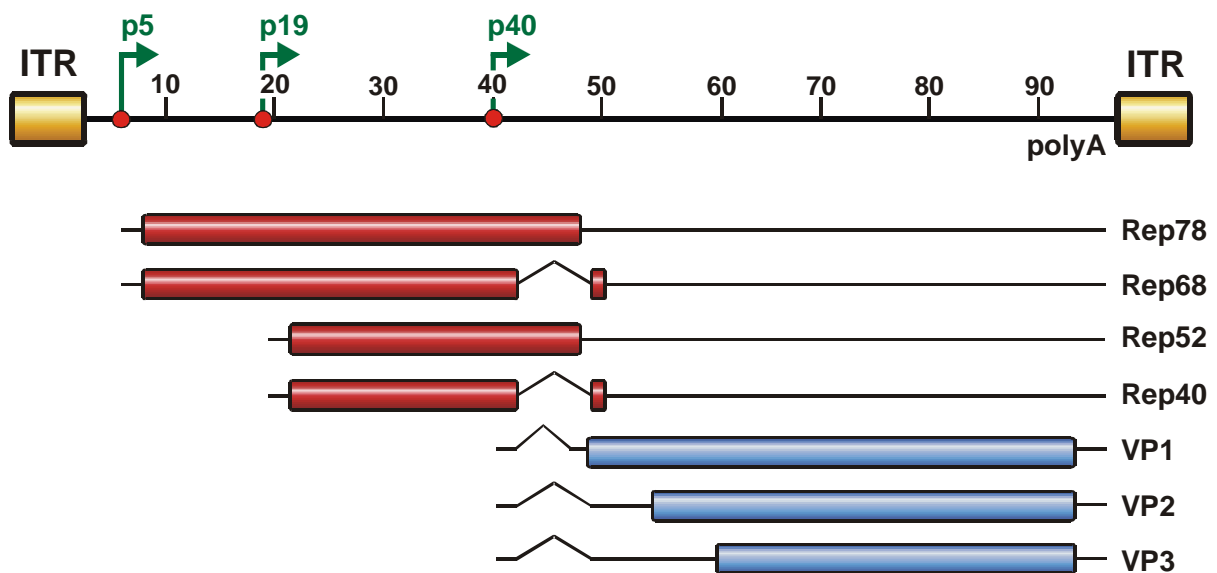


**Figure 2. Organisation of the AAV genome and gene products.** The AAV genome contains 4680 nucleotides, divided into 100 map units (46.8 nucleotides per unit). Shown are the inverted terminal repeats (ITRs), the three viral promoters positioned at units 5, 19 and 40 (p5, p19, p40) and the polyadenylation signal at unit position 96 (poly A). Open reading frames are shown as cylinders, untranslated regions as solid lines and introns as kinks. Promoters p5 and p19 regulate the four Rep proteins which exist as spliced and unspliced isoforms. The p40 promoter controls the three different capsid subunits VP1, VP2 and VP3 on the cap gene.

The 3'-ORF *cap* codes for the three structural proteins VP1, VP2 and VP3, which are transcribed from the p40 promoter and expressed at a 1:1:8 ratio (Kronenberg *et al.*, 2001). Since all three capsid proteins use a common stop codon, VP2 and VP3 are N-terminally shortened variants of VP1. The different translation efficiencies are a consequence of the alternative splicing of the VP1-coding intron and the existence of an unusual initiation codon (ACG) for VP2 translation. Accordingly, the VP3 initiation codon AUG results in a 10-fold higher translation frequency (Laughlin *et al.*, 1979; Becerra *et al.*, 1985; Becerra *et al.*, 1988).

## Infection Biology of AAV-2

Despite continuous progress, details about the infectious process of AAV-2 remain largely unknown. For successful infection, AAV has to attach to the cell surface via receptor binding followed by internalisation of the virion, intracellular trafficking and transport to the nucleus, where the genome is replicated and packaged in newly synthesised capsids (Fig. 3). Binding of AAV to the widely expressed proteoglycane HSPG functioning as primary receptor has been proposed, thus explaining the broad tropism of the virus (Summerford and Samulski, 1998). Internalisation of bound AAV seems then to be mediated by three co-receptors,  $\alpha_v\beta_5$  integrin, human fibroblast growth factor receptor 1 (hFGFR1) and hepatocyte growth factor receptor (HGFR) (Qing *et al.*, 1999; Summerford *et al.*, 1999; Kashiwakura, 2005). While the cell attachment is supposedly enhanced by FGFR-binding,  $\alpha_v\beta_5$  integrin seems to be involved in the predominant but not exclusive receptor mediated endocytosis via clathrin coated pits. In rare cases, AAV-5 was found to be endocytosed in noncoated vesicles, presumably caveolae (Bantel-Schaal *et al.*, 2002). Clustering of  $\alpha_v\beta_5$  has been proposed facilitate localization of viral particles to clathrin coated pits. The function of HGFR remains unknown, yet. The virions are then internalized in a dynamin dependent manner involving a cytosolic GTPase (Bartlett *et al.*, 2000, Wang *et al.*, 1998; Duan *et al.*, 1999) by formation of a dynamin ring responsible for the pinching of coated pits from the cell membrane (Sever *et al.*, 2000; Hinshaw and Schmid, 1995; Hinshaw, 2000). In addition, like many integrins  $\alpha_v\beta_5$  is involved in signal transduction. By attachment to AAV the small GTP binding protein Rac1 is activated leading to a stimulation of phosphoinositol-3 kinase (PI3K) and the subsequent rearrangement of microfilaments and microtubule which is necessary for efficient trafficking to the nucleus (Sangioglu *et al.*, 2000).

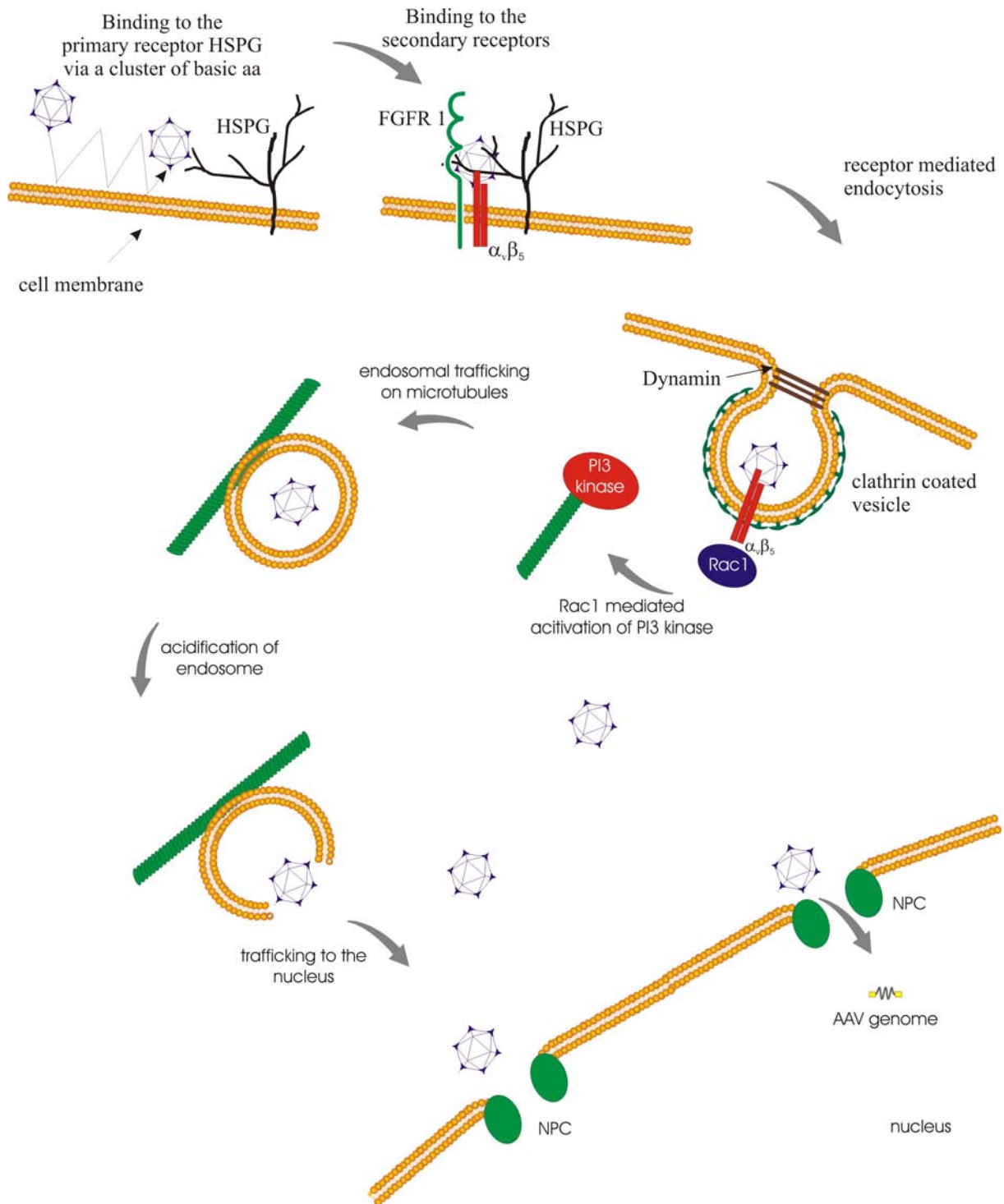


**Figure 3. Model of AAV-2 infection on the cervix carcinoma cell line HeLa (adapted from Büning et al., 2003).** Following repetitive touches, AAV binding to its negatively charged primary receptor heparin sulphate proteoglycane (HSPG) on the cell membrane is mediated by a cluster of five basic amino acids (aas). The attachment is enhanced via fibroblast growth factor receptor 1 (FGFR1) binding. Subsequent binding to  $\alpha_v\beta_5$  integrins leads to endocytosis by clathrin coated pits. Integrin binding is assumed to activate the small GTP binding protein Rac1, which stimulates the phosphatidylinositol-3-kinase (PIK3) pathway. The resulting rearrangement of the cytoskeleton allows a trafficking of AAV containing endosomes. Acidification of the endosomal milieu may lead to the release of AAV-2, possibly mediated by conformational changes of the AAV capsid. After transport of the AAV genome into the nucleus, probably via nuclear pore complex (NPC), the genome is replicated or integrated into the host cell. Whether AAV-2 virions or only the genome are translocated into the nucleus is unclear.

The exit of AAV-2 from endosomal compartments is controversial. Current hypotheses propose release from early endosome or late endosome, or even an accumulation in the golgi compartment (Xiao *et al.*, 2002; Douar *et al.*, 2001; Hansen *et al.*, 2001; Bantel-Schaal *et al.*, 2002; Pajusola *et al.*, 2002). However, acidification of the endosomal milieu is crucial for priming AAV for nuclear entry. Low pH could trigger conformational changes of the viral capsid and lead to exposure of previously hidden domains which mediate the escape. Similar conformational changes following acidification of the endosome have been observed with other viruses and recent studies of AAV have reported the exposure of the hidden N-terminus of VP1 after heat shock (Root *et al.*, 2000; Zadori *et al.*, 2001; Kronenberg *et al.*, 2005). Interestingly, this N-terminal region contains a phospholipase A<sub>2</sub> (PLA<sub>2</sub>) motif, which is conserved among parvoviruses (Girod *et al.*, 2002; Zadori *et al.*, 2001). Accordingly, the PLA<sub>2</sub> domain might play a role in the endosomal escape, although no experimental data support this hypothesis, yet.

Little is also known about the mechanism of nuclear import and viral uncoating. Due to their small diameter, intact capsids could enter the nucleus through nuclear pore complexes (NPC) but controversial data have been presented. While an interaction of the AAV capsid with the nuclear shuttle protein nucleolin has been reported (Qiu *et al.*, 1999), Hansen *et al.* (2001) suggested an NPC independent pathway. VP2 contains a nuclear localisation sequence essential for viral assembly (Hoque *et al.*, 1999), but further functions are unknown. Regarding uncoating, evidence of viral capsids in the nucleus (Bartlett *et al.*, 2000; Sanlioglu *et al.*, 2000) is in marked contrast with other reports (Lux *et al.*, 2005).

## **Structural and Functional Properties of AAV-2 and other Serotypes**

During the past decade, several atomic structures of autonomous parvoviruses, including human parvovirus B19, feline panleukopenia virus (FPV), canine parvovirus (CPV), Aleutian mink disease virus (ADV) and minute virus of mice (MVM) have been solved (Agbandje *et al.*, 1994; Agbandje-McKenna *et al.*, 1998; Chang *et al.*, 1992; Chapman and Rossmann, 1993; Chipman *et al.*, 1996; McKenna *et al.*, 1999; Strassheim *et al.*, 1994; Tsao *et al.*, 1991). However, it took until 2002, about 40 years after its discovery, to solve the first crystal structure of an AAV serotype. Xie *et al.* determined the structure of AAV-2 to a resolution of 3 Å by X-ray crystallography (Xie *et al.*, 2002) (Fig. 4A). Since then, lower resolution structures of other serotypes, such as AAV-4 and AAV-5 have been mapped by a combination of cryo-electron microscopy (cryo-EM) and pseudo-atomic model building

(Walters *et al.*, 2004; Padron *et al.*, 2005). Described structures contain only a 13 aa N-terminally shortened VP3, while VP1, VP2 and the N-terminus of VP3 could not be determined because of the low electron density of these regions. However, cryo-electron microscopy provides some evidence, that globular structures at the inner surface of the capsid at the twofold symmetry axis can be attributed to these N-terminal extensions (Kronenberg *et al.*, 2001).

The increasing number of available atomic models of different serotypes reveals a variety of similarities and differences in comparison to AAV-2. In all cases, the viral capsid exhibits a T=1 icosahedral symmetry and is composed of 60 copies of the three related structural proteins, VP1-3, at a ratio of 1:1:8 (Xie *et al.*, 2002; Kronenberg *et al.*, 2001). The core of each subunit contains an eight-stranded anti-parallel  $\beta$ -barrel motif, which is highly conserved among parvoviruses (Agbandje *et al.*, 1994; Chapman and Rossmann, 1993) (Fig. 4B). The majority of the variable surface structure consists of large loops inserted between the strands of the  $\beta$ -barrel. These loops comprising approx. two-thirds of the capsid structure constitute the capsid features, which mediate interaction with antibodies and cellular receptors. These structural features on the surface of the virus include a depression at the twofold axis (dimple) and a hollow cylinder formed by symmetry-related  $\beta$ -ribbons surrounded by a circular depression (canyon) at the fivefold axis. The most prominent features are three mound-like protrusions surrounding the threefold axis, which derive from the interaction of two neighbouring subunits. These peaks are formed by the longest loop insertion, a loop of 220 amino acids connecting  $\beta$ -sheets G and H (GH loop). Similar interactions of adjacent subunits are observed at the fivefold cylinder which is composed by interacting residues of the HI, BC and EF loops. The highest variability between parvoviruses is observed in the loops that form the surface of the viral capsid. The resulting variations convey host-specific interactions, such as tissue tropism, pathogenicity, receptor attachment and antigenicity (Agbandje *et al.*, 1994; Hueffer *et al.*, 2003a; Hueffer *et al.*, 2003b). In this context, superimposition of the crystal structure of AAV-2 and the pseudoatomic models of AAV-4 and AAV-5 show the localisation of a majority of the most variable regions on or close to the threefold protrusions (Padron *et al.*, 2005). The canyons between the protrusions in AAV-2 correspond to basic patches (Fig. 5C,D), which have been proposed as binding site for the negatively charged primary receptor heparan sulphate proteoglycan (HSPG) (Opie *et al.*, 2003; Wu *et al.*, 2000). In particular, basic clusters containing amino acids R484, R487, K 532, R585 and R588 (VP1 numbering) seem to play an important role for this interaction (Opie *et al.*, 2003; Grifman *et al.*, 2001; Wu *et al.*, 2000; Xie *et al.*, 2002).

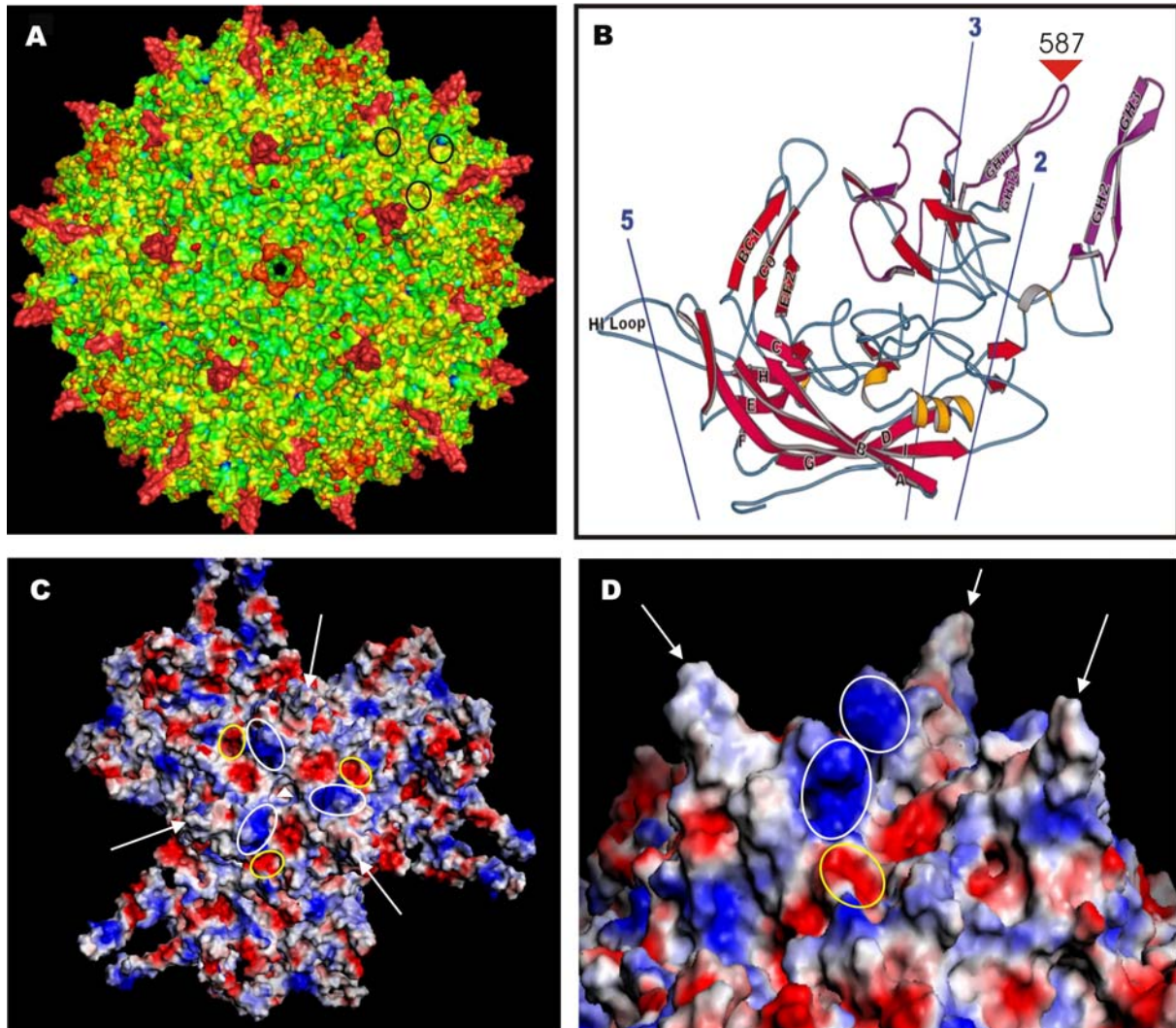


**Figure 4. Structural properties of the AAV capsid.** (A) Surface topology of AAV-2. For contrast the protruding spikes at the 3-fold axis are coloured red. The view is down the 5-fold axis. The 587 position located the shoulder of each 3-fold peak is marked by circles. (B) Ribbon drawing of a VP3 protein. The positions of the 2-, 3- and 5-fold axis are indicated, as well as the 587 position. The  $\beta$ -barrel core at the inner surface of the capsid is composed of two anti-parallel  $\beta$ -sheets (strands A to I) (Xie *et al.*, 2002). (C) Top view on a 3-fold axis composed of three subunits. The surface is coloured according to electrostatic potential. (blue = positive, red = negative). White arrows indicate the peaks around the 3-fold axis (white triangle). The positively charged HSPG binding region is marked by white ellipses, the suggested secondary receptor binding region (negatively charged) by yellow ellipses. (D) Corresponding side view on the 3-fold peak region.

Interestingly, the distance between neighbouring clusters was measured to 20 Å, which is compatible with the binding of adjacent disaccharids (Margalit *et al.*, 1993), whereas different threefold axes are separated by approx. 70 Å, which matches the spacing of highly sulfonated regions of HSPG (Fry *et al.*, 1999). Alignments of AAV-2, AAV-4 and AAV-5 showed the lack of the positive cluster for AAV-4 and -5. Accordingly, heparin inhibition assays revealed HSPG-independent infection pathways for these serotypes, for which sialic acids have been proposed as primary receptors, even if no binding regions could be determined until now (Walters *et al.*, 2001; Walters *et al.*, 2002; Kaludov *et al.*, 2001). Mapping of binding sites of

AAV-2-neutralizing monoclonal antibodies (e.g. A20 or C37b) also showed the importance of the threefold axis as antigenic region (Wobus *et al.*, 2000). While the epitope recognized by C37b is situated on the shoulder of the peak facing the threefold axis, A20 was mapped to the valley between threefold peaks. Negative charged clusters are mainly observed at the sides of the twofold dimple and on top of the fivefold cylinder, but no special functions could be attributed as of today. However, a negatively charged and highly conserved cluster adjacent to the heparin binding site has been proposed as binding region for secondary receptors (Lochrie *et al.*, 2006) (Fig. 4C, D).

## Production of Recombinant AAV Vectors

For the generation of recombinant AAV vectors (rAAV), *rep* and *cap* genes can be replaced by a gene of interest of up to 4.5 kb (Fig. 5) (Tal, 2000). The flanking ITR sequences will serve as packaging signals. *Rep* and *cap*, which are needed for AAV replication and capsid formation, can be provided *in trans* on an exogenous plasmid devoid of ITRs (Lauglin *et al.*, 1983; Samulski *et al.*, 1982). The two plasmids carrying transgene and *rep/cap* are co-transfected into 293 cells with a third plasmid encoding adenoviral helper genes necessary to provide the helper function required for AAV genome replication (Collaco *et al.*, 1999). In contrast to co-infection with adeno virus, no contamination with adeno particles takes place in this case. 48 h post transfection, viral progeny can be harvested from the lysate of transfected cells and purified to high titers of up to  $10^{14}$  particles/ml by one of several described protocols (Anderson *et al.*, 2000; Collaco *et al.*, 1999; Allen *et al.*, 2000; Gao *et al.*, 2000; Grimm and Kleinschmidt, 1999; Monahan and Samulski, 2000a; Monahan and Samulski, 2000b; Tamayose *et al.*, 1996; Zolotukhin *et al.*, 1999; Rolling and Samulski, 1995; Vincent *et al.*, 1997; Xiao *et al.*, 1998; Inoue and Russell, 1998; Auricchio *et al.*, 2001).

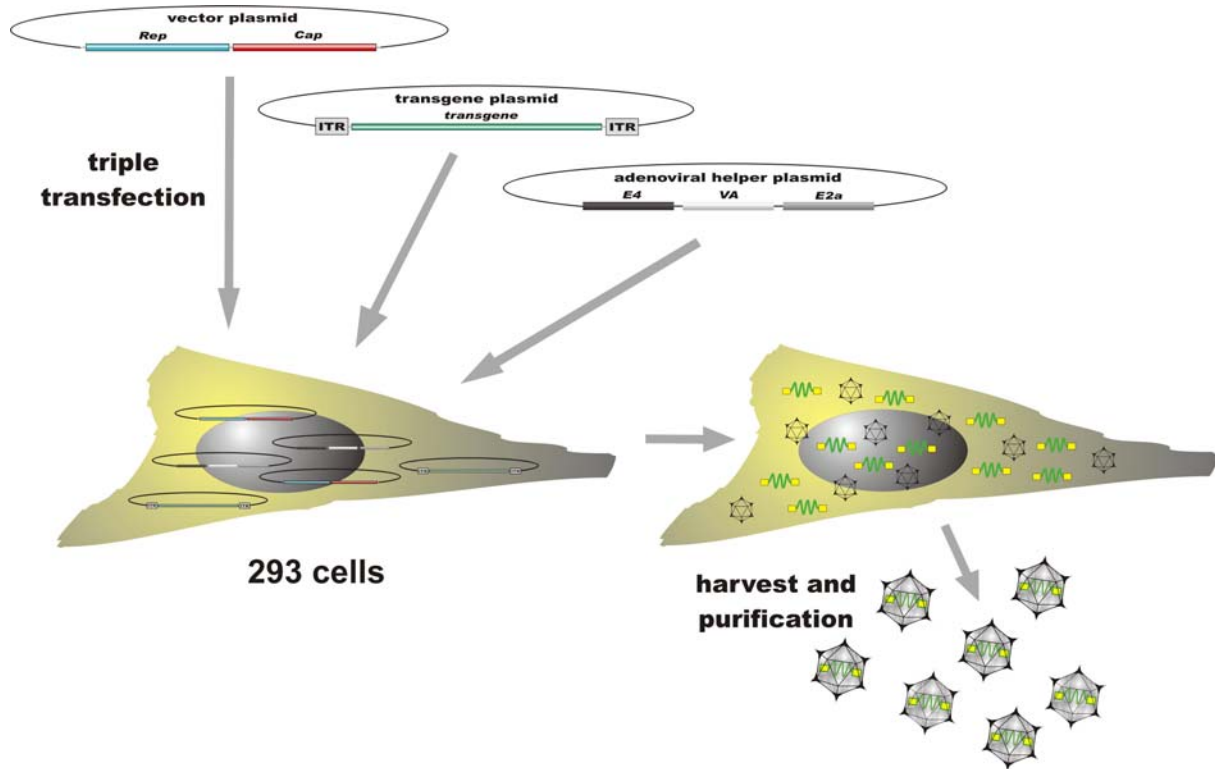


**Figure 5. Packaging of rAAV.** Three plasmid constructs are required for packaging of rAAV. The vector plasmid containing all viral genes without ITRs is needed to provide Rep and Cap proteins. The transgene is flanked by ITRs to allow transgene packaging in empty particles. The adenoviral helper plasmid provides helper functions required for AAV replication. In a triple transfection the plasmids are introduced into 293 cells. 48 hrs post transfection the viral progeny is harvested by lysis and purified by subsequent ultra centrifugation.

## AAV as a Vector for Gene Therapy

During the last 20 years, gene transfer vectors based on AAV-2 have been developed, evaluated in pre-clinical studies and are currently being tested in clinical trials (Kay *et al.*, 2000; Wendtner *et al.*, 2002; Griesenbach *et al.*, 2002; Crystal *et al.*, 2004; Mandel and Burger, 2004; Flotte, 2005). So far, these studies have provided evidence that AAV-2 vectors feature a variety of attractive properties for therapeutic gene delivery to humans. In this context, an important factor is the apparent lack of pathogenicity of AAV vectors (Berns and Linden, 1995; Blacklow, 1988; Blacklow *et al.*, 1968; Blacklow *et al.*, 1971). Moreover, due to lack of activation of cytotoxic T-lymphocytes (CTL), no inflammatory immune response has been observed after vector injection. This has been attributed to the inability of AAV to efficiently infect dendritic cells, as well as the absence of viral genes in rAAV vectors. In general, only a humoral immune response is initiated. Questions that still need to be addressed are the potential of rAAV ITRs to activate cellular genes after unspecific integration of the viral DNA in the host genome (Kotin, 1994; Blacklow *et al.*, 1971) and the discussed ability

of AAV to transduce germinal cell lines (Rohde *et al.*, 1999; Burguete *et al.*, 1999). However, site-specific integration of AAV taking place in the presence of Rep proteins is advantageous for long term expression and does not seem to influence host cell biology (Monahan and Samulski, 2000a; Monahan and Samulski, 2000b; Samulski *et al.*, 1991; Hallek and Wendtner, 1996). Although the *rep* gene is absent in rAAV, it can be provided *in trans* (Kotin *et al.*, 1990; Young *et al.*, 2000a; Young *et al.*, 2000b; Young and Samulski, 2001; Owens, 2002; Philpott *et al.*, 2002; Huttner *et al.*, 2003). Even without stable integration, AAV persistence in episomal form has been shown to convey long term gene expression of more than one year (Fisher *et al.*, 1997). Due to the limited packaging capacity of approx. 4.9 kb (Dong *et al.*, 1996) several therapeutically interesting transgenes or large promoters cannot be inserted in rAAV vectors. For that matter, so called “splicing vectors” have been developed that contain only parts of the transgene, which can be reassembled as head-to-tail concatamers by employing appropriate splicing signals present in both vectors (Nakai *et al.*, 2000; Sun *et al.*, 2000; Yan *et al.*, 2000).

## Retargeting of AAV Vectors

AAV has the ability to infect both dividing and non-dividing cells including tissues such as central nervous system (CNS), retina, muscle, liver, lung and hematopoietic system (Fisher-Adams *et al.*, 1996; Flannery *et al.*, 1997; Flotte *et al.*, 1993; Fisher *et al.*, 1997; Kaplitt *et al.*, 1994; Snyder *et al.*, 1997). This broad host range allows theoretical application of AAV vectors for a variety of diseases but is a drawback in terms of safety because tissues or organs different from the target could be transduced. To generate tissue specific vectors, viral particles have to be engineered and provided with selective receptor binding domain, which enables a stringent interaction with a receptor specific for the targeted cell type (vector re-targeting).

In the past, several attempts have been made to develop universal retargeting strategies for AAV by binding of antibodies to the capsid (Bartlett *et al.*, 1999; Ried *et al.*, 2002) (Fig. 6). However, the low transduction efficiency and the unstable capsid-antibody complex were insufficient for gene therapy purposes. In addition, antibody binding might interfere with post-internalization processing. Another approach is to redirect AAV tropism by genetic engineering of the viral capsid (Baranowski *et al.*, 2001; Girod *et al.*, 1999; Grifman *et al.*, 2001; Nicklin *et al.*, 2001; Wu *et al.*, 2000; Perabo *et al.*, 2003; Büning *et al.*, 2003a).

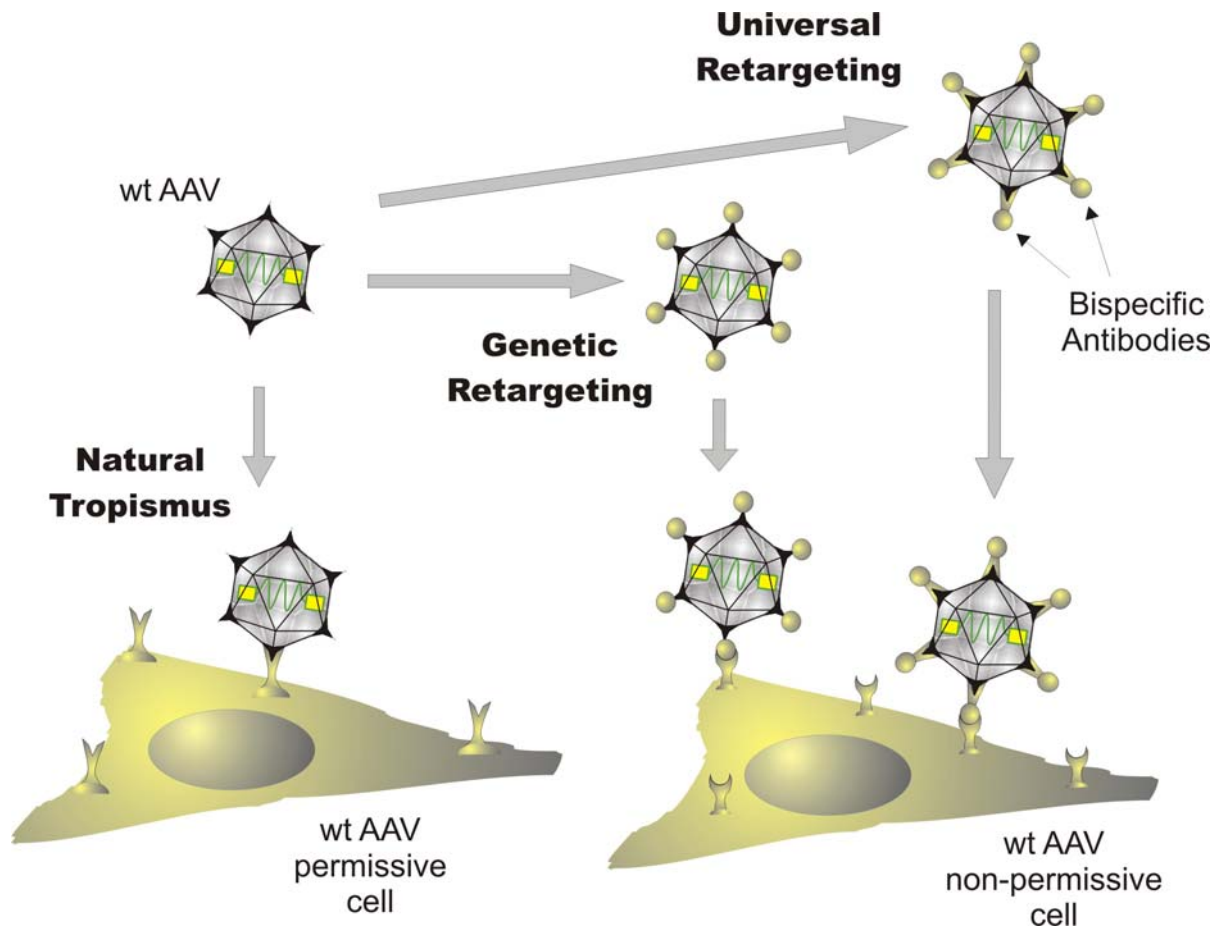


**Figure 6. Targeting strategies for AAV.** Targeting to new cellular receptors can be achieved by providing the capsid with an appropriate receptor binding motif, either by genetic engineering of the capsid (e.g. insertion of peptides) or via bispecific antibodies carrying specific binding motifs for AAV on one side and for the cellular receptor on the other side.

In this case, the DNA encoding the structural proteins is manipulated by point mutations or by insertion at specific capsid locations of DNA sequences coding for ligand peptides (insertional mutagenesis). For example, the insertion of an Arg-Gly-Asp (RGD) integrin binding motif at amino acid position 587 (VP1 numbering) allowed efficient transduction of formerly AAV non-permissive cells (Girod *et al.*, 1999). However, engineering by rational design often leads to unpredictable results. Modifications of the capsid may interfere with the stability of the capsid or with the infectious process. For example, point mutations at crucial arginins allowed the disruption of AAV binding to its primary receptor HSPG (Opie *et al.*, 2003), which is mainly responsible for the broad host range. However, those mutants showed a severely reduced infectivity. Likewise, the insertion of targeting sequences could disrupt capsid domains that exert fundamental functions in the infection process, or the inserted peptides might be expressed in a non-functional three-dimensional structure when inserted in the capsid context. Last but not least, the insertion of a particular sequence requires the *knowledge* of receptor-specific binding peptides, which are unknown for a large number of

clinically interesting tissues. An elegant solution to these problems is the use of combinatorial engineering of the capsid and high-throughput selection protocols to screen mutants with desired phenotype. Using a AAV library of capsids carrying a random insertion at amino acid position 587, an efficient retargeting to various cell types *in vitro* and *in vivo* could be achieved (Perabo *et al.*, 2003; Muller *et al.*, 2003). Moreover, it was observed that the degree of HSPG affinity was influenced by the different selected peptide insertions (Perabo *et al.*, 2003). Due to the role of HSPG as primary receptor and the importance of HSPG-independent vectors for efficient *in vivo* re-targeting, we investigated the molecular mechanisms responsible for this phenotypes (Perabo *et al.*, in revision). Interestingly, insertions carrying negatively charged amino acids are likely to ablate HSPG binding and allow detargeting from HSPG-rich tissues such as liver and spleen.

## Humoral Immune Response against AAV

A major issue in the development of viral vectors for gene therapy concerns the immune response of the host. Immune reactions upon vector injection may limit long term transgene expression or a potential readministration and could unleash severe side-effects for the patient. While recombinant AAV shows a relatively low immunogenicity generally lacking cellular response due to the absence of viral genes, viral infection triggers the production of antibodies against the capsid (humoral immune response). Depending on age and ethnic group, 30 to 96 % of humans are positive for AAV specific antibodies. Of these, 18 to 67.5 % exhibit neutralizing antibodies (Moskalenko *et al.*, 2000; Blacklow *et al.*, 1968b; Chirmule *et al.*, 1999; Erles *et al.*, 1999). In pre-clinical studies, the presence of neutralizing antibodies has been shown to eliminate or greatly reduce the levels of gene expression after vector readministration (Xiao *et al.*, 1996; Fisher *et al.*, 1997; Xiao *et al.*, 2000; Chirmule *et al.*, 2000). The observed humoral response via B-cell dependent T-cell activation seems to be exclusively directed against the vector, but not the transgene (Hernandez *et al.*, 1999; Chirmule *et al.*, 2000). Possible solutions might be a transient immunosuppression during the first administration by anti-CD40-ligand Ab, anti-CD4 Ab or a CTLA4-immunoglobulin fusion protein (CTLA4Ig) (Halbert *et al.*, 1998; Manning *et al.*, 1998), thus preventing Ab formation. An alternative solution is the engineering of the virus (Fig. 7). Insertion of peptides in surface exposed regions was shown to lead to reduced neutralization by human antibodies (Huttner *et al.*, 2003). However, insertion of peptides is likely to result in modified tropism

and/or biological properties of the capsid. In addition, only few capsid regions are known to tolerate insertions. Other natural AAV serotypes that are not recognized by AAV-2 antibodies could be employed to evade neutralization. However, each serotype has a unique tropism that might not be appropriate for the targeted tissue. In addition, the number of administrations would be limited by the number of existing serotypes. In another study, Lochrie *et al.* (2006) addressed the problem by generating and testing over 120 mutants (generated by site directed mutagenesis to introduce point mutations in different capsid sites) for their ability to evade Ab-mediated neutralisation. This approach however is extremely labor intensive. In addition, obtained mutants were mostly non-infectious.

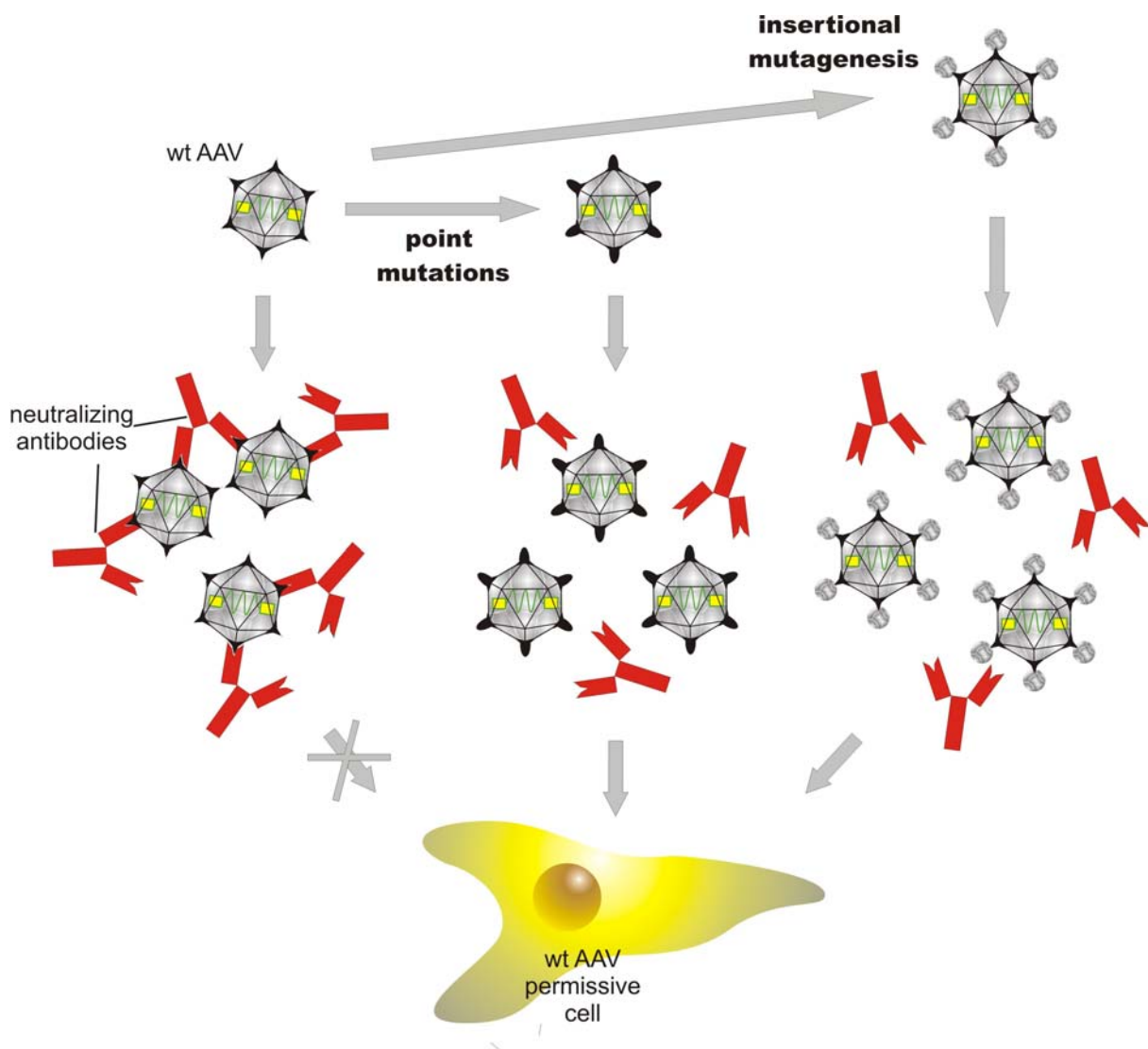


**Figure 7. Immune escape by genetic engineering of immunogenic AAV epitopes.** While the wt is efficiently neutralized by serum antibodies the introduction of point mutations or peptide insertions at antigenic sites prevents antibody-mediated neutralization thus allowing efficient infection of cells.

We therefore developed a directed evolution approach that allows the identification of mutants that were less efficiently neutralized by human Ab, from a large combinatorial library. This method does not require any knowledge about AAV infection biology or immunogenic epitopes and can be applied to screen mutants with a variety of desired phenotypes. The same technology is likely to be applicable for several classes of viruses.

## **Chapter II**

### Specific Goals of this Work (Summary)

Despite promising advance in the development of viral vectors based on AAV for human gene therapy, several major hurdles for a more general use remain. Among these, efficient *in vivo* applications are limited by the high prevalence of neutralizing antibodies in the human population, which can reduce or eliminate transgene expression.

A successful prevention of antibody-mediated vector neutralisation requires the modification of specific epitopes of the viral capsid responsible for Ab binding. The aim of this work was to demonstrate that immune-escaping capsid variants can be generated through genetic modifications of the virus by taking advantage of combinatorial engineering and directed evolution protocols.

A library of  $10^7$  AAV mutants carrying random point mutations scattered throughout the capsid gene of AAV was created by *error prone* PCR and screened for clones that were able to avoid neutralization by AAV-neutralizing human sera. Three mutants carrying the mutations R459G, R459K and N551D respectively and a double mutant with a combined R459K/N551D mutation were strongly enriched after the selection procedure. Characterisation of these clones showed an immune-escaping phenotype for all mutants. However, the combination mutant proved to be superior in both evasion of neutralization and infectivity, leading to the assumption that multiple mutations convey enhanced effects. Therefore, the remaining pool was subjected to DNA shuffling and additional *error prone* PCR, yielding a second-generation library, which was screened for further improved phenotypes. In this context, a method which we called *evolution monitoring* was devised allowing optimization of several experimental conditions that are typically critical for successful outcome of library panning. These refinements yielded novel variants with further enhanced immune-escape abilities and infectivity in comparison to previously selected mutants. Finally, obtained data suggests an enormous potential for using the here developed tools to study infection biology of viruses by reverse genetics.

This work showed for the first time that *error prone* PCR and DNA shuffling can be successfully applied for genetic engineering of a virus by a directed evolution approach. In principle, using appropriate selection protocols these techniques should be adaptable for addressing a wide variety of challenges concerning AAV in particular and virology in general.

## **Chapter III**

# Combinatorial Engineering of a Gene Therapy Vector: Directed Evolution of Adeno- Associated Virus

Published in *Journal of Gene Medicine* (2006) 8: 155-162 as:

Perabo L and Endell J, King S, Lux K, Goldnau D, Hallek M, and Büning H

## Abstract

**Background:** Viruses are being exploited as vectors to deliver therapeutic genetic information into target cells. The success of this approach will depend on the ability to overcome current limitations, especially in terms of safety and efficiency, through molecular engineering of the viral particles.

**Methods:** Here we show that *in vitro* directed evolution can be successfully performed to randomize the viral capsid by *error prone PCR* and to obtain mutants with improved phenotype.

**Results:** To demonstrate the potential of this technology we selected several adeno-associated virus (AAV) capsid variants that are less efficiently neutralized by human antibodies. These mutations can be used to generate novel vectors for the treatment of patients with preexisting immunity to AAV.

**Conclusions:** Our results demonstrate that combinatorial engineering overcomes the limitations of rational design approaches posed by incomplete understanding of the infectious process and at the same time offers a powerful tool to dissect basic viral biology by reverse genetics.

## Introduction

The viral families (e.g adeno-, retro-, herpes- and adeno-associated viruses) used as gene transfer vectors for human gene therapy (Pfeifer and Verma, 2001) all have limitations that need to be addressed. Common concerns are safety, viral tropism (target specificity), immunogenicity, ability to elicit strong and stable transgene expression and the possibility to produce the vector at high titers (Kay *et al.*, 2001; Thomas *et al.*, 2003). Recently, the adeno-associated virus of type 2 (AAV-2) has received increasing attention as a vector (Monahan and Samulski, 2000). AAV-2 is non-pathogenic in humans, does not induce a strong immune response and can transduce both dividing and quiescent cells. Viral particles are stable and can be produced at high titers. Current efforts to improve AAV vectors aim to control the tropism of the vector and to overcome barriers to infection such as neutralization by human antibodies (Huttner *et al.*, 2003; Girod *et al.*, 1999; Grifman *et al.*, 2001; Shi, Arnold *et al.*, 2001; Wu *et al.*, 2000; Nicklin *et al.*, 2001). Although unveiling of the atomic structure of AAV-2 (Xie *et al.*, 2002) boosted these efforts, the manipulation of the virions by rational design remains a difficult task due to our still incomplete knowledge of the capsid biology. Therefore, the goal of engineering tailored viral vectors could be achieved more easily if one

could take advantage of combinatorial techniques that have been extensively used to optimize protein function in the past decade (Neylon, 2004; Christians *et al.*, 1999; Cramer, Raillard *et al.*, 1998; Kolkman and Thomas, 2001; Zhang *et al.*, 1997; Cramer *et al.*, 1996a; Cramer *et al.*, 1996b; Stemmer, 1994).

Recently, two reports demonstrated that AAV peptide-display libraries can be generated by insertion of randomized peptides at a specific capsid location (Perabo *et al.*, 2003; Muller *et al.*, 2003). These viral libraries could be screened for the selection of receptor specific clones that infected wild type (wt) AAV-2 resistant cell types. However, ultimate optimization of gene therapy vectors will require manipulation of the whole capsid to be able to control different features of viral biology. In other studies, different strains of murine leukemia virus (MLV) were bred by DNA shuffling of their envelope genes to modify their tropism and stability (Soong *et al.*, 2000; Powell *et al.*, 2000). Here we describe a novel *directed evolution* approach based on randomization of the viral capsid by *error prone PCR*. To demonstrate the potential of this technology we applied it for the selection of AAV vectors that escape neutralization by human antibodies.

## Materials and methods

### Generation of a randomized AAV library and rAAV mutants

*Error prone PCR* was performed (primers: 5'-AAT GAT TAA CCC GCC ATG CT-3' and 5'-GGT ACG ACG ACG ATT GCC-3') on the fragment of the *cap* gene of AAV-2 coding for amino acids 353 to 767 (VP1 numbering). 150 ng target DNA were amplified in a 50  $\mu$ l-PCR using 0.2 mM dNTPs, 0.4 mM primers, 1 unit of Mutazyme II and 5  $\mu$ l reaction buffer (GeneMorph II, Stratagene). The reaction was conducted as follows: 95°C/2 min.; 35 cycles x (95°C/30 sec., 48.5°C/30 sec., 72°C/100 sec.); 72°C/10 min. The amplified DNA was digested with BsiWI and SnaBI restriction enzymes and cloned in an AAV-2 genome-containing plasmid (pUC-AAV2 [6]) to replace the corresponding wild type sequence. A DNA library of approx.  $2.5 \times 10^7$  clones was obtained by electroporation into XL1-Blue MRF'E. coli. The entire mutagenized region of 96 clones was sequenced to determine the average rate of mutations (5.7 mutations/clone) and to verify the random distribution of amino acid substitutions. Viral library and rAAV mutants were produced and titrated as previously described (Perabo *et al.*, 2003; Grimm *et al.*, 1999). Empty particles were generated by

transfecting 293 cells with a 1:2 molar ratio of pXX6 (helper plasmid) and a Rep-Cap containing plasmid which is devoid of AAV packaging signals (ITRs).

### **Selection protocol**

$2 \times 10^6$  HeLa cells were seeded on 150 mm Petri-dishes 24 hrs before infection. 29 human sera were obtained with informed consent from the Klinikum Großhadern in Munich, Germany, and tested for their ability to neutralize AAV-2 infection (Huttner *et al.*, 2003). 10  $\mu$ l of a strongly neutralizing serum (Huttner *et al.*, 2003) and  $2 \times 10^{10}$  genomic particles of the viral library were incubated in 10 ml of Dulbecco's Modified Eagle Medium (DMEM) containing 10% FCS for 2 hrs at 4°C. The amount of viral particles used corresponded to an MOI of 50 and allowed us to apply approximately up to 1000 copies of each viral clone increasing the possibility that efficient clones could really infect at least one cell, whilst keeping the risk fairly low of generating chimeric viruses with no correspondence between genotype and phenotype. The solution was diluted in 10 additional ml of DMEM/10% FCS and used to incubate the cells in the presence of adenovirus (700 pfu/cell). 48 hrs post infection cells were collected by centrifugation and resuspended in lysis buffer (150 mM NaCl, 50 mM Tris-Cl, pH 8.5). Cells were lysed by 3 freeze/thaw rounds and debris was removed by centrifugation. Adenovirus was heat inactivated (60°C, 30 min) and the viral progeny-containing supernatant was used for further selection rounds. After each round, viral DNA was extracted from 200  $\mu$ l of the lysate and sequenced.

### **Sequence analysis**

Sequencing was performed (Agowa GmbH, Berlin) after DNA extraction and PCR amplification from cultured bacteria (DNA library) or from viral preparations (viral library and viral pool after selections). Single viral genomes were obtained by cloning amplified DNA into pUC-AAV2 and electroporation into E coli (XL1-Blue MRF<sup>+</sup>). For each analysis >70 clones were sequenced.

### **Infection assays**

$2 \times 10^4$  HeLa cells were seeded in 48 well plates 24 hrs before infection. Identical numbers of transducing (MOI of 5) and total particles ( $6.5 \times 10^8$ , adding wt AAV-2 empty particles when needed) were incubated with serial dilutions (1:40 to 1:2560 in PBS) of human sera for 2 hrs at 4°C in a total volume of 40  $\mu$ l. Before addition to the cells, 240  $\mu$ l of DMEM/10 % FCS were added to each sample. At least 5000 cells were analyzed by FACS (Beckman Coulter

XL/MCL) 48 hrs post infection to determine the amount of GFP expressing cells. For determination of the decoy effect of wt and double mutant capsids,  $2 \times 10^4$  HeLa cells were seeded in 48 well plates 24 hrs before infection. No empty particles, or  $3.9 \times 10^8$  of either empty wt or double mutant particles were added to identical amounts of double mutant total particles ( $1.7 \times 10^7$ ). Incubation, infection and FACS analysis were performed as described above.

### **Heparin inhibition assay**

24 hrs prior to infection  $2 \times 10^4$  HeLa cells were seeded per well in 48 well plates. Equal amounts of infectious particles (MOI of 5) were incubated in a total volume of 200  $\mu$ l of DMEM/10% FCS in the presence or absence of soluble heparin (85 U/ml) at 37°C for 30 min. This solution was then used to infect cells. 48 hrs p.i. the percentage of transduced cells was determined by FACS analysis.

## **Results**

### **Production of a library of AAV-2 particles with random capsid mutations**

A library of  $2.5 \times 10^7$  capsid variants with scattered point mutations throughout the capsid protein gene (*cap*) of AAV-2 was obtained by *error prone PCR* (Fig. 1). The PCR primers allowed us to target 82% of the amino acids expressed on the viral surface, minimizing at the same time mutagenesis of the structural core of the capsid subunit (Xie *et al.*, 2002) in order to reduce loss of biodiversity after packaging. Sequence analysis confirmed that after PCR the mutations were evenly distributed along the *cap* gene. As expected, after packaging of the DNA pool into viral particles, a major amount of biodiversity was lost and the average number of amino acid mutations per clone dropped from 5.7 to 0.9, suggesting that clones with impaired assembly were eliminated. In addition a preferential localization of the mutations on surface epitopes was observed (data not shown). This can be explained by a greater tolerance of the surface structure, mainly composed of flexible loops (Xie *et al.*, 2002), to structural modifications.

### **Selection of capsid variants that escape human serum neutralization**

Depending on age and ethnic group, between 50 and 96% of the human population is seropositive for AAV-2, and 18-67.5% of these individuals have neutralizing antibodies (Moskalenko *et al.*, 2000; Chirmule *et al.*, 1999; Erles *et al.*, 1999). Animal experiments have shown that neutralizing antibodies may reduce or even prevent AAV-2 transduction *in vivo* (Xiao *et al.*, 2000; Fisher *et al.*, 1997). For this reason it is likely that application of AAV-2 vectors to patients with preexisting immunity would require higher viral doses. Although other AAV serotypes could prove useful to escape neutralization by anti-AAV-2 antibodies, different AAV serotypes often have different tropism, restricting this possibility. Moreover, since it is likely that even immune-escaping mutants will trigger the production of neutralizing antibodies, it is desirable to increase the number of capsid alternatives at our disposal for repeated applications of the vector.

Therefore, we designed a biopanning protocol for the selection of viral mutants that are less efficiently neutralized by human antibodies (Fig. 1). The randomized library was pre-incubated with an AAV-2 neutralizing human serum and applied to a cell line (HeLa) that supports AAV-2 replication. In a control experiment we pre-incubated the library with an AAV-2 seropositive but non-neutralizing human serum. In both cases, to support AAV replication cells were coinfecting with the maximum amount of Ad that allowed infection of cells without inducing cytotoxic effects after 48 hrs, therefore maximizing the probability that the helper effect is provided to all AAV infected cells. Viral progenies were harvested 48 hours p.i. and applied to new cells for further selection rounds. Thus the amplification of the clones carrying successful mutations occurs during the virus infection cycle obviating the need to introduce artificial re-amplification steps. These experimental conditions apply a selective pressure to the initial viral population and the pool is progressively enriched with mutants that are better able to infect the cells despite the presence of neutralizing antibodies. It is important to note that in this way viruses are not only selected for their ability to escape antibody binding, but also for their overall biological fitness (e.g. efficiency of infection and progeny production).

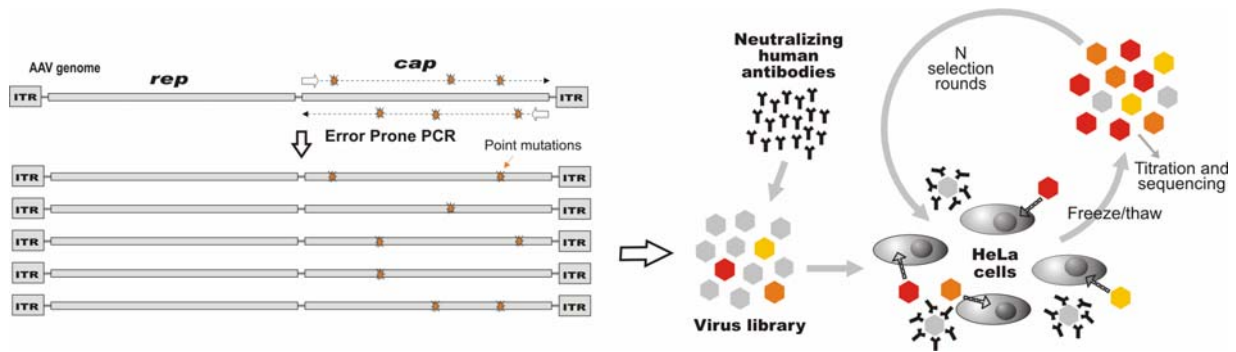


**Figure 1: Production of a library of viral particles by error prone PCR of the AAV-2 capsid gene (*cap*) and biopanning protocol.** ITRs (Inverted Terminal Repeats) are the packaging signals of the AAV genome. The *rep* gene codes for 4 proteins involved in viral replication.

### Characterization of neutralization escaping mutants

After each selection round the viral progeny DNA was extracted from cell lysates and single viral clones were analyzed by sequencing. After 3 selection rounds, 3 point mutations occurring at 2 different amino acid positions were strongly selected (Fig. 2A): an arginine to glycine mutation (R459G according to VP1 numbering) was found in 9 of 94 sequenced clones, an arginine to lysine mutation (R459K) was found in 3 clones, and an asparagine to aspartate mutation (N551D) was found in 17 clones. Two clones carried the double mutation R459K-N551D. Mutations of 22 other residues occurred only once. Of the 31 clones carrying a mutation in either of the two frequently mutated sites, 25 did not carry any additional amino acid substitution at other sites. Strikingly, although these two residues are separated by 92 amino acids in the primary sequence of the protein, they are located very closely in the three-dimensional structure of the viral particle (Fig.2B). Moreover these residues are located on the capsid surface and are therefore accessible to antibody binding, suggesting their importance as immunogenic residues. Although N551 has lower surface exposure than R459 (Xie *et al.*, 2002), it has been previously reported that even amino acids that are buried in the inner VP3 protein structure can nonetheless influence the surface topology and biology of the virus (Wu *et al.*, 2000; Rabinowitz *et al.*, 1999). Moreover, once the N is exchanged with a D this latter residue could find its way through the structure and become more exposed on the surface, where it could impair the binding of a pre-existing antibody.

Remarkably, mapping all the other (less frequently occurring) selected sites on the three-dimensional structure shows that 73% of all the recovered mutation sites clustered in the same capsid region and are expressed on the capsid surface (Fig. 2B). A previous epitope-scanning study failed to identify this region as immunogenic (Wobus *et al.*, 2000). Another



**Figure 2: (A) Selection of neutralization-escaping viral mutants.** The sequence of 30 representative clones is presented to show the biodiversity of the viral library and of the viral pools after selection in the presence of a neutralizing human serum. **(B) Mapping of the selected amino acid mutations on the capsid structure.** Red: frequently occurring mutations (positions 459 and 551). Yellow: other selected mutations mapping in the same region; these appeared only once out of 94 sequenced clones and represent 73% of the overall number of identified mutations. The three peaks are symmetrical and coloured to facilitate the visualization of the capsid structure. The yellow box on the complete viral particle (adapted from Xie et al., PNAS 2002<sup>11</sup>, Copyright 2002 National Academy of Sciences, U.S.A.) depicts the magnified region.

A control selection performed with the library in presence of a non-neutralizing human serum yielded wt AAV-2 clones in 68 of 79 cases (data not shown). Each of the 11 mutants carried a single point mutation. The 11 mutations were scattered throughout the capsid sequence and occurred only once; only 3 of them involved a charge shift. These results suggest that the wild type capsid (that has already been subject to natural selection pressure) is the structure that is most fitted to the task of performing a productive infection on HeLa cells in the presence of an AAV-2 non-neutralizing human serum. This control also demonstrates that the selection of mutants in the presence of neutralizing antibodies is not due to other factors (e.g. the presence of adenovirus). To exclude that viral immune escaping mutants can be generated through spontaneously occurring mutations (in the absence of capsid modification by error prone PCR), wt AAV-2 was applied to HeLa cells in the presence of neutralizing antibodies and three selection rounds were performed (same experimental conditions as for the real selection). None of 30 sequenced viral clones was found to carry a single point mutation.

**Table 1: Viral titers per  $\mu$ l of GFP expressing rAAV-2 and selected mutants.**

|                               | Genomic titer | Infectious titer | Particle titer | Heparin inhibition |
|-------------------------------|---------------|------------------|----------------|--------------------|
| wt                            | 1.2x10(8)     | 5.9x10(5)        | 1.49x10(9)     | 99.2%              |
| R459G                         | 3.45x10(8)    | 4.9x10(5)        | 1.65x10(9)     | 98.7%              |
| N551D                         | 4.18x10(8)    | 8.8x10(5)        | 2.2x10(9)      | 99.4%              |
| double mut                    | 2.36x10(8)    | 1.8x10(6)        | 1.36x10(9)     | 99.4%              |
| AAV2<br>Empty particles       | ---           | ---              | 1.25x10(9)     | n.d.               |
| Double mut<br>Empty particles | ---           | ---              | 1.58x10(9)     | n.d.               |

*Titers in this table refer to the viral preparations used for the infection experiments shown in figures 3 and 4. All mutants have been packaged at least twice resulting in titers consistent with those provided here.*

To confirm that immune escaping viral mutants had been selected, recombinant GFP expressing AAV particles carrying the mutations R459G, N551D or the R459K-N551D double mutation were produced. Genomic and particle titers of the mutants showed no significant difference to wt vector titers (Tab. 1). This was expected because the selection process should yield clones with good packaging efficiency since mutations interfering with efficient packaging are assumed to be negatively selected when the viral progeny is generated. However, to demonstrate that this kind of selection really applies, evaluation of titers obtained from a larger repertoire of mutants would be required. Infectious titers showed a better infectivity of the double mutant in comparison to wt and single-mutation clones (Tab.1). This could reflect the selective pressure applied to the pool during the selection procedure. An increase in the infection efficiency (e.g. ability to bind to cellular receptors or to perform post-entry steps) would contribute to the amplification of a mutant additionally to its ability to escape neutralization. The selected mutations could not only allow escape from antibody neutralization, but at the same time improve the generic efficiency of the infection process. However, further investigations are required to confirm this observation and this hypothesis.

Equal infectious titers were used to infect HeLa cells in the presence of serial dilutions of the same neutralizing human serum that was used for the selection (Fig. 3). In addition, amounts of total viral particles were normalized by addition of AAV-2 empty capsids in order to exclude the influence of particle titers on antibody sequestration. The amount of serum needed to halve the number of transduced cells was defined as  $N_{50}$ .  $N_{50}$  values for wt virus and mutants were determined using figure 3. The values obtained for R459G, N551D and R459K-N551D were respectively 4.1-, 3.3- and 5.5-fold higher than the corresponding  $N_{50}$  obtained for wt, demonstrating that the selected mutations improved the ability of the virus to escape neutralization. Similar results were obtained after preincubation with AAV-2 neutralizing sera obtained from 7 different donors: all tested sera showed a weaker neutralization of the double mutant in comparison to wt (single mutants were not tested).  $N_{50}$  values of R459K-N551D were 1.3- to 5.3-fold higher than for wt AAV-2 (data not shown), demonstrating that the ability to escape neutralization was not limited to the particular serum used for the selection.

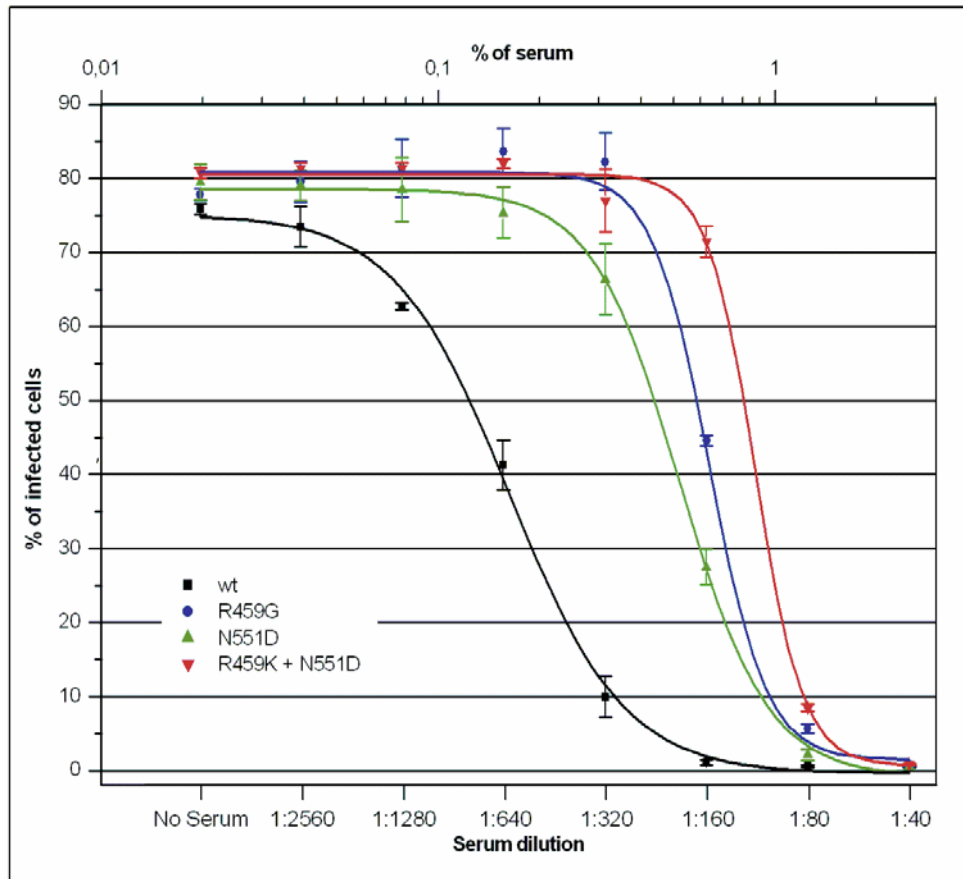


**Figure 3: Transduction of HeLa cells in the presence of an AAV-2 neutralizing serum.** Cells were infected with same infectious titers of GFP expressing rAAV virions. Particle titers were adjusted by the addition of wt AAV-2 empty capsids. Black: wild type rAAV-2; blue: R459G mutant; green: N551D; red: double mutant (R459K+N551D). Results are expressed as mean and standard error of triplicate values. Serum concentrations are expressed in the x-axis as dilution factor (below) or as percentage to facilitate calculation of  $N_{50}$  values (above).

Additionally, to further prove that the selected mutations diminish antibody recognition of the viral capsids, the ability of wt and mutant empty particles to act as decoys for human neutralizing antibodies was tested by infecting HeLa cells with the R459K-N551D mutant in the absence or presence of wt or R459K-N551D empty particles (Fig.4). When empty particles carrying the double mutation were added, the  $N_{50}$  value was only slightly increased (+35%). However,  $N_{50}$  was substantially increased (+190%) if the same amount of empty wt particles was added, showing that wt capsids were better at sequestering the neutralizing antibodies which hindered transduction. The ratio between these values calculates to a 5.4-fold higher increase after addition of wt empty particles compared to the addition of double mutant empty particles. This is in good agreement with the 5.5-fold value obtained from figure 3.

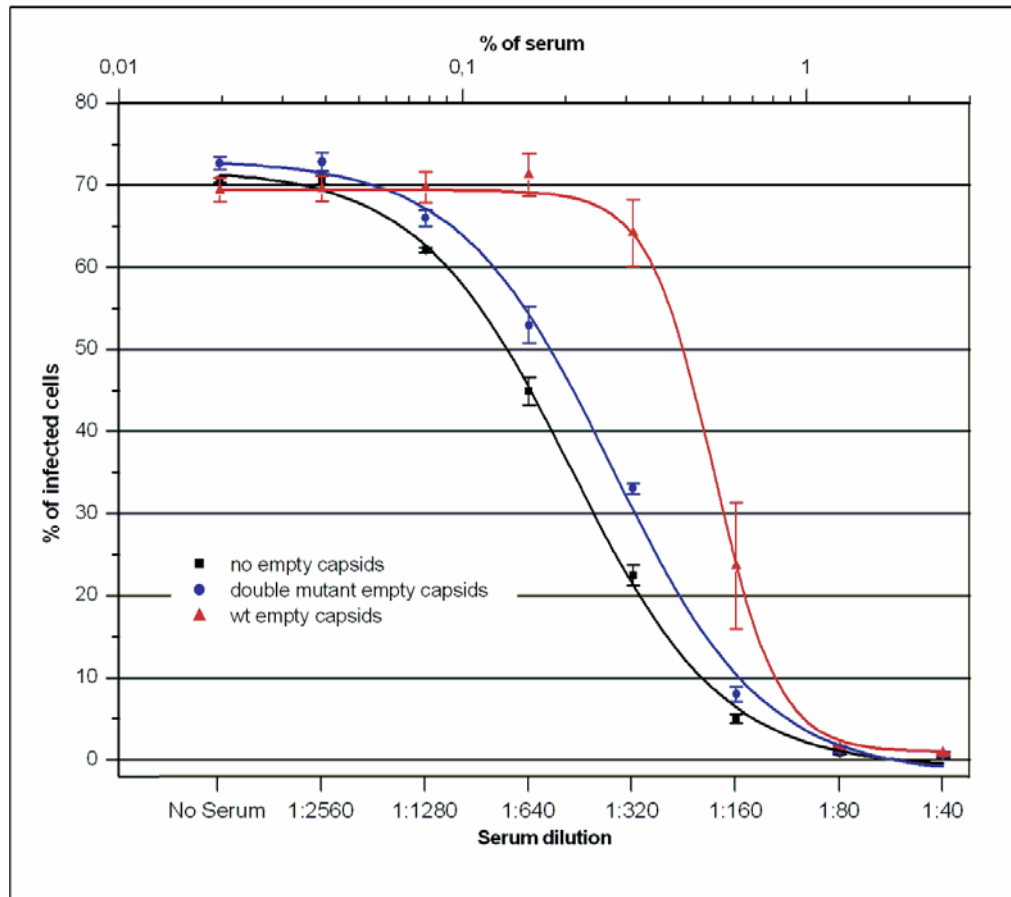


**Figure 4: Decoy activity of wt and mutated empty capsids.** HeLa cells were infected with R459K-N551D in the presence of neutralizing serum without addition of empty particles (black line) or after addition of double mutant empty particles (blue line) or wt empty capsids (red line). Serum concentrations are expressed in the x-axis as the dilution factor (below) or as percentage (above).

No differences in infectivity were detectable in the infections performed with additional empty capsids without serum, showing that the differences observed using wt and mutant empty particles were not due to a different level of cellular receptor competition for the viral attachment or any other infection step.

In conclusion, these experiments demonstrate that the mutations reduce the affinity of neutralizing antibodies for the viral capsids.

Finally, we investigated if the selected capsid mutations had an influence on the viral tropism. We used soluble heparin, an analogue of the AAV-2 primary receptor heparin sulfate proteoglycan (HSPG), to show that cell transduction could be blocked in a similar manner and to a similar level to wt AAV-2 (Table 1). Moreover, tropism of the immune-escaping clones was unchanged in comparison to wt AAV-2 when tested on HeLa (Table 1), a very permissive cell line for wt AAV-2 and on M-07e (data not shown), a wt AAV-2 resistant cell line (Perabo *et al.*, 2003).

## Discussion

These results demonstrate that randomized mutagenesis of the viral capsid can be successfully applied for the generation of improved viral vectors for gene therapy.

The described protocol for the production of a viral library is based on transfection of cells with a pool of viral genomes. Since it is possible that some cells are transduced by more than one AAV genome, this procedure yields a certain amount of chimeric viral particles where the genotype is not coupled to phenotype, as demonstrated by the presence of viral DNA sequences carrying stop codons, an event that can be explained only by genotype-phenotype uncoupling. Although this could initially lead to a loss of biodiversity of the viral library in comparison to the DNA library, after the first selection round no stop codons could be detected in the viral pool demonstrating that, as expected, the selection process eliminates such chimeric particles. The initial loss of biodiversity could be avoided by initially infecting permissive cells with AAV hybrid (wt and mutant) virions at low MOI (Muller *et al.*, 2003). Although it was not necessary to perform this step for the experiments presented here, this solution could be recommended for screenings where the biodiversity could represent a limiting factor for the success of the procedure.

The mutants described here carry amino acid substitutions that involve changes in charged amino acids and might therefore alter regional surface electron potential, local pKa, or even local quaternary structure, and might affect a significantly larger region of the AAV capsid surface. Based on this, it is currently unclear whether the strongly selected amino acid mutations correspond to immunogenic sites or if their substitution exerts influence on nearby capsid regions, maximizing phenotypic change per single genotypic change. However, the clustering of the selected mutations suggests an immunogenic site to be located on the external side of the 3-fold symmetry peak.

Despite increased ability to escape neutralization, the mutants generated can still be inactivated by relatively high sera dilutions and further optimization will be required for clinical application. However, the double mutant was more efficient than single mutants suggesting that better variants could be generated by combining several additional mutations on one capsid at the same time. This is also suggested by the observation that polyclonal antibodies contained in human serum are probably able to interact with different epitopes on the viral capsid. Complete escaping of neutralization will require engineering of all these distinct epitopes. Given the limited size of the library described here and considering the low average number of mutations per clone, combinations of multiple mutations are unlikely to be

selected. Application of increasing selective pressure or performing further selection rounds could have led to the identification of some of these mutants. However, these will be more easily isolated by screening libraries obtained by consecutive rounds of mutagenesis and selection or by gene shuffling of previously mutants used as parental strains (Crameri, Raillard *et al.*, 1998; Stemmer, 1994). High-throughput breeding of different retrovirus strains yielded viral vectors with increased stability and with modified tropism in previously reported experiments (Soong, Namura *et al.*, 2000; Powell, Kaloss *et al.*, 2000). This interesting approach could be also applied to AAV. It is noteworthy that this procedure usually yields complex chimera derived from several parental strains, from which it is difficult to understand how the selected mutations contribute to the phenotype. It should be also noted that despite a clear selection for the two described mutations, the number of recovered wt clones after the 3<sup>rd</sup> selection round was still high. Additionally, the same experimental setup allowed us to recover viral clones after three rounds of selection applied to wt AAV-2. This was possible because the selective pressure was kept low by the high serum dilution used in these experiments. Moreover, the ability of the selected mutants to escape neutralization could be proven for all the 7 tested AAV-2 neutralizing human sera but ranged quantitatively, suggesting that the pool of neutralizing antibody differs from one individual to the other. Taken together, these observations suggest that introduction of the refinements proposed here to the library, in parallel with application of a stronger selective pressure (increasing serum concentration and/or pooling of different sera), should result in the selection of capsid variants with greater ability to escape antibody neutralization. In addition, due to the statistical nature of the process, it is likely that other important immune-escaping mutations could be identified simply by repeating the selection experiment described here. These speculations are also supported by the observation that we only identified a maximum of two alternative amino acids for every selected mutation site while it is reasonable that other amino acid substitutions could generate clones with similar or even improved phenotype. Moreover, the identified amino acid substitutions originated in all cases from the same codon types (no alternative codons for the same amino acid were found). These observations are in agreement with statistical expectations from a library of  $10^7$  clones that cannot represent all the possible combinations of 400 positions and 20 amino acids and once more underline the importance of upgrading the selection protocols with repeated mutagenesis and DNA shuffling.

Heparin binding phenotypes and the infection experiment performed on a cell line (M-07e) that is not permissive to wt AAV-2 infection suggest that the mutations described here

do not influence the tropism of the mutants. However, it cannot be excluded that tropism alterations could be detected on other cell types or induced by different immune-escaping mutations that could be identified with error prone PCR technology. In this case, protocols should be applied to specifically select mutations that do not interfere with the desired viral tropism. This can be achieved by alternating infections in the presence of neutralizing antibodies and infections on target cells.

It remains to be elucidated whether these novel mutants would generate neutralizing human antibodies after their first application. However, even in this case, one or more immune-escaping clones could provide patients with preexisting immunity with the chance to receive at least one or a few successful vector applications. The pool of capsid mutations required for this goal could be generated by combined efforts that employ different mutagenesis techniques. Finally, successful escape from neutralization *in vivo* will require the resolution of a number of additional factors. Some of these complications can be addressed by the further development of capsid randomization technology and by setup of selection procedures that more closely mimic the *in vivo environment*. However, the production of ideal vectors is likely to be achieved by designing procedures that exploit combinations of several different engineering approaches including educated guess-work.

We anticipate that further development of this technology could yield virus variants with modified tropism, increased genome size capacity and reduced toxicity. Finally, the study of viral biology will benefit from the use of such combinatorial techniques as reverse genetics.

## **Acknowledgements**

We thank Heidi Feldmann, Nadja Huttner and Tony Meinhart for technical assistance. Also we are grateful to Patrick Cramer and Karim Armache for help in the preparation of this manuscript. The files for the computation of AAV-2 atomic structure were kindly provided by Michael S. Chapman and Qing Xie. This work has been supported by grants of the Deutsche Forschungsgemeinschaft (SFB 455) to L.P., J.E., M.H. and H.B. and of the Bayerische Forschungstiftung (FORGEN) to M.H. and H.B.

## **Chapter IV**

Improving Viral Phenotypes by DNA  
Shuffling and *Evolution Monitoring*

## Introduction

As described in chapter III, we have screened a library of AAV-2 particles carrying random point mutations to isolate mutants exhibiting immune-escaping properties. Clones carrying mutations R459G, N551D or the double mutation R459K/N551D were strongly selected, while several other mutations appeared with lower frequency in other mutants. The finding that the double mutant showed the best phenotype in terms of infectivity and ability to escape neutralization suggested that more efficient immune escaping mutants could be obtained by introducing more mutations in the same clone (also see *Discussion* in chapter III). This can be achieved by applying DNA shuffling protocols to the previously selected pool in order to generate a viral library consisting of clones carrying different combinations of previously selected mutations. At the same time, additional randomization of the target region can be performed by *error prone* PCR in order to introduce new point mutations in the pool.

This chapter describes the setup of a DNA shuffling protocol for AAV libraries and its application for the screening of AAV mutants with improved immune-escaping phenotype. Moreover, to improve efficiency of the selection procedure and reduce experimental costs, a new method was devised to monitor evolution of the pool at each selection round through light cycler PCR (*evolution monitoring*).

These refinements yielded the first proof of principle that DNA shuffling can be applied to *error prone* PCR viral libraries. Several novel mutants with interesting potential for human gene therapy were identified. In addition, analysis of the results provided interesting insights on viral capsid function, suggesting the potential of this technology as reverse genetic tool for the study of infection biology.

## Material and Methods

### DNA shuffling of selected viral clones

PCR was performed (primers 5'-TAC CAG CTC CCG TAC GTC CTC GGC-3' and 5'-CGC CAT GCT ACT TAT CTA CG-3') on a fragment of the *cap* gene of AAV-2 coding for the amino acids 333 to 763 (VP1 numbering) of two AAV-2 capsid mutants (double mutant T410A/R459G and triple mutant R459K/N551D/E555G) and wtAAV-2. Target DNA (100 ng) was amplified in a 50 µl reaction using 0.2 mM dNTPs, 0.4 µM primers, 2x reaction

buffer, 2x enhancer solution and 2.5 U of *pfx platinum* polymerase (Invitrogen). The reaction was conducted as follows: 95 °C/3 min; 35 cycles (95 °C/40 s, 55 °C/30 s, 68°C /2 min); 68 °C/10 min. 3 µg of each plasmid were mixed and digested in a 50 µl reaction using 1 U of DNase I for 5 min at 15 °C. The digestion was stopped adding 5 µl 0.5 M EDTA followed by heat inactivation for 10 min at 95 °C. The digestion was loaded on a 1.5 % agarose gel and fragments of size between 50 and 100 bp were purified using *QIAEX II Gel Extraction Kit* (Qiagen). 300 ng of DNA fragments were reassembled in a 50 µl reassembly reaction without primers using the reagents described above. The reaction was conducted as follows: 95 °C/3 min; 40 cycles (95 °C/45 s, 55 °C/30 s, 68 °C /1 min + 2 s per additional cycle); 68 °C/10 min. For replication of correctly assembled fragments a regular PCR as described above was performed using 1 µl of the reassembly reaction. The amplified DNA was sequenced as previously described (see Chapter III).

### **Generation of a second-generation library by DNA shuffling and *error prone* PCR**

Viral genomes were obtained from the third selection cycle of a previous selection, in which a randomized AAV-2 library was screened on a neutralizing human serum (see Chapter III). DNA shuffling of viral DNA was performed as described above. Since plasmids proved to be more reliable templates for *error prone* PCR than PCR fragments, the shuffled DNA was cloned into an AAV-2 genome containing plasmid (pUC AAV-2, see Chapter III) yielding a preliminary library of approx.  $10^7$  clones. A second-generation library of approx.  $4 \times 10^7$  clones was created by further randomization of the preliminary library by *error prone* PCR and cloning into XL1-Blue MRF' *E. coli* (see Chapter III). The second generation library was packaged and analysed as described in chapter III.

### **Selection protocols**

Selections were performed as described in chapter III with the following modifications: for the selections two new neutralizing human sera, serum A and B, and a mixed serum composed of equal volumes of four different human sera (S2, S3, S4, S5) were used. Selection pressures were diversified by changing the effective serum concentration through variation of the total incubation volume using lysis buffer and adding equal volumes of

Dulbecco's Modified Eagle Medium (DMEM) with 10 % fetal calf serum (FCS). With each serum two selections were performed applying a high or a low selection pressure. Selections parameters are summarized in Table 1. The viral progeny was monitored as described below (see paragraph *Evolution monitoring during selections*) and a maximum of  $5 \times 10^9$  genomic particles corresponding to a multiplicity of infection (MOI) of below 1 after serum incubation was used during the selection cycles to maintain a constant selection pressure and a permanent genotype-phenotype coupling.

In addition, each of these selections was repeated with identical parameters but without limitation of genomic particles. Accordingly, the whole viral progeny harvested after the infection step was applied to the next round. In this case, and 5 cycles (instead of 3) were performed. Initial serum concentrations of all performed selection were kept low in order to minimize the risk of losing chimeric capsids with potentially beneficial genotypes during the first cycle. As discussed in chapter III (see *Discussion*) the presence of chimeric capsids in the library is a direct consequence of the packaging protocol. In addition, a low stringency during the first cycle prevents accidental loss of the initially rare library mutants with the desired phenotype. After enrichment of enhanced mutants due to amplification stringency can be increased to insure selection of the fittest variants.

**Table 1. Selection parameters.**

| selection                 | serum volume    | serum dilution 1.<br>cycle | serum dilution 2.<br>cycle | serum dilution 3.<br>cycle |
|---------------------------|-----------------|----------------------------|----------------------------|----------------------------|
| serum A low pressure      | 10 $\mu$ l      | 1:100                      | 1:50                       | 1:50                       |
| serum A high pressure     | 30 $\mu$ l      | 1:50                       | 1:25                       | 1:25                       |
| serum B low pressure      | 5 $\mu$ l       | 1:500                      | 1:250                      | 1:250                      |
| serum B high pressure     | 5 $\mu$ l       | 1:250                      | 1:125                      | 1:125                      |
| mixed serum low pressure  | 10 $\mu$ l each | 1:200 each                 | 1:100 each                 | 1:100 each                 |
| mixed serum high pressure | 30 $\mu$ l each | 1:100 each                 | 1:50 each                  | 1:50 each                  |

## Evolution monitoring during selections

After DNA extraction with a *DNeasy Kit* (Qiagen) the total number of produced viral genomes after each selection cycle was monitored by *light cycler*-PCR (*LC*-PCR) by using the primers 5'-ATG TCC GTC CGT GTG TGG-3' and 5'-GGT ACG ACG ACG ATT GCC-3'. Target DNA was amplified in a *light cycler* (Roche Diagnostics) in a 20  $\mu$ l-reaction using the *light cycler kit* LC-FastStart DNA Master SYBR Green I (Roche Diagnostics) and the following protocol: 0.5  $\mu$ M primers, 5 mM MgCl<sub>2</sub>, 1 x LC-FastStart DNA Master SYBR

Green I. The reaction was conducted as follows: denaturation: 95 °C/10 min; amplification: 35 cycles (95 °C/10 s, 60 °C/10 s, 72 °C /35 s); melting: 95 °C/0 s, 68 °C/10 s, 95 °C /0 s; cooling 40 °C/30 s.

## Infection assays

$2 \times 10^4$  HeLa cells were seeded in 48-well plates 24 h prior to infection. Identical numbers of genomic particles ( $1.5 \times 10^7$ ) and total particles ( $1.3 \times 10^9$ , adding wtAAV-2 empty capsids, when needed) were incubated with serial dilutions of different human sera in phosphate-buffered saline (PBS) for 2 h at 4 °C in a total volume of 40  $\mu$ l (see Table 2) and subsequently added to the HeLa cells. 48 h p.i. the cells were analysed by FACS analysis.

*Table 2. Dilutions of sera for infection assays.*

| serum                        | dilutions                           |
|------------------------------|-------------------------------------|
| S1                           | no serum, 1:20 to 1:2560            |
| S2                           | no serum, 1:20 to 1:1280            |
| S3                           | no serum, 1:20 to 1:1280            |
| mixed serum (S2, S3, S4, S5) | no serum, each serum 1:80 to 1:2560 |

*Sera of healthy patients were obtained from the Klinikum Großhadern.*

## Results

### DNA shuffling of selected clones

DNA shuffling can be used to generate clones that carry random combinations of mutations, which are present in an initial pool. DNA fragments to be shuffled are amplified by PCR from the initial pool. The product is briefly digested with DNase I yielding randomly-cut DNA fragments, which average length depends on digestion time and concentration of DNase I. Fragments of a desired size are purified from agarose gel and full-length DNA is reassembled by PCR performed in absence of primers: overlapping regions of different short fragments can anneal after denaturation followed by a fill-in by the polymerase (Fig. 1).

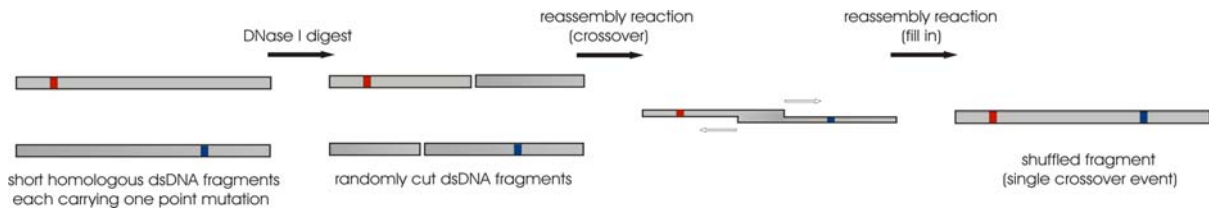


**Figure 1. Principle of DNA shuffling.** A single crossover event is shown. Two short homologous double stranded (ds) DNA fragments each carrying a point mutation at different positions are digested with DNase I yielding randomly cut DNA fragments. In a polymerase chain reaction (PCR) without primers (reassembly reaction) the fragments first anneal at the homologous regions (crossover) followed by a fill-in reaction.

To empirically set up appropriate reaction conditions, a pilot experiment was conducted by shuffling a 1273-base pair (bp) PCR fragment of the *cap* gene of AAV-2 of three selected clones, a T410A/R459G double mutant, a R459K/N551D/E555G triple mutant and wtAAV-2 (Fig. 2). DNA fragments were mixed and briefly digested with an amount of DNase that maximized the amount of fragments ranging in size between 50 and 100 base pairs that were purified from an agarose gel and reassembled as described above. Full-length molecules were then amplified by PCR. For statistical analysis of the generated recombination mutants the DNA amplified from the reassembly reaction was cloned back into a pUC-AAV-2 plasmid and single clones were sequenced.

As seen in Fig. 2c, the product of the reassembly is highly heterogeneous consisting of a large variety of single and double stranded fragments in different states of reassembly. Due to the high homology of the initial fragments the amount of correctly assembled fragments is not so much influenced by the stringency of the annealing process but rather by the size of the digestion fragments, their concentration during the reassembly and the number of reassembly cycles.

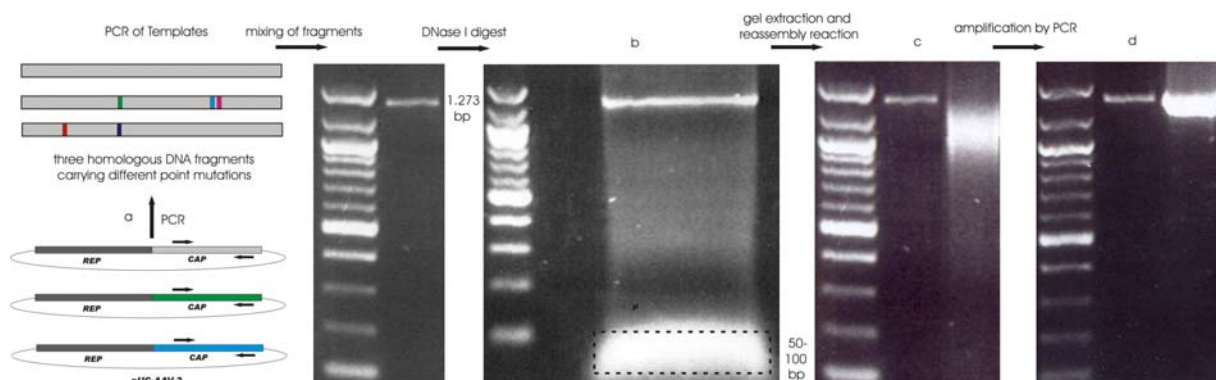


**Figure 2. DNA shuffling of three AAV-2 *cap* gene clones.** (a) A 1.273 bp DNA fragment of three AAV-2 *cap* gene mutants was amplified by PCR. After mixing and DNase I digestion, fragments of 50-100 bases were purified (b). Purified fragments were reassembled by a PCR performed in the absence of primers and full-length molecules are reconstituted (c). The heterogeneous appearance of the product is largely due to incompletely assembled fragments and the partial single-stranded nature of the product. The full-length product is then amplified by PCR with primers (d).

In general, reassembly of smaller digestion fragments requires more cycles and higher DNA concentration. The size of the digestion fragments is an important parameter for the quality of the shuffling result. The smaller the fragments, the more crossover events are necessary to reassemble the full-sized PCR fragment. The number of crossover events (*crossover rate*) determines the probability for shuffling two point mutations which are separated by a given distance. However, with decreasing fragment size the probability of obtaining the correctly reassembled full-length fragments is also decreasing. This explains the need for a pilot experiment: sub-optimal reaction conditions would result in the generation of a shuffled pool that is too similar to the original pool, or in the loss of the pool biodiversity (size of the library).

The clones for the pilot experiment were chosen in order to meet several requirements. The overall number of mutations (5) was kept small to allow adequate statistical analysis without requiring extensive (expensive) sequencing. The distances between the chosen point mutations, ranging from 4 amino acids (12 bp) to 91 amino acids (273 bp), were ideal to determine if *crossover rate* and PCR conditions were suitable to generate combinations of mutations that were close or far from each other. Since fragments used for the reassembly reaction have a maximum length of 100 bp (33 aa), all mutations, which are separated by more than 33 aa can be treated as statistically independent (crossover probability of 1). This condition is fulfilled for all the mutations of the chosen clones, except for the mutations at position 551 and 555, which are located on the same clone. Their distance of 12 bp is much smaller than the length of the digestion fragments (50-100bp). Therefore, the probability of a crossover event is strongly reduced and mutants that can be generated by a crossover between those positions are unlikely to occur. Accordingly, these two positions can be treated as statistically dependent (coupled). To calculate the probability of generating a certain mutant, the two mutations are regarded for simplicity as a single independent mutation. Therefore, the probability for all mutants, that carry either both or none of these mutations, is calculated as though only three mutated positions (410, 459, 551/555) instead of four were existing. The probability  $P_P$  for a clone to carry a given mutation of one clone from a certain *position* is determined by the number of clones used for the shuffling. If  $N$  clones are used the probability is

$$P_P = \frac{1}{N}.$$

The probability  $P_X$  for generating a mutant  $X$  carrying a particular combination of independent mutations at  $M$  positions equals the product of the probabilities of observing each mutation at the given position.

$$P_X = \prod_{P=1}^M P_P$$

Due to the simplification of having only three independent mutated positions,  $M$  equals  $N$ . Therefore, it can be written as

$$P_X \approx \left(\frac{1}{N}\right)^N.$$

Since three independent positions are assumed the expected frequency of observing a certain clone is approximately 1 out of 27 ( $\frac{1}{3} \times \frac{1}{3} \times \frac{1}{3}$ ). The probability for observing a clone showing either of the two dependent mutations is here described as  $\ll 1/27$  for simplicity and because a more sophisticated analysis would provide a result that would require extensive sequencing to be statistically verified. Clones with a probability higher than  $1/27$  result from the fact that they can be theoretically assembled from fragments originating from *two* instead of one initial clone. This is the case for all newly generated clones, which carry wt amino acids in position 1 or 3, or both, since two of the initial clones encode wt at these positions. Accordingly, the probability to obtain the wt aa at these positions would be  $2/3$  instead of  $1/3$ .

After shuffling, the observed frequency of each clone was found to be in good agreement statistical expectations (Table 3). Variations between expected and observed frequency of single clones are likely due to the relatively small number of sequenced clones (43). However, the different groups of mutants with equal probabilities showed a good correlation. The six mutants with an expected frequency of  $2/27$  were observed a total of 11.8 times out of 27 instead of the expected 12, while the three mutants with a probability of  $4/27$  were found 11.3 times instead of 12. Mutants with a probability of  $1/27$  were observed 2 times instead of 3. Interestingly, even two of the highly unlikely mutants carrying either of the two dependent mutations were found (mutant 13 and 14). Even if no statistical test was performed, which would have required extensive and money consuming sequencing, these results suggest that the applied DNA shuffling protocol is suitable to generate recombination mutants. Furthermore, experimental conditions allow shuffling of mutations that are located as close to each other as a 4 aa distance. Due to its simplicity and rapidity, this approach seems to be a better alternative to site-directed mutagenesis for the generation of large numbers of capsid variants with combined mutations.

**Table 3. Expected and observed frequency of all possible mutants generated by DNA shuffling.**

| Mutant | aa position<br>410 | aa position<br>459 | aa position<br>551 | aa position<br>555 | observed<br>frequency in<br>43 sequences | expected<br>frequency in<br>27 sequences | approx.<br>probability<br>$P_{\text{approx.}}$ |
|--------|--------------------|--------------------|--------------------|--------------------|--|--|--|
| 1      | -                  | -                  | -                  | -                  | 4  | 2.5                                      | 4/27   |
| 2      | -                  | R459K              | -                  | -                  | 7  | 4.4                                      | 4/27   |
| 3      | -                  | R459G              | -                  | -                  | 7  | 4.4                                      | 4/27   |
| 4      | T410A              | -                  | -                  | -                  | 6  | 3.8                                      | 2/27   |
| 5      | T410A              | R459G              | -                  | -                  | 1  | 0.6                                      | 2/27   |
| 6      | T410A              | R459K              | -                  | -                  | 4  | 2.5                                      | 2/27   |
| 7      | -                  | -                  | N551D              | E555G              | 2  | 1.2                                      | 2/27   |
| 8      | -                  | R459K              | N551D              | E555G              | 1  | 0.6                                      | 2/27   |
| 9      | -                  | R459G              | N551D              | E555G              | 5  | 3.1                                      | 2/27   |
| 10     | T410A              | -                  | N551D              | E555G              | 1  | 0.6                                      | 1/27   |
| 11     | T410A              | R459K              | N551D              | E555G              | -  | -  | 1/27   |
| 12     | T410A              | R459G              | N551D              | E555G              | 2  | 1.2                                      | 1/27   |
| 13     | -                  | R459K              | -                  | E555G              | 2  | 1.2                                      | $\ll 1/27$                                     |
| 14     | -                  | R459G              | N551D              | -                  | 1  | 0.6                                      | $\ll 1/27$                                     |
| 15     | -                  | -                  | N551D              | -                  | -  | -  | $\ll 1/27$                                     |
| 16     | -                  | -                  | -                  | E555G              | -  | -  | $\ll 1/27$                                     |
| 17     | -                  | R459K              | N551D              | -                  | -  | -  | $\ll 1/27$                                     |
| 18     | T410A              | R459K              | -                  | E555G              | -  | -  | $\ll 1/27$                                     |
| 19     | T410A              | R459K              | N551D              | -                  | -  | -  | $\ll 1/27$                                     |
| 20     | T410A              | R459G              | -                  | E555G              | -  | -  | $\ll 1/27$                                     |
| 21     | T410A              | R459G              | N551D              | -                  | -  | -  | $\ll 1/27$                                     |
| 22     | T410A              | -                  | -                  | E555G              | -  | -  | $\ll 1/27$                                     |
| 23     | T410A              | -                  | N551D              | -                  | -  | -  | $\ll 1/27$                                     |
| 24     | -                  | R459G              | -                  | E555G              | -  | -  | $\ll 1/27$                                     |

Three DNA fragments of the cap gene (wt, T410A/R459G double mutant and R459K/N551D/E555G triple mutant) were shuffled. After cloning of shuffled fragments into pUC-AAV-2, 43 mutants were sequenced. As an approximation for statistical analysis, the crossover probability between distant point mutations ( $\geq 100$  bp/33 aa) was assumed to be 1, allowing a simplified statistical analysis as independent mutations. Accordingly, the probability to incorporate a mutation at a given position by shuffling of three clones is  $P_{\text{Mutation}} = 1/3$ . The crossover probability of the two closely located mutations (N551D/E555G) was assumed to be  $\ll 1$ , requiring statistical treatment as dependent (coupled) mutations ( $P_{\text{coupled}} = 1/3$ ,  $P_{\text{individual}} = \ll 1/3$ ). Therefore, mutants separating these mutations are rarely observed. The probability to carry wt at positions 1 or 3 is  $P_{\text{wt}} = 2/3$  each, since two of the initial clones encode wt aa at these positions. Amino acid (aa) positions are according to VP1 numbering.

### Production of a second-generation library of AAV-2 particles carrying shuffled mutations from previous selections combined with new randomization

Viral DNA collected after the third round of a previous selection (see chapter III) was subjected to DNA shuffling following the above described protocol. Further randomization by error prone PCR was also performed to introduce novel point mutations in the obtained pool (see *Materials and Methods*). This yielded a library of approx.  $4 \times 10^7$  clones. Sequence analysis after packaging showed an average number of 1.7 aa mutations per clone. Since the

pool used for production of the second-generation library contained besides the three strongly selected mutations (R459G, R459K, N551D) only an average number of 0.2 mutations per clone, at least 1.5 mutations per clone had to be newly generated. Including the shuffled mutations (0.5 per clone) the error rate averaged 2.2 mutations per clone. As expected all combinations of the three previously selected mutations were found after sequencing (data not shown). Moreover, the newly generated mutations were randomly distributed throughout the *cap* gene.

### **Real time *evolution monitoring*: improving selection efficacy**

Crucial factors for the success of library-panning experiment are choice and maintenance of an appropriate selective pressure. In order to be able to test in parallel several selection conditions by a money- and time-saving procedure, we set up a method to monitor the evolution of the pool by *light cycler* PCR technology (*evolution monitoring*). This strategy is based on the reasoning that appropriate selection conditions would result in a decrease of viral titer in the first selection rounds due to elimination of strongly neutralized or infection deficient mutants followed by titer recovery during later rounds corresponding to a progressive amplification of the best escaping variants (selection of the fittest virions).

$2 \times 10^9$  genomic particles of the second generation library (MOI=5) were incubated with different concentrations of a neutralizing serum (serum B, see *Materials and Methods*) and viral particles numbers (see below) in three parallel settings (Fig. 3). After each round of selection viral DNA was extracted from a small aliquot of the harvested progeny and the genomic titer was determined. A fourth setting (low selection pressure w/o particle regulation) is not shown, since results were similar to the setting 'high pressure w/o particle regulation'. In the first two settings (blue and red in Fig. 3), a high and a low serum concentration of a serum were applied for three selection rounds. After the first selection cycle, only a maximum number of  $5 \times 10^9$  genomic particles was incubated with a new aliquot of serum and used for the next infection (regulation of genomic particle numbers). In "high pressure" conditions with regulation of genomic particles, titers showed a constant decrease during the experiment. Although the previously described N551D mutant and the R459K/N551D double mutant were enriched and only marginal amounts of wtAAV were detected, no triple or higher mutants were detected. These results suggest that a too strong selective pressure promptly eliminating most of the virions easily neutralized by antibodies, which compose the biggest proportion of the library. However, it also hampered an efficient

amplification of the fitter molecules in the pool. A selection to some extent took place, since the easily neutralized virions were lost more rapidly than the ones with an enhanced immune escape ability, but due to the lack of an amplification effect the procedure failed to identify new interesting variants.

In presence of a low selection pressure combined with the regulation of particle numbers after the first selection cycle, the viral titer showed an initial drop followed by a robust increase after the 3<sup>rd</sup> round, suggesting an enrichment of mutants with improved phenotype. Sequencing of single clones showed a strong selection for a S458P/R459K/N551D triple mutant. Several new strongly selected single mutations (R447S, N449S, P458S, Y500F, A664T) were observed, as well as three other quadruple mutants (S458P/Y500F/N551D/A664T, N551D/E563K/Q575P/A591V and S458P/R459K/H509Q/N551D) and a quintuple mutant (R459K/Y500F/G512D/N551D/A664T).

In another setup, virions were incubated with a “high” serum concentration but without limiting the applied number of genomic particles at every round. In these conditions, a stable and high titer was observed after a slight decrease during cycle 2 and 3. Nevertheless, after five cycles no distinct selection of mutants was observed and wtAAV was enriched in comparison to the initial pool. This failed selection could be a result of an insufficient selection pressure due to high amounts of virions or a lack of genotype-phenotype coupling (see *Discussion*).

Analogous results were obtained with a different human serum (serum A, or in presence of a mix of four different sera (S2, S3, S4 and S5)) (data not shown). In case of serum A, when the amount of virions during the selections was not regulated, the outcome of the selection was unsuccessful for both high and low selection pressure. A selection profile similar to the one described above (high pressure w/o particle regulation) was observed (no distinct selection of mutations; enrichment of wt). However, as in the case described above, particle regulation resulted in a successful selection. In the second case (mixed sera), a progressive loss of viral progeny was observed independently from the level of serum concentration (high or low) or particle regulation, suggesting that the mixture of sera applied too stringent conditions to the selection process. Sequencing confirmed the unsuccessful outcome of the selection.

In summary, isolation of novel mutations and multiple-site mutants always correlated with a clear rescue of titer. These findings validate this method as convenient solution to test different experimental conditions. Restricting sequencing to selections that result in good titer-evolution patterns allows more different experimental settings to be tried for a given budget.



## General characterisation of enhanced capsid mutants

As described in the previous paragraph, we performed a total of twelve selections. Clones were selected from pools that showed a rescue of titer after the 3<sup>rd</sup> selection cycle (serum A, high pressure w particle regulation; serum B, low pressure w particle regulation). The mutants were packaged as GFP-expressing rAAV particles (Table 4) and tested for packaging ability, infectivity and ability to evade neutralisation. Since strongly selected mutations were likely to convey the best immune-escaping effect, only clones were chosen that combined as many of the strongly selected mutations in one mutant as possible. Mutations were considered to be strongly selected, when they were observed in at least 10 % of the clones of a selection. According to the assumption that multiple efficient mutations on one clone should result in a superior phenotype compared to the corresponding single mutants no mutants with less than three strongly selected mutations were tested. Two of the quadruple mutants (N551D/E563K/Q575P/A591V and S458P/R459K/H509Q/N551D) and the quintuple mutant were not pursued since they carried mainly mutations that were weakly selected as single mutations in other clones, thus suggesting a neutral or negative influence. Accordingly, after preliminary tests showed a reduced transduction efficiency for these latter mutants, these clones were not further characterised. New mutations occurring frequently in single mutation clones (e.g R447S and N449S) were not further characterized because of time constraints but could represent interesting alternatives for the generation of immune-escaping clones.

All tested mutants contained the N551D mutation. C1 and C2 were based on the previously selected R459K/N551D double mutant (see Chapter III), which had exhibited the best immune-escape ability and an infectivity superior to wtAAV-2. As expected the occurrence of these two mutations was strongly increased in all successful selections, although slight variations in frequency of occurrence were observed when comparing results obtained with the two sera. In the initial second generation library about 50 % of the sequences contained the N551D mutation, while the R459K mutation was present in only 10 % of all sequences.

**Table 4. Mutants obtained after three rounds of selection in presence of different neutralizing sera**

| Clone | Number of mutations | Mutations                  |
|-------|---------------------|----------------------------|
| C1    | 3                   | S458P, R459K, N551D        |
| C2    | 3                   | R459K, A493T, N551D        |
| C3    | 3                   | R447S, S458P, N551D        |
| C4    | 3                   | N449S, S458P, N551D        |
| C5    | 4                   | S458P, Y500F, N551D, A664T |

The double mutation R459K/N551D was found in 5 % of the sequenced clones. After the new selection rounds, the occurrence of the N551D mutation increased approx. 2 fold to 90-95 %, while the proportion of double mutants was elevated 7-14 fold to 35-70 %, confirming the efficacy of these mutations in conferring immune-escaping ability to the viral capsid. Though not as frequent as the R459K and N551D mutations, the new mutations carried by tested mutants appeared in 10-60 % of the clones in the selection, in which they appeared most frequently (Table 5). It should be noted that clones that contained either a R447S or a N449S mutation in combination with a N551D mutation are likely to be a product of the shuffling procedure since both these new mutations had already been observed in the previous selection, thus demonstrating that successful combination mutants are generated by DNA shuffling.

**Table 5. Observed frequency of strongly selected mutations in the two most successful selections in %.**

|                        | R447S | N449S | S458P | R459K | A493T | Y500F | N551D | A664T |
|------------------------|-------|-------|-------|-------|-------|-------|-------|-------|
| serum A, high pressure | 3 %   | 3 %   | -     | 33 %  | 15 %  | 5 %   | 95 %  | -     |
| serum B, low pressure  | 10 %  | 12 %  | 57 %  | 75 %  | -     | 12 %  | 91 %  | 10 %  |

*Both selections were performed with reduction of particle numbers. At least 40 single clones were sequenced.*

As discussed in chapter III, enhancement of infection efficiency mediated by improved receptor binding ability or post-entry processing is an expected consequence of the screening procedure, because it would confer, independently from the ability to escape neutralization, an additional selection advantage by favouring amplification of such clones. Accordingly, genomic titers of all tested mutants were comparable to wtAAV-2 (Table 6). The infectious titers of the mutants C1, C2, C4 and C5 were higher than of wtAAV-2. However, while the ratio between infectious and genomic particles (which for simplicity we define here as “infectivity”) of C3 and C4 was slightly reduced or equal in comparison to wt AAV-2, the ratio was increased approx. 3-fold for C1 and C5, while C2 mutant was about 1.3 fold more infectious. The previously studied R459K/N551D double mutant also exhibited a 1.7-fold increased infectivity in comparison to wt. This calculates to a 1.8-fold increase of C1 and C5 in comparison to the double mutant. In case of C1 (S458P/R459K/N551D) the mutation responsible is the S458P mutation, while the C5 quadruple mutant (S458P/Y500F/N551D/A664T) has three new mutations (S458P, Y500F and A664T) compared to the double mutant, thus allowing no distinction between single or cumulative effects. The C2 mutant differs from the double mutant in one additional mutation (A493T), accordingly being responsible for the slight drop of infectivity from 1.7-fold to 1.3-fold.

**Table 6. Viral titers per  $\mu$ l of GFP-expressing rAAV-2 selected mutants**

| Clone                 | Genomic titer     | Infectious titer  | Particle titer     | Ratio genomic to infectious titer | n-fold infectivity compared to wt |
|-----------------------|-------------------|-------------------|--------------------|-----------------------------------|-----------------------------------|
| wt                    | $1.2 \times 10^8$ | $5.9 \times 10^5$ | $1.5 \times 10^9$  | 203                               | 1                                 |
| Double mutant         | $2.3 \times 10^8$ | $1.9 \times 10^6$ | $1.4 \times 10^9$  | 121                               | 1.7                               |
| C1                    | $1.6 \times 10^8$ | $2.4 \times 10^6$ | $1.5 \times 10^9$  | 67                                | 3.0                               |
| C2                    | $2.2 \times 10^8$ | $1.4 \times 10^6$ | $1.45 \times 10^8$ | 156                               | 1.3                               |
| C3                    | $2.1 \times 10^8$ | $5.1 \times 10^5$ | n.d.               | 408                               | 0.5                               |
| C4                    | $2.1 \times 10^8$ | $1.1 \times 10^6$ | n.d.               | 198                               | 1                                 |
| C5                    | $1 \times 10^8$   | $1.5 \times 10^6$ | n.d.               | 67                                | 3.0                               |
| AAV-2 empty particles | –                 | –                 | $1.25 \times 10^9$ | –                                 | –                                 |

In the mutant C3 the R447S seems to be responsible for the slight decrease in infectivity, while the N449S mutation does not influence infectivity. Since C2 was strongly selected despite the drop in infectivity this disadvantage should be compensated by better immune-evading properties which was in fact the case (see below).

Interestingly, only one of the newly identified mutations conveys a remarkable change in local pKa on the capsid surface. In the R477S mutation a large and highly basic arginine (positively charged) is replaced by a polar serine (neutral) with a 50 % reduced *van der Waals* volume. As in case of the R459K and N551D mutations, this would correspond to a loss of positive charge at the side of the threefold peak. All other mutations cause no local charge shifts. However, the S458P and A493T mutations lead to an increase of *van der Waals* volume of approx. 25 % and 40 % respectively. The Y500F mutation does not modify the volume, but like all mutations mentioned above it induces a local change in hydrophilicity which could result in a rearrangement of aa in this area. The hydrophilic S459 and Y500 are exchanged for a hydrophobic P and F respectively, while A493 (hydrophobic) is changed to T (hydrophilic). The N479S mutation results in a slight loss of hydrophilicity and *van der Waals* volume (20 %). Besides a local influence on the contact area involved in the interaction with receptors or antibodies, these changes could lead to more general structural rearrangements of the capsid and therefore to modification of antibody binding sites located elsewhere. Moreover, an amino acid with unique characteristics as proline could influence secondary, tertiary and quaternary structure by introducing kinks in the protein structure.

As already observed in chapter III strongly selected mutations are located at the surface of the capsid. This was expected since surface exposed amino acids are more likely to tolerate mutations and are directly responsible for any kind of interactions with their environment like receptors or antibodies. As seen in Figure 4A and B, mapping of the mutated amino acids on tested mutants showed a clustering of the strongly selected new mutations (R447S, N449S, S458P, A493T, Y500F) at the base of the large peaks of the three-fold symmetry axis.

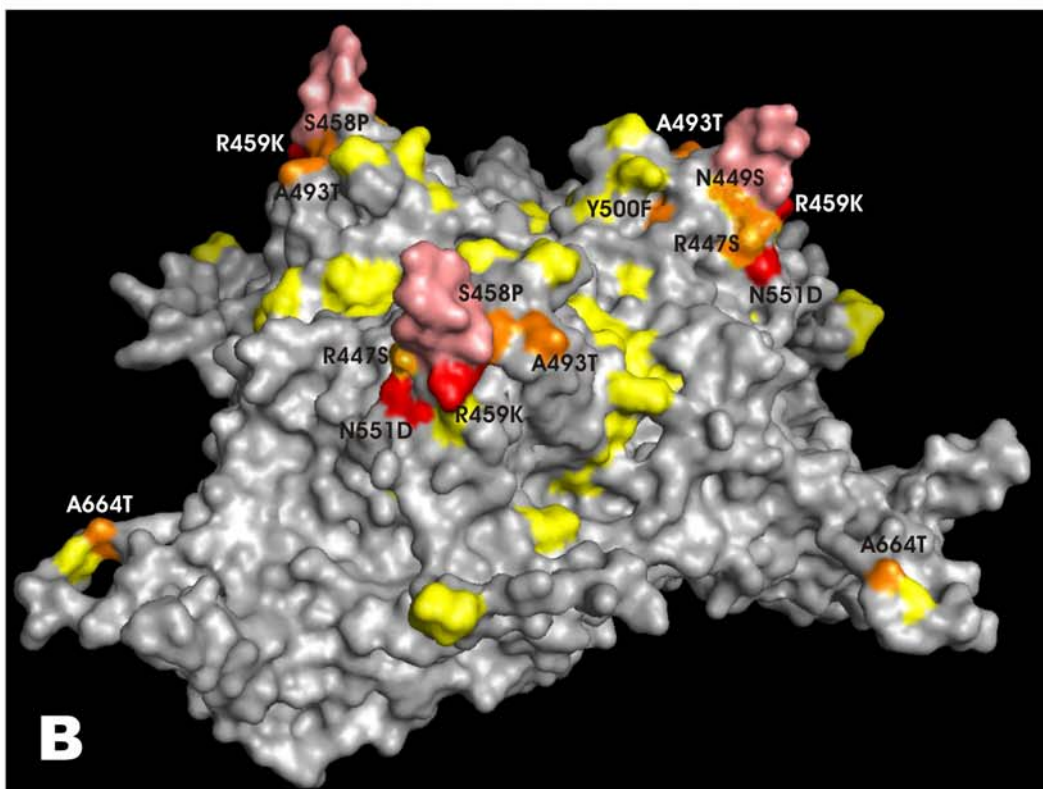
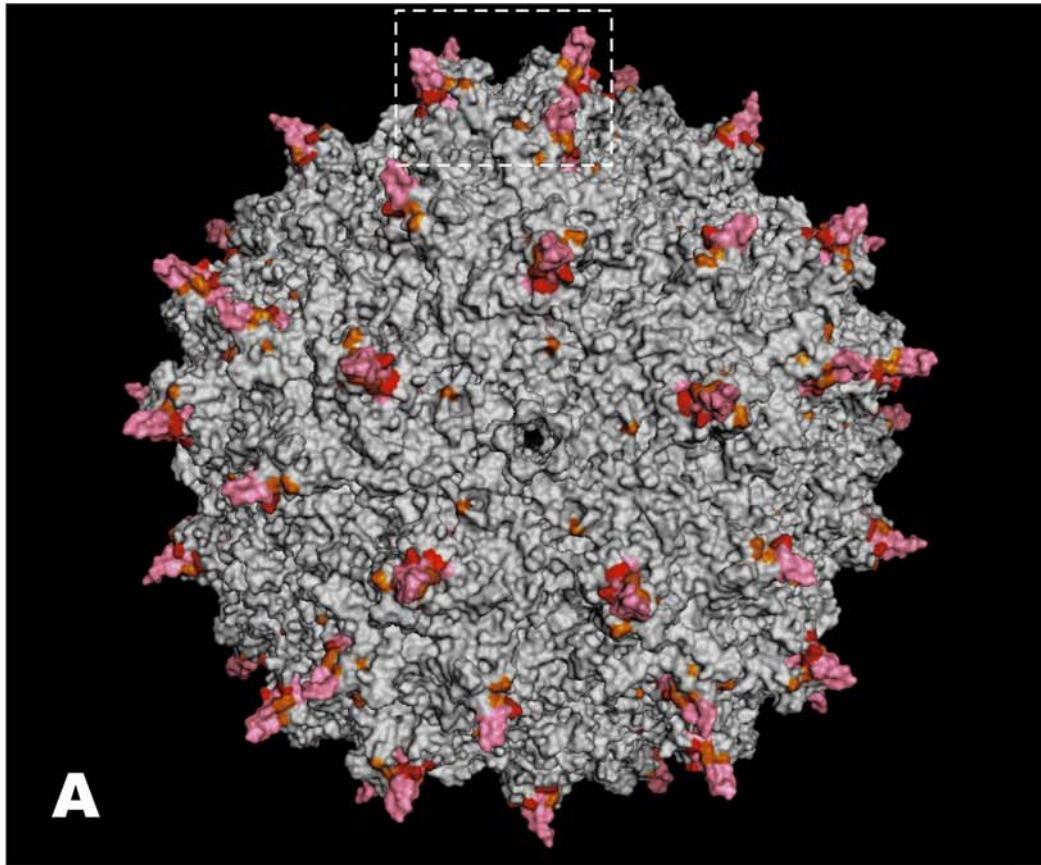


**Figure 4. Mapping of mutations found after the selections on the 3D structural model of the viral capsid.** (A) Mapping of strongly selected mutations on a 3D structural model of the AAV capsid. Mutations observed in more than 10 % of the clones are depicted in orange. The previously selected R459K and N551D mutations are coloured in red. To facilitate visualization, the protruding spikes are coloured in pink. (B) The pictures show a magnified view of the three-fold symmetry axis composed of three viral capsid subunits. In addition to strongly selected mutations (orange and red) mutations that appeared in less than 10 % of the clones were depicted in yellow. (C) Mapping of strongly selected second- (orange) and first-generation mutations (red) on the amino acid sequence. Numbering is according to VP1.

As sole exception, the strongly selected A664T mutation was not located at the peak of the three-fold axis but instead close to the five-fold axis. Looking towards the three-fold axis, the newly selected S458P and A493T mutations are located close to each other at the right side of the peaks (looking towards the threefold axis), while the R447S and N449S mutations are found adjacent to each other on the left side. In contrast to the second-generation mutations, previously selected mutations R459K and N551D locate at the back of the peak, facing away from the three-fold axis. Strikingly, the distance of the mutations on the protein sequence is not necessarily mirrored by their position on the 3D-structure. Although being separated in the primary structure by a distance of 34 and 104 amino acids respectively (Figure 4C), the mapping of S458 and A493 as well as R447 and N551 on the three dimensional structure reveal a proximity of approx. 5 and 4 Ångström (Å) respectively between functional groups. Similarly, despite the distance of 91 amino acids in the primary structure between the previously studied R459 and N551 functional groups are approximately 7 Å apart. Finally, the distance between neighbouring side chains of S458 and the R459 as well as R447 and N449 are of approximately 2.5 Å. This clustering around the base of the peaks strengthens the hypothesis, discussed in chapter III, of this being a highly immunogenic region.

### **Characterisation of immune-evading abilities of enhanced mutants**

To evaluate antibody-evading abilities of the selected mutants, equal genomic titers were used to infect HeLa cells in the presence of serial dilutions of different neutralizing human sera. The mutants were tested on sera different from those used during the selection procedure in order to test if immune-escaping ability was rather a serum-specific (patient-specific) or a universal characteristic. In order to exclude the influence of particle titers on the effective antibody concentration, the total number of viral particles was normalized by addition of AAV-2 empty capsids. A preliminary test of all packaged mutants was conducted using the previously described mixed serum in order to select the best mutants for further evaluation (data not shown).

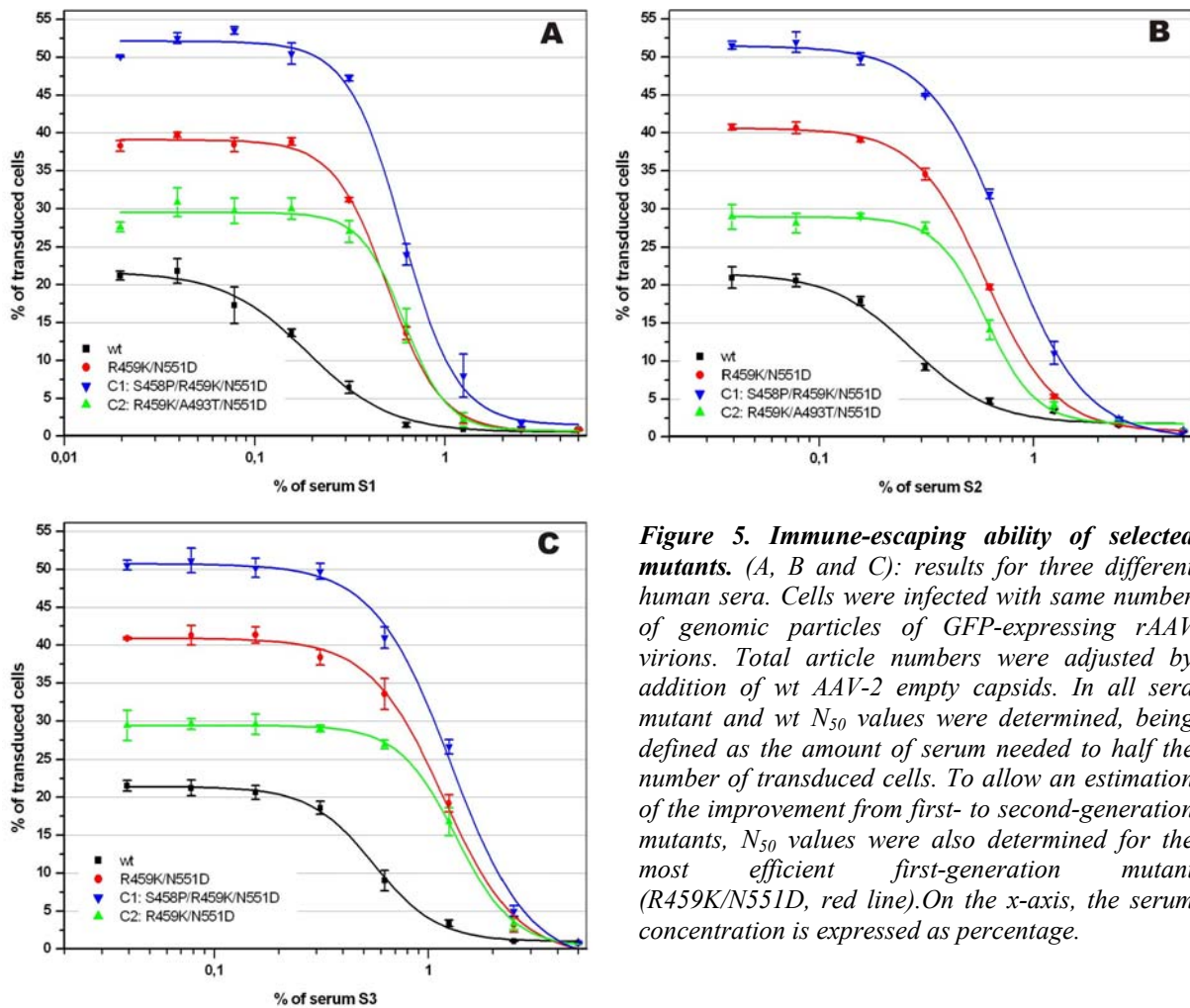


**Figure 5. Immune-escaping ability of selected mutants.** (A, B and C): results for three different human sera. Cells were infected with same number of genomic particles of GFP-expressing rAAV virions. Total article numbers were adjusted by addition of wt AAV-2 empty capsids. In all sera mutant and wt  $N_{50}$  values were determined, being defined as the amount of serum needed to half the number of transduced cells. To allow an estimation of the improvement from first- to second-generation mutants,  $N_{50}$  values were also determined for the most efficient first-generation mutant (R459K/N551D, red line). On the x-axis, the serum concentration is expressed as percentage.

As indicated by the genomic-to-infectious titer ratio, differences in infectivity were observed in the neutralisation assays, when equal genomic particles were applied. To allow quantification of immune-evading ability independently from differences in infectivity of tested mutants, the amount of serum needed to half the number of transduced cells was defined as  $N_{50}$ . Values were determined using Figure 5. The best results were obtained by mutants C1 and C2, which were therefore used for additional testing on three single test sera (S1-S3) in parallel with the R459K/N551D double mutant to estimate the improvement of newly selected mutants to the first-generation mutant.  $N_{50}$  values of the new mutants, the R459K/N551D double mutant and wt were determined using Figure 6. To allow quantification of the immune-evading properties of the mutants the ratio of mutant to wt  $N_{50}$  was calculated (Fig. 6A). Compared to wt, the mutant C1 (S458P/R459K/N551D) in presence of S1, S2 and S3 required a 3.7-, 3- and 2.3-fold respectively higher serum concentration to halve the number of transduced cells. The C2 mutant (R459K/A493T/N551D) showed an

improvement of 3.4-, 2.8- and 2.6-fold. In contrast, the double mutant yielded slightly lower values of 2.7-, 2.4- and 2-fold of wt- $N_{50}$ . In S1 and S2 the C1 mutant was the most successful, while C2 showed the highest value in S3. As expected, the immune-escaping abilities varied in the different sera. All mutants showed the strongest phenotype in S1 and the weakest in S3. A direct comparison of the immune escape abilities of the new second-generation mutants compared to the first-generation double mutant revealed an enhanced phenotype in all tested sera, although the increase varied between 15 and 37 %.(Fig. 6B). This was expected, since antibodies composition of different sera is likely to differ for ability to recognize the different capsid epitopes.

In summary, this data demonstrate that generation of viral mutants with immune-escaping properties can be achieved by successive re-iteration of a directed evolution procedure based on *error prone* PCR, DNA shuffling and *evolution monitoring*.

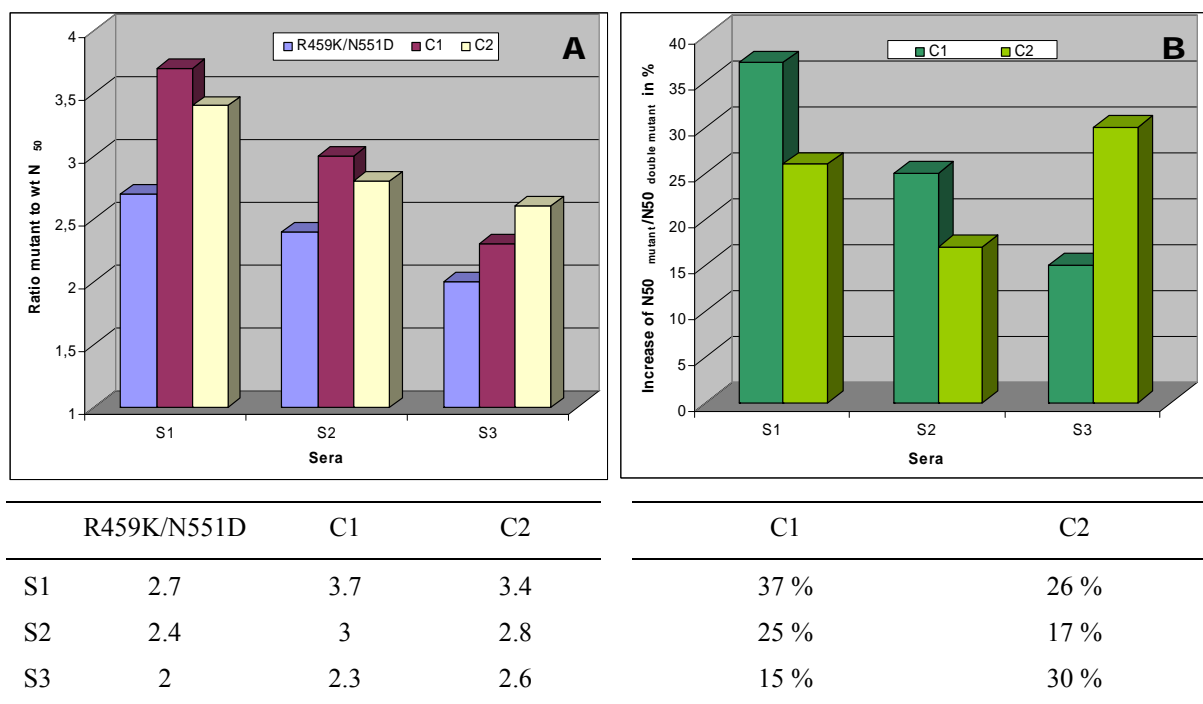


**Figure 6. Immune-escaping properties of newly selected mutants and the R459K/N551D double mutant.** (A) Immune-evading abilities of the mutants in the three test sera were quantified by comparison of mutant and wt  $N_{50}$  values obtained from Fig. 5. (B) Improvement of the immune-escaping properties of newly selected mutants compared to the R459K/N551D double mutant in %. Shown results are summarized in the table below.

## Discussion

As described in chapter III, a directed evolution approach could be successfully applied to the problem of antibody-mediated neutralization of AAV vectors. Obtained results suggested the possibility to obtain further enhanced mutants by additional directed evolution. The resulting accumulation of multiple effective mutations on the capsid should confer a better ability to evade neutralizing antibodies. Accordingly, we introduced DNA shuffling for the creation of a large second-generation library ( $\sim 4 \times 10^7$  clones).

A pilot experiment allowed setup of a DNA shuffling procedure for *error prone* PCR-generated AAV libraries. In this setup, three single clones carrying a total of 5 mutations were shuffled, which should have resulted in 24 combination mutants of the 5 point mutations. Considering that for more complex pools carrying a higher number of mutations, the number of possible combinations is accordingly higher, it becomes clear that DNA shuffling is an elegant alternative to labour intensive site directed mutagenesis.

Although DNA shuffling can be used to generate new point mutations during recombination, a high fidelity protocol was used in order to allow a methodical separation between recombination and randomization (Stemmer, 1994; Zhao and Arnold, 1997). After limited sequence analysis of obtained mutants, 13 of the possible 24 clones were found. Even the clones with a statistical expectation of only 1/27 were found with one single exception which is likely due to the low number of sequenced clones (43). All other missing clones had a statistically expected frequency of significantly less than 1 in 27 clones due to the close proximity (only 4 aa) between mutations N551D and E555G which reduces the probability of a crossover event to occur between the two sites. Interestingly, two of these clones were actually observed, suggesting that missing clones could indeed have been generated although not all found. The observation that all groups of clones with an equal expected frequency showed a good correlation between expected and observed occurrence is also a good indication for successful shuffling, while the weak correlation found for individual mutants is likely to be a consequence of the small number of sequenced clones.

After establishment, DNA shuffling was applied to the entire pool of virions generated after 3 rounds of a previous selection using a neutralizing human serum (see chapter III), although only three mutations R459G, R459K and N551D had been strongly selected. This is based on the rationale that combinations of weakly selected mutations alone or together with strongly selected mutations might also confer a positive effect. As expected all combinations of the three frequent mutations were observed in the second-generation library. In general, libraries

with a mutational rate between one and two mutations per clone have been shown to yield best selection results (Moore *et al.*, 1997). However, since the shuffled pool contained only an average of 0.5 mutations per clone, new mutations were introduced by *error prone* PCR. The obtained rate of 1.7 new aa exchanges per clone found in the resulting library of  $4 \times 10^7$  clones were well within the desired range.

*Evolution monitoring* has been introduced as an efficient tool to improve the efficacy of selections. Success of a selection is strongly dependent on the choice of an appropriate selective pressure. This is in turn dictated by the complex requirements that a mutant has to meet in order to be successfully selected against other variants (in our case ability to escape neutralization, infectivity, efficient replication and packaging).

The fact that only selections with regulation of particle numbers were successful showed that the effective selection pressure was dependent not only on the amount of serum but on the number of free virions, as well. Since the amount of serum was held constant, it can be speculated that variations in the ratio between virions and antibodies mediates a direct effect on the selection pressure because high numbers of virions reduce the selective pressure by sequestering binding antibodies. In addition, higher numbers of virions would result in multiple infections of single cells by different mutants. Subsequent capsid assembly and DNA packaging would generate chimeric virions, in which no correspondence between genotype and phenotype is given (uncoupling). In this case no efficient selection could take place in the next round. The sequencing profile after the reduction of total genomic particles to  $5 \times 10^9$  during the selection did not show stop codons. This suggests a MOI after incubation with neutralizing sera of below 1 (less than one mutant genome per cell) since only in this case an efficient genotype-phenotype coupling takes place. As a result each mutant genome is packaged in the capsid, which it encodes. Accordingly, mutants carrying stop codons could not be packaged due to their inability to allow production of complete capsid proteins. On the contrary, a high frequency of stop codons as found without reduction of particle numbers (data not shown) is a good indicator for a lack of genotype-phenotype coupling caused by a MOI of significantly above 1.

Therefore, the selective pressure is the result of a complex mixture of experimental conditions and the optimal setup for any given goal has to be determined by trial-and-error experiments followed by sequencing of high numbers of clones. This problem was addressed by *evolution monitoring*. During the whole panning procedure, reliable indication about the progress of the selection can be obtained by titrating of the viral pool after each screening round and selection pressure and/or particle numbers can be adjusted accordingly. Selections for which a strong

rescue of titer is observed have been shown to correlate with a successful outcome. Restricting sequencing to experiments where viral titer is rescued after an initial drop allowed to test a larger number of experimental conditions, reducing experimental times and costs at the same time.

Screening of the second-generation AAV library for efficient gene delivery in the presence of two different neutralizing human sera allowed the selection of several successful variants, the majority of which were based on the previously studied R459K/N551D double mutant. An alignment of different AAV serotypes disclosed a preferential location of the strongly selected mutations in capsid regions that are either highly variable (S458, R459, A493) or at least only moderately conserved between serotypes (N449, Y500, N551) (Fig. 7). The R447S mutation could be considered an exception, since the R is conserved in 7 out of 9 shown serotypes. However, an S is found in the other two serotypes, which could explain the tolerance and the relatively moderate drop of infectivity to 50 % of wt.

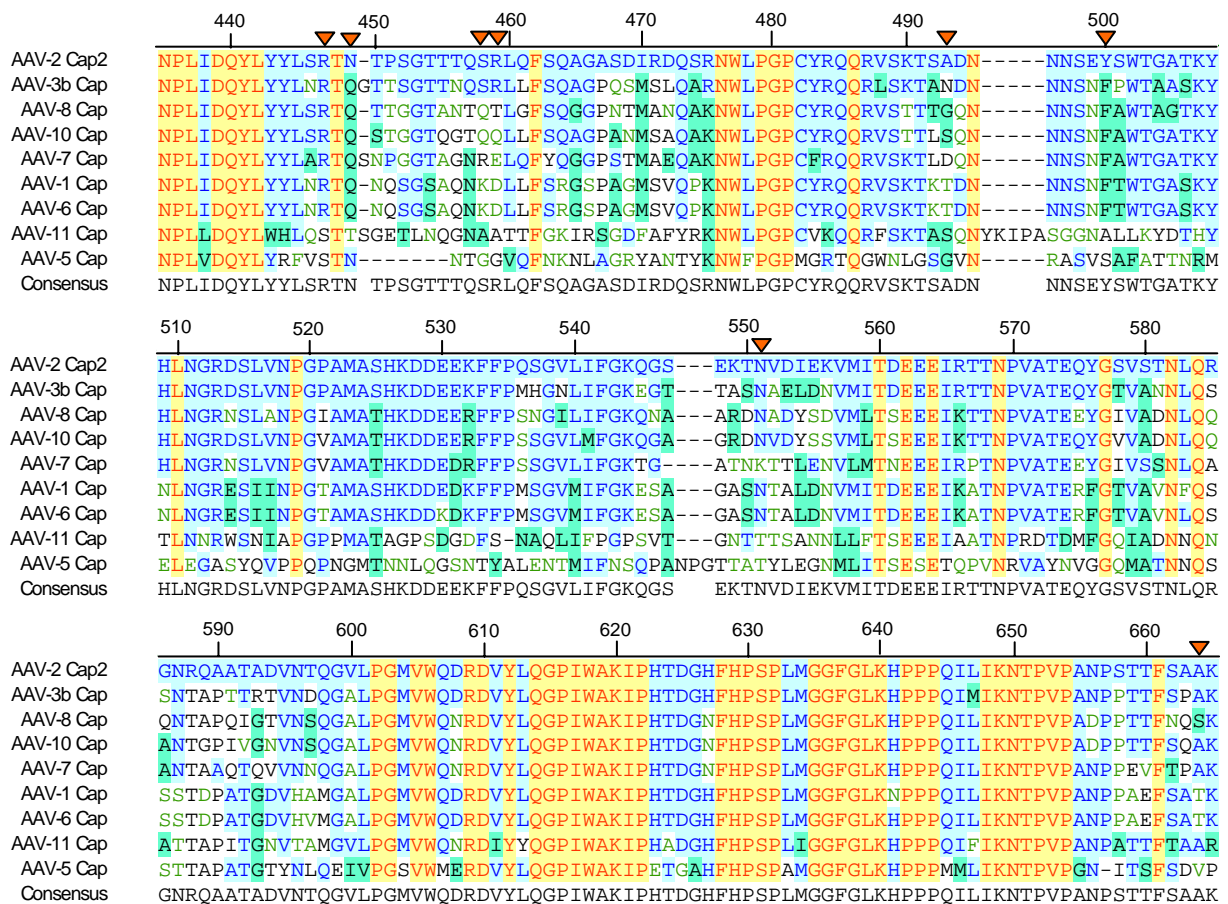


**Figure 7. Alignment of different AAV serotypes.** In the shown part all positions mentioned in the text are marked by triangles (orange). To simplify comparison with the text, the numbering is according to VP1 in AAV-2 (upper row).

Interestingly, with exception of the Y500F mutation, which is located on the peak facing towards the axis, all strongly selected mutations are positioned outside of the threefold crater. This might be due to a preferential location of immunogenic epitopes on the outside of the 3-fold crater because of a higher accessibility. Another possible reason could be due to the importance of the crater for the infectious process (Kern *et al.*, 2003, Opie *et al.*, 2003). Mutations in this area are therefore more likely to negatively influence the infectivity. The observed exception could result from the fact that the newly generated F is conserved in six of the nine serotypes in the alignment (AAV-3, AAV-1, AAV-6, AAV-7, AAV-8 and AAV-10), while the Y is unique for AAV-2, which might explain the tolerance for this aa. Accordingly, the Y500F mutation could correspond to a local reversion of the evolutionary diversification of AAV-2 from other serotypes. An analogous example of a reversion, although observed only once, is provided by a R475K mutation. The R is only found in serotypes 2 and 3, while all other serotypes in the alignment show a K at this position. The new amino acids P (S458P), K (R459K) and D (N551D) were not observed in other serotypes, but it should be noted that a number of new AAV serotypes have been recently discovered, suggesting that more might exist. Strikingly, the new amino acids of half of the strongly selected mutations (R447S, A493T, Y500F, A664T) are found in other serotypes. When using a directed evolution approach the selected aa should constitute the best compromise regarding tolerance and immune-escaping effect. Since a significantly large proportion of strongly selected aa are found in other serotypes, this suggests that AAV might have evolved in a variety of serotypes to circumvent the host immune system. In this regard it is conceivable that beside the generation of useful gene therapy vectors, *error prone* PCR libraries could help scientists to backtrack natural evolution of viral families.

Two of the tested mutants carried additionally an S458P mutation (clone C1) and an A493T mutation (clone C2) and showed enhanced immune-evading abilities in comparison to the double mutant. This strengthens the hypothesis that improved phenotypes can be generated by accumulation of multiple beneficial mutations on one clone. Clones were tested on three human sera that had not been used during the selections in order to assess if immune-escaping phenotype was serum specific or rather an universal characteristic. Our results partially suggest the second hypothesis, since a certain degree of immune escape could be observed for all mutants in the tested sera. However, the effect of a given mutant varied quantitatively for each serum, probably because of recognition of different epitopes by antibodies contained in different sera. These differences could also explain the selection of new mutations which did not yield particularly strong immune-escaping properties when tested on sera different from

those used for the selections (e.g. R447S and N449S). Accordingly it is possible that, although tests on three sera showed a better effect for clones C1 and C2, clones carrying the other four strongly selected mutations R447S, N449S, Y500F and A664T might be more effective on other sera. Interestingly in this respect, all mutations carried by clones C1 and C2 except for the A493T mutation are not found in any analyzed AAV serotype (1, 2, 3, 5, 6, 7, 8, 10 and 11), while three of the four mutations present in the less successful clones (R447S, N449S, Y500F and A664T) appear in other serotypes with N449S as sole exception. Since patients might not only be seropositive for AAV-2 but also for other serotypes in parallel, it can be speculated that the widest immune-escape phenotype might be conveyed by mutations that are not present in other common serotypes. However, demonstration of this hypothesis requires further investigation.

In addition to immune escape, selected mutations affected other biological characteristics of the virions. The double mutant, C1 and C2 showed a better infectivity than wtAAV (1.7-fold, 1.3-fold and 3-fold respectively). These data suggests that this directed evolution approach may also be used to optimize vectors in respect to infectivity. Improvement of infectivity of the double mutant has also been observed in preliminary *in vivo* experiments conducted by our collaborators at the University College of London, UK (A. Nathwani, personal communication). The double mutant was able to express significantly enhanced levels of factor IX after systemic injection in mice (n = 3) in comparison to wt AAV-2. Similarly, other groups have also observed significant improvement of infectivity mediated by single point mutations (Lochrie *et al.*, 2006; Opie *et al.*, 2003, Maheshri *et al.*, 2006), although *in vitro* and *in vivo* data did not always correlate (Lochrie *et al.*, 2006).

In a rational design approach, Lochrie and coworkers (Lochrie *et al.*, 2006) generated over 120 point mutants at different surface exposed positions and tested them for infectivity and immune-escaping abilities. Interestingly, more than 60 % of the mutants lead to a severely reduced transduction efficiency, showing that introduction of new mutations in the capsid structure is likely to negatively interfere with biological function. In addition, not only the mutated position but also the nature of the substituted amino acid is crucial for the phenotype. Accordingly, Lochrie *et al.* observed a 50-fold drop in infectivity in case of a A493R mutation generated by site directed mutagenesis, while the here reported A493T mutation shows only a reduction by 25 %. These issues complicate the process of capsid optimization by site directed mutagenesis. Evolutionary approaches circumvent this obstacle because deleterious mutations are automatically sorted out from the pool, while the best suited amino acids are selected.

In addition, combinatorial technology can be exploited to gain information about structural or biologically important regions of the capsid. A mapping of all mutations found after the selection did not show the random distribution featured by the library but rather a distinct pattern in which some areas were devoid of mutations (Fig 8A). Two explanations might account for that finding. First, it is possible that the mapping reflects the location of immunogenic regions. However, this is more likely to be the case for the strongly selected mutations, while a weak selection could just reflect tolerance to a neutral amino acid change in a specific position. Some areas, on the other hand, are functionally crucial for structure or infection biology and are therefore less likely to tolerate mutations. In this case, mapping all observed mutations should allow an indirect identification of those important regions. This hypothesis is supported by comparison of the mapping of all selected mutations with the location of transduction-abolishing mutations found by Opie *et al.* (2003) and Lochrie *et al.* (2006) (Fig. 8B). Transduction-abolishing mutations found by Opie *et al.* and Lochrie *et al.* are shown in red and constitute an area of the capsid which Lochrie and colleagues defined as the “dead zone”: mutations of these residues led in their study to dramatic loss in infectivity. Strikingly, nearly all 30 surface-exposed mutations found after selections in our approach (depicted in yellow) mapped in an area surrounded by the dead zone, while only two of these (depicted in orange) overlapped with “dead zone” residues.

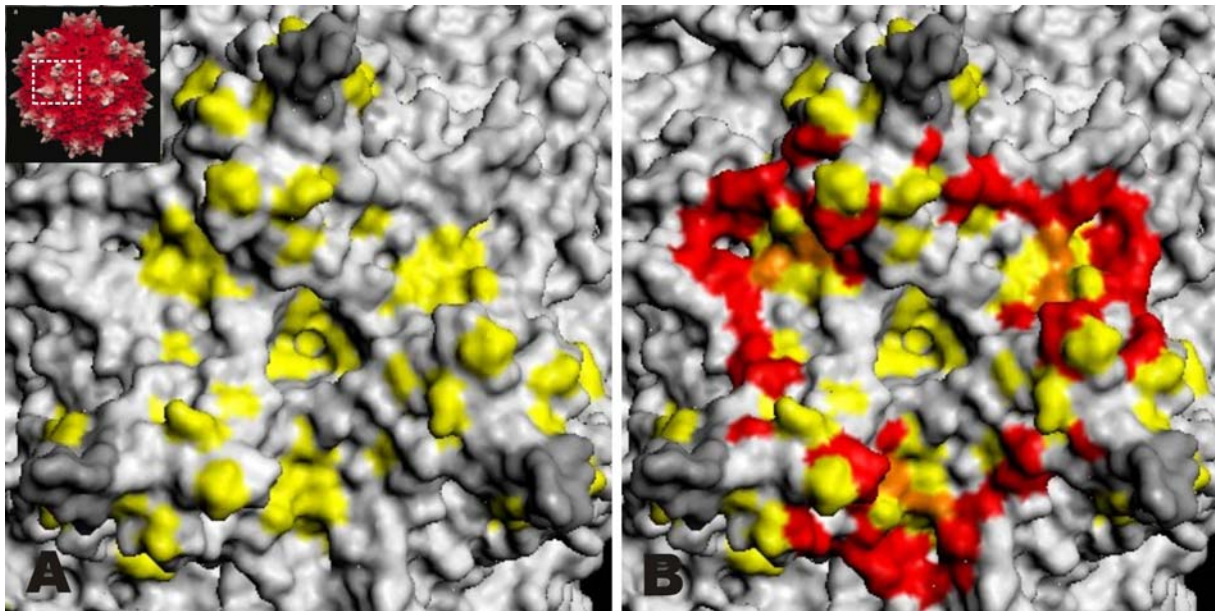


**Figure 8. Mapping of tolerated and transduction-abolishing mutations.** (A) Mapping of all surface-exposed mutations (yellow) found after the selections in the area of the 3-fold axis. (B) Additional co-mapping of transduction-abolishing point mutations found by Opie *et al.* (2003) and Lochrie *et al.* (2006) (depicted in red). The mutated positions include the binding motif for AAV's primary receptor HSPG and the area proposed to be involved in secondary receptor interaction. In the positions depicted in orange mutations were observed after the selection, although positions were reported to be intolerant of mutations.

This observation suggests the potential of combinatorial technology as tool to investigate capsid function. In addition, it should be noted that in the case of the overlapping positions, the amino acid introduced by mutagenesis was different in this case than in the study by Lochrie and coworkers, demonstrating once more the importance of the amino acid nature for the phenotype and suggesting that a combinatorial approach is a more powerful tool for the study of capsid biology by reverse genetics. These data suggest a yet unknown biological importance for the amino-acids located directly in the 3-fold crater around the symmetry axis, where no mutations were found after the selection procedure.

Like the mutations of the double mutant, both new mutations are located at the base of the threefold peak. The preferred localisation of all strongly selected mutations around the sides of the threefold peak supports previous findings identifying it as immunogenic region (Moskalenko *et al.*, 2000; Huttner *et al.*, 2003; Lochrie *et al.*, 2006). Although all mutants were less efficiently neutralized by test sera than the wt, stronger influences of point mutations on immune evasion have been reported (Lochrie *et al.*, 2006 and Maheshri *et al.*, 2006). However, the differences could be due to the different experimental settings applied to characterize the mutants. First of all in both studies different cell lines were used to test immune-evasion. In addition, Lochrie and coworkers used a  $\beta$ -Galactosidase readout system to quantify the immune-escaping effect by visual determination of positive cells in small areas of the sample and also applied transduction-enhancing agents such as ectoposide or adenovirus co-infection. In this regard the use of FACS analysis should allow a more unbiased evaluation. Moreover, the influence of transduction-enhancing agents is difficult to assess. Maheshri and coworkers, on the other hand, did not use human sera but instead serum obtained from an AAV-2 immunized rabbit. It is possible that human sera contained antibodies against several AAV serotypes that conferred resistance against a wider spectrum of capsid variants. For example, mutations that were selected in our experiments like R447S, A493T, Y500F and A664T are present in other serotypes and might not be effective in a serum containing Ab against these serotypes. In this case more or different mutations might be needed to achieve a stronger immune-escaping phenotype. These aspects are currently under investigation and further selection protocols are being performed to identify more beneficial mutations.

A library of  $10^7$  clones and an average mutation rate of only 1.7 aa per clone is unlikely to contain mutants with multiple effective mutations at the needed positions. Therefore, further evolved libraries would be needed to achieve better results on pooled sera. As starting point efficient mutations on various epitopes could be selected by screening a first-generation

library on a larger number of different sera in parallel. After shuffling, a second-generation library could be selected on pooled human sera. This step-by-step process should lead to the generation of a pool of mutants, which allow efficient gene therapy for a major proportion of patients with pre-existing immunity.

It is important to observe that mutants with improved infectivity were selected, demonstrating the potential of this approach for the generation of capsid variants with enhanced transduction efficiency of problematic cells, such as stem cells resistant to all tested AAV serotypes (Smith-Arica *et al.*, 2003; Hughes *et al.*, 2002).

In summary, these data demonstrate that directed evolution methods employing *error prone* PCR, DNA shuffling, *evolution monitoring* are applicable to AAV for the generation of engineered capsid variants with tailored phenotype. In addition we could show the potential of this technology as reverse-genetics tool to investigate capsid biology. We speculate that similar techniques can be applied to viral systems different than AAV.

## Chapter V

# HSPG Binding Properties of Adeno-Associated Virus (AAV) Retargeting Mutants and their Consequence for *in vivo* Tropism

In press in *Journal of Virology* as:

Perabo L and Goldnau D and White K and Endell J, Humme S, Work L, Janiki H, Hallek M, Baker A, and Büning H.

## Abstract

AAV-2 targeting vectors have been generated by insertion of ligand peptides into the viral capsid at amino acid position 587. This procedure ablates binding of heparan sulphate proteoglycan (HSPG), AAV-2s' primary receptor, in some, but not all mutants. Using an AAV-2 Display library, we investigated molecular mechanisms responsible for this phenotype, demonstrating that peptides containing a net negative charge are prone to confer a HSPG non-binding phenotype. Interestingly, *in vivo* studies correlated the inability to bind to HSPG with liver and spleen detargeting in mice after systemic application, suggesting several strategies to improve efficiency of AAV-2 re-targeting to alternative tissues.

## Results and Discussion

AAV-2 is gaining increasing attention as gene therapy vector. However, the wide distribution of its primary receptor, HSPG (Summerford and Samulski, 1998), hampers selective transduction of target tissue. Vectors aiming to re-direct AAV-2s' tropism have been generated by insertion of ligands at position 587/588 of the capsid (Büning *et al.*, 2003a; Büning *et al.*, 2003b). This is likely to interfere with the HSPG binding of at least two (R585 and R588) of the five positively charged amino acids of the recently identified HSPG binding motif (Kern *et al.*, 2003; Opie *et al.*, 2003), explaining the ablation of HSPG binding of some targeting vectors (Girod *et al.*, 1999; Grifman *et al.*, 2001; Nicklin *et al.*, 2001; Perabo *et al.*, 2003; Ried *et al.*, 2002). In some cases, however, binding was only partially affected (White *et al.*, 2004), or even restored (Grifman *et al.*, 2001; Perabo *et al.*, 2003; Work *et al.*, 2004). To investigate molecular mechanisms responsible for these differences, we applied a previously described library of AAV capsids carrying insertions of 7 randomized amino acids at position 587 (Perabo *et al.*, 2003) to a heparin affinity column (Work *et al.*, in press) to separate binding from non-binding mutants. We sequenced and statistically analyzed (Table 1) at least 80 clones from: 1) the original DNA-library, 2) the viral AAV-Display-library, 3) the flow-through fraction (non-binders = NB-AAV-pool) and 4) the 1M NaCl eluted fraction (binders = B-AAV-pool).

The DNA-library showed a higher than expected presence of alanines which originates from the oligonucleotides synthesis procedure. Occurrence of every other amino acid met statistical expectations for an unselected library.

The AAV-Display-library showed an excess of the amino acids P, G and A and a defect of C, L, F, W and Y (Table 1B). Since P, G and A are three of the four smallest amino acids, whereas F, Y and W are three of the four biggest, this bias suggests that the packaging process selects against bulky inserts which would introduce dramatic structural rearrangements and have a deleterious effect on capsid structure. In addition, prolines could favour spatial accommodation of the peptide by introducing kinks and reducing its bulkiness.

The B-AAV-pool showed a significant increase of arginine residues (Figure 1B). Strikingly, arginines were particularly frequent at the 7<sup>th</sup> position of the peptide (30%). In contrast, in the AAV-Display-library and the NB-AAV-pool, the frequency of arginine at this position (15% and 9% respectively) was equal or lower than the expectation for a randomized distribution among the seven amino acid positions (14.3%).

| A | B-AAV-pool | net charge | NB-AAV-pool | net charge |
|---|------------|------------|-------------|------------|
|   | DRDRPQR    | +          | ADRQEAN     | -          |
|   | KSSDLSR    | +          | ADSDHSS     | -          |
|   | HPSGVGK    | +          | ASLSHDD     | -          |
|   | SGVEGGR    |            | GSGTTQA     |            |
|   | KKPSGAV    | +          | DRAYGEQ     | -          |
|   | PPKVAQT    | +          | DSQGEAE     | -          |
|   | SPRSDRP    | +          | EALSTRD     | -          |
|   | ARDPGKA    | +          | EPTGSDL     | -          |
|   | SSRATAD    |            | GASSVSG     |            |
|   | AGRITIE    |            | GLDQGEEQ    | -          |
|   | VKSRDQQ    | +          | GPGATST     |            |
|   | CDQRDRC    |            | HTTSAAS     | (+)        |
|   | APEARLS    |            | DHDDPEW     | -          |
|   | NSATGSK    | +          | NTAGANA     |            |
|   | PNPAAVH    | (+)        | QDPTPPA     | -          |
|   | ASLGGRP    | +          | SNADKVS     |            |
|   | DRATPTR    | +          | TEDESPD     | -          |
|   | ALTGAPG    |            | TERPGAD     | -          |
|   | ASQQHAH    | +          | TTPSPA      | (+)        |
|   | RVDPEAK    |            | VGSDPSV     | -          |

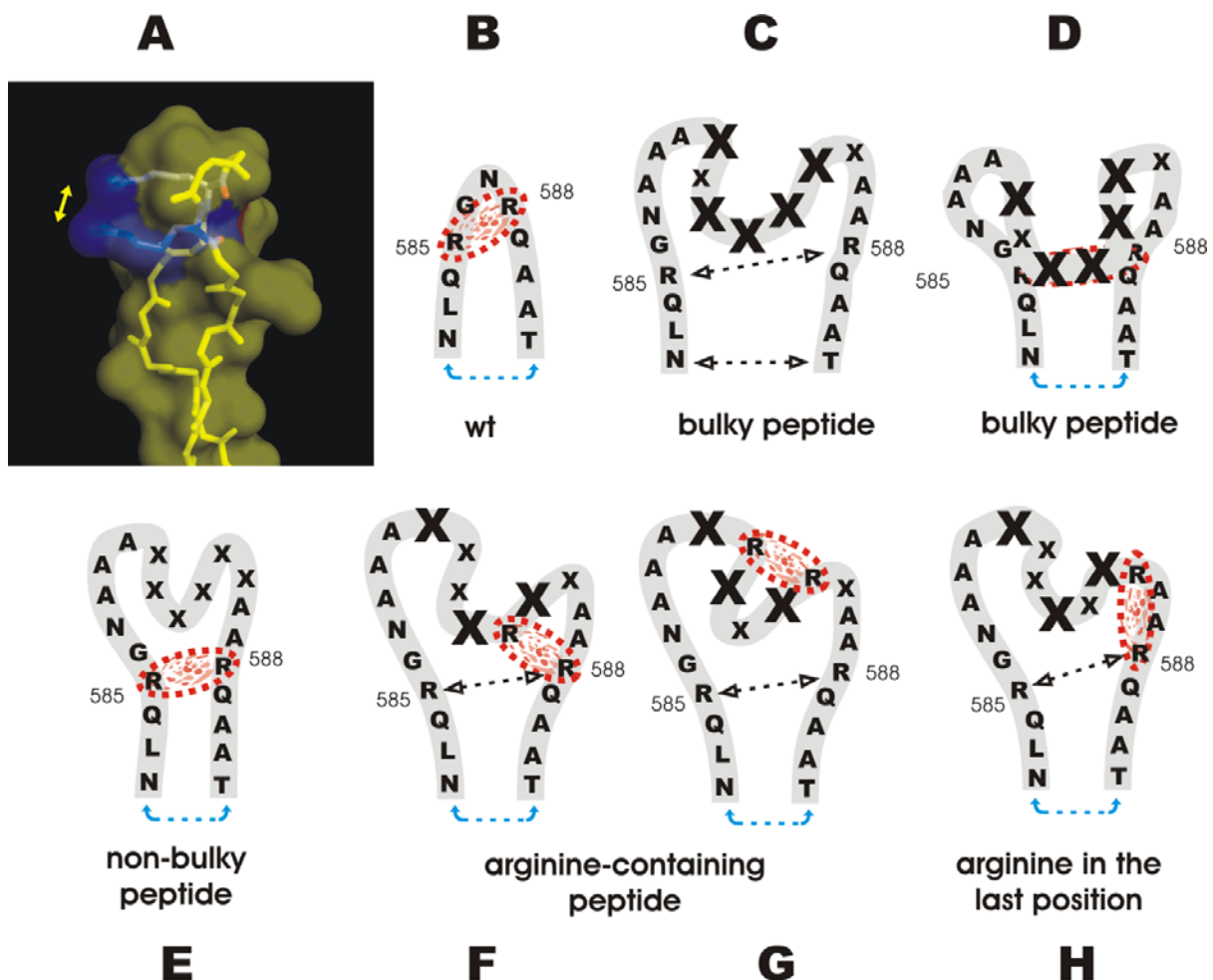
  

| B | DNA-library | AAV-library | B-AAV-pool | NB-AAV-pool |
|---|-------------|-------------|------------|-------------|
|   | R           | R           | R          | R           |
|   | H           | H           | H          | H           |
|   | K           | K           | K          | K           |
|   | E           | E           | E          | E           |
|   | D           | D           | D          | D           |
|   | N           | N           | N          | N           |
|   | S           | S           | S          | S           |
|   | T           | T           | T          | T           |
|   | G           | G           | G          | G           |
|   | A           | A           | A          | A           |
|   | P           | P           | P          | P           |
|   | C           | C           | C          | C           |
|   | Q           | Q           | Q          | Q           |
|   | I           | I*          | I          | I           |
|   | L           | L           | L          | L           |
|   | M           | M           | M          | M           |
|   | F           | F           | F          | F           |
|   | W           | W*          | W          | W*          |
|   | Y           | Y           | Y          | Y           |
|   | V           | V           | V          | V           |

**Table 1:** A) Representative example of 20 peptides detected in B-AAV and NB-AAV pool. Net charge of the insertions is provided. Parentheses indicate a weak charge considering the low pKa of histidine B) Statistical analysis of the occurrence of amino acids. Based on the  $\chi^2$ -test, the colours indicate a higher (red), lower (blue) or expected (black) occurrence of each amino acid in the analyzed populations ( $P=0,0001$ ). For each population >80 clones were sequenced. \*These amino acids were found at clearly lower frequencies than expected but statistical assessment of the significance was not possible without sequencing a higher number of clones.

Interestingly, B-AAV-pool insertions carrying no positive amino acids displayed an exceptionally high amount of A, G and S (data not shown), the three smallest amino acids, suggesting a reduced impact on the wild-type capsid structure, which is less likely to interfere with binding of heparin.

The NB-AAV-pool showed clearly a higher presence of negative charged amino acids (D and E) (Table 1A, B). Moreover, although the number of negative residues observed in the B-AAV-pool matched statistical expectations, only 2% of the clones carried a net negative charge in its insertion, while 76% carried a positive and 21.5% a neutral charge. In clear contrast, the NB-AAV-pool consisted of 53% negative, 8% positive and 39% neutral net charged inserts. This bias becomes even clearer if histidine is considered neutral due to its low pKa: B-AAV-pool insertions would then be 2% negative, 64% positive and 34% neutral while NB-AAV-pool consisted of 64% negative, 2% positive and 34% neutral. These observations strongly suggest that the presence of negative charges is deleterious for functional binding of AAV-2 vectors to negatively charged heparin/HSPG.



**Figure 1: Proposed model for the influence of several peptide classes on capsid stability and on binding to heparin.** A) Three dimensional atomic structure of the 587 region. The side chains of R585 and R588 are pointed by the yellow arrow. B) The two arginines are part of the binding motif. C) A bulky peptide disrupts the heparin binding motif taking the arginines apart. D) A bulky peptide obstructs the HSPG binding motif. E) Small peptides could preserve the original structure of the loop and heparin binding motif. F) and G) The presence of one or more arginines in the inserted peptide restores the heparin binding ability. H) Due to its proximity to R588, an arginine in the last amino acid position of the insertion is prone to restore heparin binding. In all panels, a functional heparin binding site is indicated by a red pattern. A loop conformation that confers capsid stability is indicated by the blue arrow.

Taken together, these data suggest a model in which peptide insertions at 587 can either disrupt or conserve the capsid ability to bind heparin by different mechanisms. Insertion of a peptide between R585 and R588 (Figure 1A, B) could cause their spatial separation or sterically block the heparin binding ability. In either case, bulky amino acids are prone to lead to one or both of these results (Figure 1C, D). If the peptide consists of small residues, the insertion could be less invasive and the structure of the HSPG binding motif maintained functional (Figure 1E). Insertion of positively charged peptides could lead to a HSPG binding phenotype by reconstituting a binding motif in combination with one of the original arginines (Figure 1F) or independently from them (Figure 1G). The proximity of R588 to the last position of the inserted peptide could facilitate reconstitution of a functional motif if an arginine is present at this latter position (Figure 1H). It should be noted that this behaviour could be due to the particular sequence of the construct we used, where the 7<sup>th</sup> position of the randomized peptide and R588 are separated by two residues resembling the wild-type situation.

We previously described an AAV targeting vector, rAAV-MTP, that allowed systemic vascular targeting (White *et al.*, 2004). Simultaneous detargeting of this vector from liver and spleen was observed. This vector showed a reduced ability to bind to heparin (White *et al.*, 2004). Here, we analysed whether the inability of AAV insertion mutants to bind heparin directly correlates with detargeting from liver and spleen. Therefore, binding and non-binding pools were produced as beta-galactosidase expressing recombinant AAV vectors (rAAV) as previously described (Perabo, Endell *et al.*, 2006). rAAV with wild-type capsid (rAAV-RC) was used as a control. First, the ability to infect the hepatocellular carcinoma cell line HepG2 was determined (Figure 2). All three viral preparations were able to transduce HepG2. rAAV-RC and B-rAAV-pool showed a comparable transduction efficiency. Since the addition of heparin completely abolished rAAV-RC mediated transduction (data not shown), it can be assumed that AAV-2 infection of this cell line depends on HSPG binding.

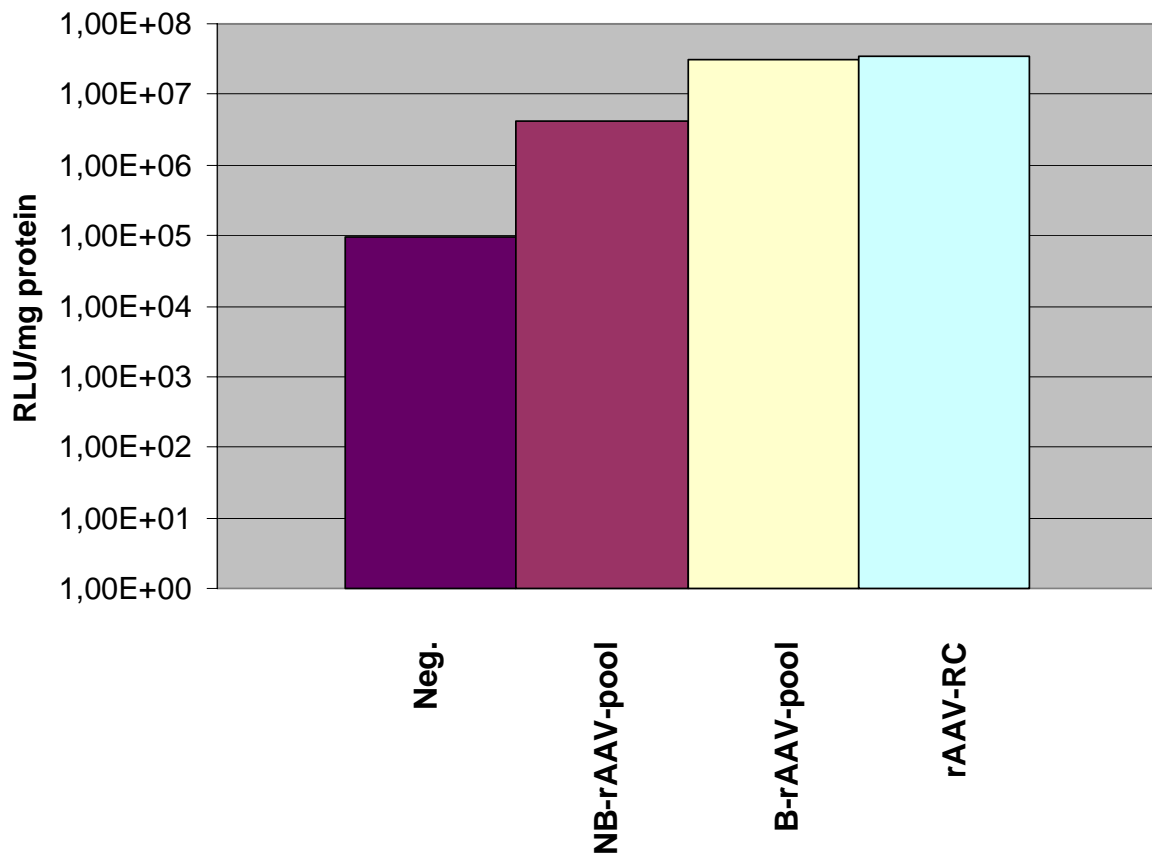


**Figure 2: Transduction efficiency of rAAV-RC, B-rAAV-pool and NB-rAAV-pool on HepG2.** HepG2 were infected in the presence of adenovirus (1 pfu/cell) with 1000 genomic particles per cell of rAAV-RC, B-rAAV-pool or NB-rAAV-pool and analysed 48 h p.i. Cells were lysed in Galactolight Plus beta galactosidase lysis buffer (Tropix, USA) and beta-galactosidase expression was determined by Galactolight Plus beta galactosidase assay according to manufacturer instructions. Detection was performed using a Wallac 1420 (Victor2) multilabel counter with beta-galactosidase as standard. Gene expression was normalized for total protein using BCA (Perbio, UK) and expressed as RLU/ mg protein.

The mutants within the NB-rAAV-pool are unable to bind to HSPG. This suggests that the observed HepG2 transduction is mediated by some but not all inserts displayed within the pool, explaining the 1 log reduction in infectivity and pointing towards new and specific ligand-receptor interactions.

Thereafter,  $4 \times 10^9$  genomic particles were injected intravenously into C57/B6 mice (n=4) and biodistribution studies were performed as described (White *et al.*, 2004). Animals injected with rAAV-RC and B-rAAV-pool showed a comparable biodistribution with the highest vector DNA level in spleen and liver (Figure 3). In contrast, the NB-rAAV-pool showed a 102- and 31.8-fold reduction in vector DNA level in the spleen in comparison to rAAV-RC and B-rAAV-pool, respectively, whereas in the liver an 8.8- and 6.7-fold reduction was detected.

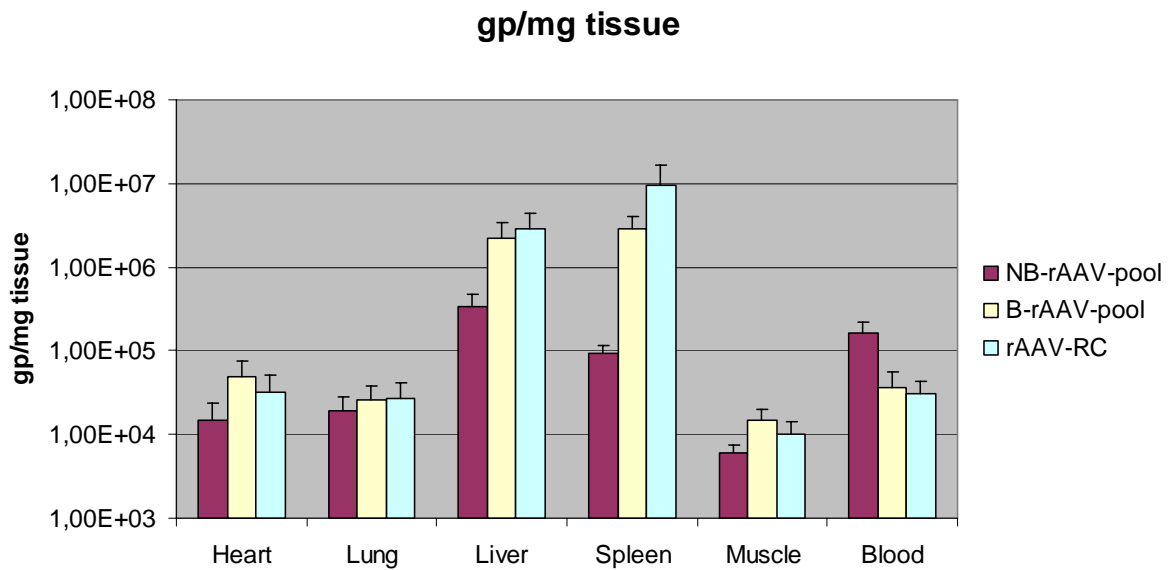


**Figure 3: Bioistribution of rAAV-RC, B-rAAV-pool and NB-rAAV-pool in C57/B6 mice**  $4.2 \times 10^9$  genomic particles of the different vector preparations were injected into the tail vein of 12 week old C57/B6 mice. 24 h p.i. mice were sacrificed. DNA was extracted from blood and tissues. Vector genomes per tissue were quantified by PCR (Taqman).

In addition, elevated levels of viral DNA in the blood were measured for the NB-rAAV-pool consistently with the level of liver and spleen detargeting. This suggests an unspecific HSPG-dependent retention of rAAV-2 and HSPG-binding rAAV-targeting vectors in liver and spleen and an HSPG-independent, receptor-specific infection of cells in the liver mediated by some peptide insertions of the NB-rAAV-pool. This hypothesis is in agreement with results previously obtained for a HSPG-knock-out mutant (Kern *et al.*, 2003) and explains the liver and spleen detargeting observed for rAAV-MTP (White *et al.*, 2004).

These results are a clear rationale to use the NB-AAV-pool for AAV Display selections of cell/tissue type specific AAV targeting vectors to avoid unspecific HSPG-dependent retention in liver and spleen and increasing thereby the in-vivo-targeting-ability of the respective vectors. Furthermore, our studies revealed different ways by which an inserted peptide is able to confer HSPG-binding abilities to AAV targeting vectors and may help to fine tune the peptide insertion in order to ablate HSPG binding and to obtain tissue specific vectors. This knowledge could also improve targeting mutants where R585 and/or R588 are substituted by other amino acids, since even in this case, some peptides (Figure 2G) would restore HSPG binding.

## **Acknowledgements**

This work was supported by the Center for Molecular Medicine of University of Cologne (S.H., M.H., H.B.), Köln Fortune (M.H.), the Deutsche Forschungsgemeinschaft (Forschergruppe Xenotransplantation) (M.H., L.P.), the European Union, Deutsche Krebshilfe (J.E., H.J.), Medical Research Council (A.H.B) and Biotechnology and Biophysical Research Council (A.H.B.). Furthermore, we would like to thank Prof. Dr. Richard Jude Samulski (University of North Carolina at Chapel Hill, USA) for kindly providing pXX6.

## Chapter VI

# Green Fluorescence Protein-Tagged Adeno-Associated Virus Particles Allow the Study of Cytosolic and Nuclear Trafficking

Published in *Journal of Virology* (2005) 79:11776-11787 as:

Lux K, Goerlitz N, Schlemminger S, Perabo L, Goldnau D, Endell J, Leike K, Kofler D, Finke S, Hallek, and Büning H.

## Abstract

In order to allow the direct visualization of viral trafficking, we genetically incorporated enhanced green fluorescent protein (GFP) into the AAV capsid by substitution of wild-type VP2 with GFP-VP2 fusion proteins. High titer viral progeny was obtained and used to elucidate the process of nuclear entry. In the absence of Adenovirus 5 (Ad5) nuclear translocation of AAV capsids was a slow and inefficient process: At 2 hours (h) and 4 h post infection (p.i.), GFP-VP2-AAV particles were found in the perinuclear area and in nuclear invaginations but not within the nucleus. In Ad5 coinfecting cells, isolated GFP-VP2-AAV particles were already detectable in the nucleus at 2 h p.i., suggesting that Ad5 enhanced the nuclear translocation of AAV capsids. The number of cells displaying viral capsids within the nucleus increased independently of helpervirus slightly with time, but the majority of the AAV capsids remained in the perinuclear area in all conditions analyzed. In contrast, independently of helpervirus and with 10x less virions per cell already 2 h p.i. viral genomes were visible within the nucleus. Under these conditions even with prolonged incubation times (up to 11 p.i.) no intact viral capsids were detectable within the nucleus.

In summary, the results show that GFP-tagged AAV particles can be used to study the cellular trafficking and nuclear entry of AAV. Moreover, our findings argue against an efficient nuclear entry mechanism of intact AAV capsids and favour the occurrence of viral uncoating before or during nuclear entry.

## Introduction

Adeno-Associated Virus serotype 2 (AAV) was discovered as a coinfecting agent during an adenovirus outbreak, without any apparent pathogenicity contributed by AAV (Blacklow, 1988). Recombinant AAV (rAAV) vectors based on AAV type 2 or one of the other known serotypes hold attractive potential for the development of efficient and safe gene therapy vectors. Clinical trials are ongoing for the treatment of cystic fibrosis and haemophilia B (High *et al.*, 2004; Wagner *et al.*, 2002). Elucidating the molecular mechanisms of viral infection and cellular processing of AAV is critical for the success of these approaches.

Besides conventional biochemical studies, microscopic techniques are emerging as powerful tools for the study of viral infection. A promising development for the investigation of AAV was the finding that viral particles can be labelled by cyanine dyes generating a stable NHS

ester with amino groups at the capsid surface (Bartlett, Wilcher and Samulski, 2000). However, this labelling method is labor intensive and hampered by the low efficiency of the labelling reaction (on average one dye per capsid) (Seisenberger *et al.*, 2001). High particle numbers need to be used for fluorescence microscopy studies to overcome this problem. This limitation was conquered by a new technique, Single Virus Tracing (SVT), recently described by our group (Seisenberger *et al.*, 2001). This method is based on the detection of single molecules using an epifluorescent microscope and a laser beam as a light source, allowing the real time observation of single virus particles inside living cells. Although it is possible to merge the transmitted-light picture of the cell with the virus-tracking movie by the SVT method, a direct co-localization of virions and cellular organelles remains difficult. Additionally, highly pure viral preparations have to be used to avoid labelling of contaminating proteins. This can not be achieved easily for many AAV retargeting vectors, since many mutants lose the ability to bind heparan sulphate proteoglycans preventing the use of heparin affinity chromatography for purification.

Therefore, we aimed to develop an alternative strategy for the labelling of the AAV capsid by using the enhanced green fluorescent protein (GFP). GFP has been extensively used as a fusion protein to study intracellular trafficking and localization of proteins. It has an effective chromophore, which absorbs UV or blue light and emits green fluorescence. No further gene products or substrates are needed. Moreover, GFP does not seem to interfere with cell growth and function. GFP fusion proteins thus provide an attractive tool for biological studies including viral tracking (Desai and Person, 1998; Elliott and O'Hare, 1999; Glotzer *et al.*, 2001; McDonals *et al.*, 2002; Sampaio *et al.*, 2005; Suomalainen *et al.*, 1999; Ward, 2004; Warrington *et al.*, 2004).

Different strategies have been previously used to incorporate peptides into the AAV capsid. The capsid is a tightly packaged icosahedron of 25 nm and is composed of three different viral proteins, VP1 (90 kDa), VP2 (72 kDa) and VP3 (60 kDa). These proteins are encoded in the same open reading frame (ORF) and share a common stop codon. They differ in their N-terminus due to alternative splicing and different initiation codons, resulting in three progressively shorter proteins. Ligand peptides of up to 34 amino acids have been inserted into amino acid (aa) position 587 of VP1 to generate targeting vectors (Girod *et al.*, 1999; Ried *et al.*, 2002). Peptides were also inserted into the VP1 unique region at aa position 34 (Wu *et al.*, 2000) and one or two residues downstream from the N-terminal methionine of the VP2 start codon (aa position 138: (Loiler *et al.*, 2003; Warrington *et al.*, 2004; Wu *et al.*,

2000; Yang *et al.*, 1998) and 139: (Shi *et al.*, 2001)). Since VP1 is an N-terminal extension of VP2, insertions at 138/139 are displayed within VP1 and VP2. The most abundant capsid protein VP3 remains unmodified. Insertions as large as 32 amino acids were tolerated with only marginally lower packaging efficiencies (Loiler *et al.*, 2003). Larger insertions, for example the rat fractalkine chemokine domain (76 aa) or the human hormone leptin (146 aa) inserted at aa position 138 resulted in a decrease in VP3 expression which prevented capsid assembly (Warrington *et al.*, 2004). Providing additional VP3 in trans (by a VP3 encoding plasmid) restored capsid assembly with a remaining 5 log decrease in infectivity (Warrington *et al.*, 2004).

However, Yang and colleagues could previously show that large insertions at the N-terminus of the VP proteins interfere with capsid assembly (Yang *et al.*, 1998). In their study a 29.4 kDa single chain antibody (sFv) was incorporated into the AAV capsid fusing the sFv gene to the N-terminus of VP1, VP2 and VP3. The fusion proteins were expressed, but neither use of all three sFv-VP fusion proteins nor combination of one sFv-VP with two other unmodified VPs resulted in detectable rAAV particles. However, when the sFv-VP2 fusion protein was included in the packaging process in the presence of all three unmodified VP proteins, intact rAAV chimeric vector particles containing sFv-VP2 fusion protein were generated. This significantly increased the transduction of target cells expressing a cellular receptor recognized by the inserted antibody.

Based on these previous results, we decided to insert the 30 kDa GFP protein as a GFP-VP2 fusion protein into the AAV capsid. Incorporation of GFP-VP2 into the AAV capsid did not interfere with viral assembly or viral genome packaging. The GFP-tagged virions produced in this study retained infectivity in marked contrast to results published by Warrington *et al.* (Warrington *et al.*, 2004). When used to visualize the process of nuclear entry in more detail, we detected virions in the nuclear area shortly after infection. In agreement to Xiao *et al.* (Xiao *et al.*, 1998) we observed that Ad5 augmented the efficiency of the nuclear entry of AAV capsids. In cells infected with GFP-VP2-AAV a colocalization of viral capsids with nuclear invaginations was observed. With prolonged incubation times the amount of cells displaying AAV capsids within the nucleus increased independent of Ad5 coinfection. However, still the majority (more than 90%) of the capsids remained detectable outside the nucleus during the whole observation period. In contrast, viral genomes were detectable by FISH hybridization within the nucleus of cells already 2 h p.i. irrespective of Ad5 coinfection although 10x less virions per cell were used. Compared to 2 p.i. an increase in the amount of

viral genomes was observed at 11 h p.i. Moreover, under these conditions ( $10^5$  instead of  $10^6$  virions per cell) no intact viral capsids were detected within the nucleus even after prolonged incubation times.

Our studies demonstrate that GFP-VP2 tagged virions are a promising alternative to the chemical labelling of AAV to study the infectious biology of AAV and derived vectors.

## Material and Methods

**Cell culture.** The human cervix epitheloid cell line HeLa (ATCC CCL 2; American Type Culture Collection, Rockville, Maryland), the HeLa-DsRed2Nuc cell line (produced by stable transfection of HeLa with pDsRed2-Nuc), and the human embryonic kidney cell line 293 were maintained as monolayer culture at 37°C and 5% CO<sub>2</sub> in Dulbecco's modified Eagle's medium (DMEM), supplemented with 10% fetal calf serum (FCS), 100 U/ml penicillin 100 mg/ml streptomycin and 2 mM L-glutamine.

**Plasmids.** pUC-AV2 (11), pSUB201<sup>+</sup> (26), pXX6 (38) and pGFP (15) were described before. The plasmid pUC-AV2-VP2k.o. was obtained by PCR amplification combined with site directed mutagenesis of pUC-AV2, changing the ACG start codon into ACC using overlapping PCR fragments (VP2ko\_for: 5'-GTTAAGACCGCTCCGGG-3' and 4066: 5'-ATGTCCGTCCGTGTGTGG-3'; VP2ko\_back: 5'-CCCGGAGCGGTCTTAAC-3' and 3201: 5'-GGTACGACGACGATTGCC-3') and ligation of the fragments in a second PCR step using the primers 3201 and 4066. The resulting fragment was digested with BsiWI and EcoNI and sticking end ligated into pUC-AV2. To obtain the plasmid pGFP-VP2 the sequence coding for VP2 was amplified from pSUB201<sup>+</sup> by PCR using the primer pair VP2-N 5'-CTCCGGGAAAAAAGAGG-3' and VP2-C: 5'-TTACAGATTACGAGTCAGGTAT-3', thereby deleting the VP2 start codon and ligated into pEGFP-C3 (Clontech), which was digested with Bgl II and filled in by Klenow polymerase. The plasmid pDsRed2Nuc was generated by deletion of the EGFP encoding region from pEGFP-Nuc (Clontech) and insertion of the DsRed2 gene, which was amplified by PCR (Primers: 5'-CGG AGT ACA TCA ATG G-3' and 5'-AGA TCC GGT GGA TCC TAC CT-3') from pDsRed2-N1 (Clontech) and cut with AgeI.

**Viral production and purification.** AAV particles were produced in HEK293 cells by the adenovirus free production method using pXX6 (38) to supplement the adenoviral helper functions. Briefly, HEK293 cells were seeded at 80% confluence and cotransfected by

calcium phosphate with a total of 37.5 µg plasmid of pUC-AV2 and pXX6 in a 1:1 molar ratio for the production of wild-type AAV. For the production of chimeric virions cells were transfected with pXX6, pUC-AV2 and pGFP-VP2, substituting 30% or 60% of pUC-AV2 with pGFP-VP2. For the production of the VP2 k.o.-AAV HEK293 cells were transfected with pUC-AV2-VP2k.o. and pXX6 in a 1:1 molar ratio. For the production of the 100%-GFP-VP2-AAV pUC-AV2-VP2k.o., pGFP-VP2 and pXX6 were transfected in 1:1:1 molar ratio. 48 h post transfection cells were harvested and pelleted by low-speed centrifugation. Cells were resuspended in 150 mM NaCl, 50 mM Tris-HCl (pH 8.5), freeze-thawed several times, and treated with Benzonase for 30 minutes at 37°C. To purify the viral preparation by iodixanol gradient centrifugation, the cell debris was spun down at 3700g for 20 minutes at 4°C and supernatant was loaded onto an iodixanol gradient as described (41).

**Determination of AAV titers.** Particle titer of vector stocks was determined by quantitative PCR (30). Therefore, viral DNA was isolated from vector stocks according to the DNeasy kit protocol (Qiagen, Hilden, Germany). Capsid titer of vector stocks was determined by A20-ELISA as previously described (11). Infectious titer was obtained by infecting HeLa cells as monolayers on cover slips with serial dilutions of viral preparations in the presence of adenovirus type 5 (MOI 5). 72 h post infection Rep protein expression was determined by immunofluorescence staining (34). Briefly, cells were fixed in methanol and acetone for 5 min, respectively. After washing with PBS, unspecific reactions were blocked by incubation with 0.2% gelatine in PBS for 10 min. The cover slips were incubated for 1 h at room temperature with the anti-Rep antibody 76/3 (kindly provided by Dr. Jürgen Kleinschmidt, DKFZ Heidelberg, Germany), cover slips were washed and blocked again and incubated for 1 h with a secondary antibody (FITC conjugated goat anti-mouse; 1:100 in PBS; Dianova). Titers were calculated from the last limiting dilution of viral stocks that led to fluorescence positive cells.

**Functional testing of GFP-VP2 fusion protein by transient transfection.** HeLa cells (grown on cover slips) were transfected by calcium phosphate precipitation (11) at 80% confluence with the plasmid pGFP-VP2. As control, HeLa cells were transfected in parallel with pGFP (15). 48 h post transfection cells were fixed for 30 minutes in 4% paraformaldehyde (PFA). The nuclear lamina was stained as described below using anti-lamin B antibody.

**Western Blot.** For the detection of viral capsid proteins  $10^{10}$  capsids were separated on a SDS-polyacrylamide gel (10%) and blotted onto a nitrocellulose membrane. The membrane

was then blocked with 0.2% I-Block (Sigma) in Tris buffered saline supplemented with Tween 20 (TBS-T) over night at 4°C. After incubation with B1-antibody (kindly provided by Dr. Jürgen Kleinschmidt (DKFZ Heidelberg, Germany); 1:10 in 0.2% I-Block) and three washing steps in TBS-T, the membrane was incubated for 1 h with a peroxidase conjugated anti-mouse IgG antibody (1:5000 in 0.2% I-Block, Sigma). The membrane was washed again, subsequently incubated for 5 min with SuperSignal West Pico Chemiluminescent Substrate (Pierce) and then exposed to Biomax Light Film (Kodak).

**Viral infection.**  $4 \times 10^4$  HeLa cells per well were seeded onto 12 mm cover slips inside 24 well plates. 24 h later HeLa cells were infected with or without 425 units heparin/ml medium with  $1.5 \times 10^6$  capsids/cell. When indicated, cells were coinfecting with adenovirus type 5 (MOI 5). The infection was carried out for 0.5 h on ice. Cells were then shifted to 37°C and incubated at 37°C and 5% CO<sub>2</sub> for the indicated time period. Cells were washed with PBS and fixed for 0.5 h with 3% PFA in PBS at room temperature, washed again with PBS and the remaining PFA was quenched for 10 min with 50 mM NH<sub>4</sub>Cl in PBS. Nuclear staining was obtained by Dapi (1 µg/ml in PBS) for 5 min or by anti-lamin B antibody staining. For antibody staining cells were permeabilized with 0.2% Triton X 100 in PBS for 10 min, blocked for 10 min with 0.2% gelatine in PBS and then incubated for 1 h at room temperature with first antibodies as indicated. As first antibodies polyclonal goat anti-lamin B IgG antibody (1:50 in PBS, Santa Cruz Biotechnology), monoclonal A20 or B1 hybridoma supernatant derived from mice (kindly provided by Dr. Jürgen Kleinschmidt, DKFZ Heidelberg, Germany) were used. After washing and blocking, the cells were incubated for 1 h with secondary antibodies. As secondary antibodies we used Texas Red or Cy5 conjugated donkey anti-goat-antibody (Dianova, diluted 1:50 or 1:100 in PBS, 0.2% gelatine) and Rhodamine Red-X (RRX) conjugated donkey anti-mouse (Dianova, diluted 1:200 in PBS, 0.2% gelatine). The cover slips were washed in PBS again, embedded in Vectashield mounting medium (Alexis) and examined.

**Fluorescence in situ hybridisation (FISH)** Plasmid pRC (15) which encodes Rep and Cap of AAV2 was linearized and labelled with 5-(3-aminoallyl)dUTPs by nick translation. Incorporated dUTPs were labelled with amino reactive Oregon Green 488 by ARES DNA labelling kit (Molecular Probes) according to manufacturers manual. To detect the AAV genome inside cells, HeLa cells were prepared as described above. Cells were infected with wild-type AAV2 ( $10^5$  capsids/cell), fixed with 3% PFA after indicated time points, quenched and permeabilized as described before. Nuclear lamina and viral capsids were stained by polyclonal goat anti-lamin B IgG antibody and monoclonal A20 hybridoma supernatant

derived from mice (kindly provided by Dr. Jürgen Kleinschmidt, DKFZ Heidelberg, Germany). Cy5 conjugated donkey anti-goat antibody (Dianova) and Rhodamine Red-X conjugated donkey anti-mouse antibody (Dianova) were used as secondary antibodies. After antibody staining cells were washed with PBS. A hybridization-mix containing 1 ng/ $\mu$ l labelled DNA probe, 50% formamide, 7.3% dextran sulphate, 15 ng/ $\mu$ l salmon sperm DNA and 0.74x SSC was denaturated for 3 min at 95°C and shock cooled on ice. Cover slips were inverted onto the denaturated hybridization-mix (only the DNA probe was denaturated since the AAV genome is single stranded). Cover slips were sealed with rubber cement and hybridization occurred at 37°C over night. Rubber cement was removed and cover slips were washed 3x in 2x SSC at 37°C, 3x in 0.1x SSC at 60°C and 2x in PBS. Cells were embedded in Vectashield mounting medium (Alexis).

**Wide field fluorescence microscopy.** Images were acquired with an immunofluorescence microscope (Zeiss, Axioskop) equipped with filters specific for GFP and Dapi using a 40x (NA1.3) objective. Images were obtained with a CCD camera (Visicam, Visitron Systems) with MetaMorph Imaging System version 3.0.

**Confocal microscopy.** To localize the GFP-VP2 signal within the cell more precisely, images were obtained by confocal laser scanning microscopy using a Leica DM IRE2 microscope with a Leica TCS SP2 laser system or a Zeiss Axiovert 200M microscope with a Zeiss LSM 510 Laser Module, using a 63x (NA 1.4) objective and filter settings optimized for respective dyes. For each sample a series of 0.2 to 0.25  $\mu$ m horizontal sections were made. The pinhole was adjusted to 1 airy unit. Images were processed by Leica confocal software or LSM 510 Meta software and Adobe Photoshop version 7.0.

**Live cell imaging (Time-laps microscopy).** For live cell images  $2 \times 10^5$  HeLa-DsRed2Nuc cells were seeded onto the glass bottom of microwell dishes (35 mm; Mat Tek). 24 h later cells were infected with or without 425 units heparin/ml media with approx.  $10^6$  capsids per cell. Cells were incubated for 20 min at 37°C and then analyzed by live cell microscopy under physiological conditions. Live cell movies were obtained with an inverse Zeiss Axiovert 200M microscope with a 63x (NA1.4) objective using Zeiss filter sets (FS)10 for GFP and DsRed. Images were taken with a Zeiss AxioCam HRm using the Axiovision 3 software with a time laps of 30 seconds.

**Fluorescence activated cell sorting (FACS) analyses.**  $4 \times 10^4$  HeLa cells were seeded per well in a 24 well plate. 24 h later cells were infected with or without 425 units of

heparin/ml medium with  $8 \times 10^7$  capsids/cell. The virus binding was carried out for 30 min. on ice. Thereafter, cells were shifted to 37°C for 1 h. Cells were harvested, resolved in 0.5 ml PBS and analyzed with a Coulter Epics XL-MCL (Beckman Coulter). A minimum of 5000 cells were analyzed for each sample. The percentage of positive cells is defined as the fraction beyond the region of 99% of the control of untransfected cells. Data were analyzed with the use of WinMDI 2.8 FACS software.

## Results

### GFP fusion does not interfere with nuclear translocation of VP2

The enhanced green fluorescent protein (GFP) has been widely used as a fusion protein to monitor the cellular localizations of proteins (Chalfie *et al.*, 1994). However, it is a relatively large protein for being inserted into a compact structure such as the AAV capsid. Based on the observation that large insertions are tolerated at the N-terminus of VP2 (Yang *et al.*, 1998), we decided to generate a GFP-VP2 fusion protein to incorporate a fluorescent marker into the AAV capsid. For this purpose, the VP2 ORF was amplified by PCR and fused to the C-terminus of the GFP open reading frame (Figure 1), with the human cytomegalovirus (CMV) promoter controlling transcription. To avoid translation from the natural VP2 start codon, the translation start codon was deleted. To test the biological properties of this GFP-VP2 fusion protein, transient transfections of HeLa cells with pGFP-VP2 were carried out.

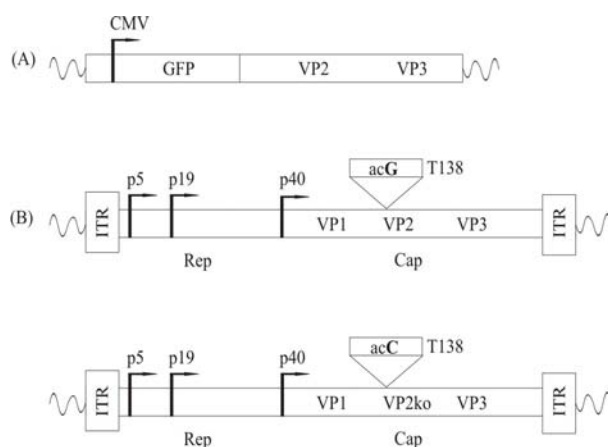


**Figure 1: Schematic representation of the plasmids.** (A) The plasmid pGFP-VP2 encodes the GFP-VP2 fusion protein. VP2 was amplified by PCR from pUC-AV2 and cloned into the multiple cloning site of pEGFP-C3 (Clontech). During this step, the VP2 start codon was deleted. (B) To produce wild-type AAV the plasmid pUC-AV2 was used (upper panel). A G-to-C substitution within the wobble position of the VP2 start codon (T138) was introduced, resulting in the plasmid pUC-AV2-VP2k.o. (lower panel). Due to the substitution, VP2 expression was abolished without altering the amino acid sequence of VP1.

As a control, HeLa cells were transfected with a GFP expressing plasmid lacking any known organelle homing signals (Ried *et al.*, 2002). 48 h post transfection, cells were fixed and the nuclear lamina stained with an anti-lamin B antibody. Since VP2 contained a nuclear localization sequence (Hoque *et al.*, 1999), GFP-VP2 was expected to be detectable in the nucleus, whereas the GFP lacking homing signals should be distributed throughout the whole cell. Figure 2 shows that this was indeed the case, allowing to conclude that the GFP fusion does not hamper the nuclear localization VP2.

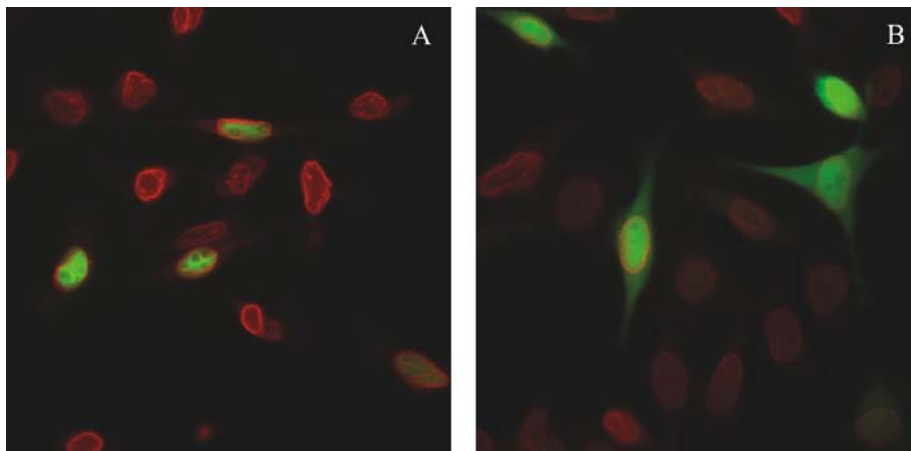


**Figure 2: Transient transfection of HeLa cells with GFP-VP2 and GFP expressing plasmids.** Cells were transfected at 80% confluence with pGFP-VP2 (A) or pGFP (B) and fixed 48 h post transfection. The nuclear lamina was stained with Texas Red conjugated anti-lamin B antibody.

### **Substitution of VP2 by GFP-VP2 fusion protein results in infectious virions**

In a prior study, scFv-VP2 fusion proteins used to generate viral particles resulted in viral progeny only when all three wild-type AAV capsid proteins were provided during the packaging process (Yang *et al.*, 1998). Since the GFP insertion was of similar size as scFv, we assumed that all three unmodified wild-type capsid proteins had to be provided during the packaging process to obtain infectious GFP-tagged viral particles. The first step was therefore to determine the amount of VP2 which could be substituted by GFP-VP2 without interfering with the production of infectious AAV particles. We tested a 30% and 60% substitution of pUC-AV2 (coding for the AAV genome) by pGFP-VP2 during packaging. The viral preparations generated were named 30%-GFP-VP2-AAV and 60%-GFP-VP2-AAV, respectively. Wild-type AAV was used as control. 48 h post transfection virus producing cells were harvested and cell lysates were purified by iodixanol step gradients. The 25% and the 40% phase of the gradient were harvested and genomic and capsid titers were determined. DNA containing viral particles with comparable titers were detected for the different viral preparations (25%-phase of the gradient:  $2.5 \times 10^{10}$ /ml; 40%-phase of the gradient:  $0.5$ -

$1 \times 10^{11}$ /ml). The amount of intact capsids was determined by ELISA using the anti-capsid antibody A20 (Wobus *et al.*, 2000). As expected, a higher amount of empty capsids was obtained in the 25%-phase of the gradient. However, all the capsid titers showed comparable values (25%-phase of the gradient:  $5-8 \times 10^{13}$ /ml; 40%-phase of the gradient:  $0.4-1 \times 10^{13}$ /ml). Thus, neither capsid assembly nor DNA packaging was affected in the 30%- and the 60%-GFP-VP2-AAV preparations in comparison to the wild-type control.

To investigate, if the GFP-VP2 fusion proteins were inserted into the AAV capsid and if the GFP-tagged virions retained infectivity, HeLa cells were incubated with the 30%- and 60%-GFP-VP2-AAV preparations, respectively. 2 h p.i. cells were washed intensively, detached from the plate by trypsin treatment and analyzed by flow cytometry. Treatment with trypsin removes all the proteins bound at the cell surface (Awedikian *et al.*, 2005; Mizukami *et al.*, 1996), thus only intracellular GFP signals should be detected. GFP positive cells were obtained in samples infected with both preparations. The highest amount of GFP positive cells (19.5%) was obtained with 60%-GFP-VP2-AAV, whereas 13.5% GFP positive cells were detected using the same amount of capsids of 30%-GFP-VP2-AAV. In contrast, no green cells were detected when wild-type AAV was used. To exclude pseudo-transduction, heparin inhibition controls were included. Heparin, a soluble analogue of the primary AAV receptor heparan sulphate proteoglycan (HSPG), blocks wild-type AAV infection by binding to the viral capsid. Since the HSPG binding region of AAV is located in the VP3 region of the capsid proteins (Wu *et al.*, 2000), the ability to bind to these molecules should be retained by the GFP-tagged virions. Incubation of both viral preparations with heparin inhibited cell transduction indicating that a viral infection and not pseudo-transduction was responsible for the GFP signal measured in the GFP-VP2-AAV infected cells.

These results demonstrate that GFP fusion proteins were incorporated into the AAV capsid of infectious virions and that the GFP signal provided by GFP-tagged virions was detectable by flow cytometry.

### **Production of GFP tagged AAV virions in the absence of wild-type VP2**

Since comparable titers were obtained for the 30%-GFP-VP2-AAV and the 60%-GFP-VP2-AAV preparations, we investigated the possibility to package a 100%-GFP-VP2-AAV preparation. A wild-type AAV encoding plasmid containing a VP2 start codon mutation was generated (pUC-AV-VP2k.o.; Figure 1) and used to package 100%-GFP-VP2-AAV.

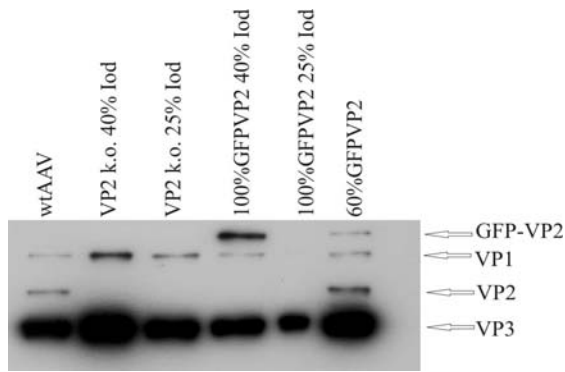


**Figure 3: Western blot analysis of iodixanol gradient purified AAV capsids.** After iodixanol gradient centrifugation same amount of viral capsids ( $10^{10}$ ) of wild-type AAV (lane 1; 40% phase of iodixanol gradient), VP2 k.o.-AAV (lane 2: 40% phase of iodixanol gradient; lane 3: 25% phase of iodixanol gradient), 100%-GFP-VP2-AAV (lane 4: 40% phase of iodixanol gradient; lane 5: 25% phase of iodixanol gradient) and 60%-GFP-VP2-AAV (lane 6; 40% phase of iodixanol gradient) were separated by SDS-10% polyacrylamide gel electrophoresis and analyzed by Western blot using the B1 antibody.

In addition “VP1/VP3 only particles” (VP2 k.o.-AAV), 60%-GFP-VP2-AAV and wild-type AAV were produced and purified by density gradient centrifugation. First, a Western blot analysis of our different preparations was performed (Figure 3). Although only virions isolated from the 40% phase of the iodixanol gradient were used for the following studies, also the 25% phase of the gradient was analyzed by Western blot. For wild-type AAV we obtained three signals corresponding to VP1, VP2 and VP3 (Figure 3, lane 1) in a ratio of approximately 1:1:20. As expected, VP2 k.o.-AAV contained only VP1 and VP3 proteins (lane 2 and 3), whereas in the 100%-GFP-VP2-AAV preparation the GFP-VP2 fusion protein, VP1 and VP3 were detected (lane 4). The 60%-GFP-VP2-AAV was packaged in the presence of all three unmodified AAV capsid proteins, four protein bands, GFP-VP2, VP1, VP2 and VP3, were visible (lane 6).

Further, we performed a detailed titer analysis. Therefore each virus mutant was packaged at least a second time. The capsid, genomic and infectious titers of these preparations were determined and empty-to-full and genomic particle-to-infectivity ratios were calculated to directly compare the different preparations for packaging efficiency and infectivity (Tab.1). No significant difference between mutants (including wild-type) was observed for genomic nor capsid titers which ranged between  $1.3 \times 10^{11}$  and  $1.5 \times 10^{12}$ , and  $7.35 \times 10^{12}$  and  $1.36 \times 10^{13}$  per ml, respectively. The ratios of empty-to-full capsids varied to nearly the same extent for different preparations of the same virus mutant (including wild-type) as between the different mutants. This reveals that the deletion of VP2 or the substitution by GFP-VP2 does not interfere with capsid formation or viral genome packaging. The genomic particle-to-infectivity ratios were slightly increased for VP2 k.o.- and the 100%-GFP-VP2-AAV-preparations, but remained within the variation described for wild-type AAV preparations (Girod *et al.*, 1999; Grimm *et al.*, 1999; Ried *et al.*, 2002). The results revealed that GFP-tagged virions with a 100 % substitution of VP2 by GFP-VP2 can be generated with high titers ( $2 \times 10^9$  infectious particles/ml).

**Table1. Characterization of the different viral preparations.** *Titers were determined by quantitative PCR, A20 ELISA and infectious titer assay, respectively (\*per ml; a, b, c: independently packaged).*

| preparation                   | genomic particle*      | physical particle*     | infectious particle*   | empty/full | genomic/infectivity |
|-------------------------------|------------------------|------------------------|------------------------|------------|---------------------|
| wild-type AAV <sup>a</sup>    | 2.49 x10 <sup>11</sup> | 1,25 x10 <sup>13</sup> | 8.38 x10 <sup>9</sup>  | 50.2       | 29                  |
| wild-type AAV <sup>b</sup>    | 1.04 x10 <sup>12</sup> | 1,19 x10 <sup>13</sup> | 1.67 x10 <sup>10</sup> | 11.4       | 62                  |
| VP2 k.o.-AAV <sup>a</sup>     | 1.30 x10 <sup>11</sup> | 9.39 x10 <sup>12</sup> | 1.31 x10 <sup>8</sup>  | 72.2       | 991                 |
| VP2 k.o.-AAV <sup>b</sup>     | 1.17 x10 <sup>12</sup> | 1.41 x10 <sup>13</sup> | 4.19 x10 <sup>9</sup>  | 12.1       | 278                 |
| 60%-GFP-VP2-AAV <sup>a</sup>  | 7.01 x10 <sup>11</sup> | 1.04 x10 <sup>13</sup> | 8.38 x10 <sup>9</sup>  | 14.8       | 84                  |
| 60%-GFP-VP2-AAV <sup>b</sup>  | 2.15 x10 <sup>11</sup> | 1.25 x10 <sup>13</sup> | 2.10 x10 <sup>9</sup>  | 58.1       | 102                 |
| 60%-GFP-VP2-AAV <sup>c</sup>  | 4.10 x10 <sup>11</sup> | 7.35 x10 <sup>12</sup> | 2.10 x10 <sup>9</sup>  | 17.9       | 195                 |
| 100%-GFP-VP2-AAV <sup>a</sup> | 3.00 x10 <sup>11</sup> | 1.36 x10 <sup>13</sup> | 1,31 x10 <sup>8</sup>  | 45.3       | 2288                |
| 100%-GFP-VP2-AAV <sup>b</sup> | 4.39 x10 <sup>11</sup> | 9.71 x10 <sup>12</sup> | 2,10 x10 <sup>9</sup>  | 22.2       | 208                 |
| 100%-GFP-VP2-AAV <sup>c</sup> | 1.5 x10 <sup>12</sup>  | 1.09x10 <sup>13</sup>  | 1.05 x10 <sup>9</sup>  | 7.2        | 1431                |

### Visualization of viral infection by GFP-VP2 tagged AAV particles

To determine, if GFP-tagged virions were suited for intracellular visualization, viral infections of HeLa cells followed by wide field fluorescent microscopic analysis 2 p.i. were performed. GFP signals seemed to localize partly in the nucleus or perinuclear area in cells infected with the 60%- and 100%-GFP-VP2-AAV preparations (Figure 4A and Figure 4B). The fluorescent microscopy images obtained thus resembled published results with unlabeled or chemically labelled virions (Bartlett *et al.*, 2000; Seisenberger *et al.*, 2001). No signal was detected inside the cell when soluble heparin was used, demonstrating that the GFP signal was not due to pseudo-transduction (Figure 4C).

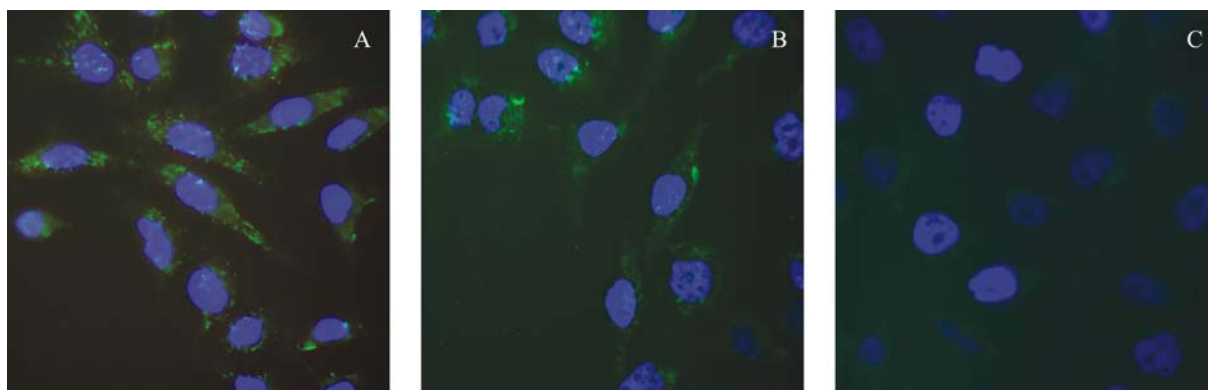


**Figure 4: GFP-tagged virions analyzed by wide field fluorescent microscopy.** Cells were infected with  $5 \times 10^6$  capsids per cell of 100%-GFP-VP2-AAV (A) and 60%-GFP-VP2-AAV (B and C) in the absence (A and B) or presence of heparin (C). Cells were fixed and nuclei were stained with Dapi.

A promising development in the field of fluorescent microscopy is live cell imaging. Infection of live HeLa cells with GFP-tagged AAV virions followed by live cell imaging microscopy allowed the visualization of virions undergoing cell membrane contact (Figure 5 as movie in supplement). Some of these virions touched the cell membrane multiple times similar to the observations, made previously by SVT (Seisenberger *et al.*, 2001). As observed in fluorescent microscopy, most of the virions stacked to the membrane, again confirming previous SVT observations, which showed that less than half of the virions enter the cell (Seisenberger *et al.*, 2001). Furthermore, GFP-tagged virions seem to move inside the cytoplasm of infected cells and in the perinuclear area (Figure 5 as movie in supplement), suggesting the potential of this technology for real-time imaging studies.

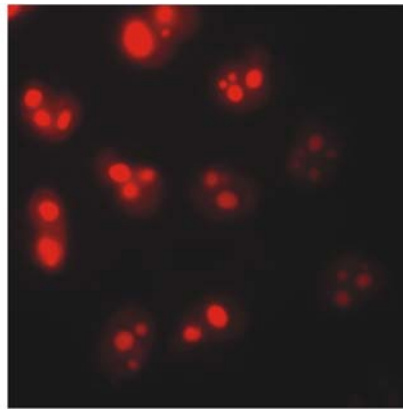
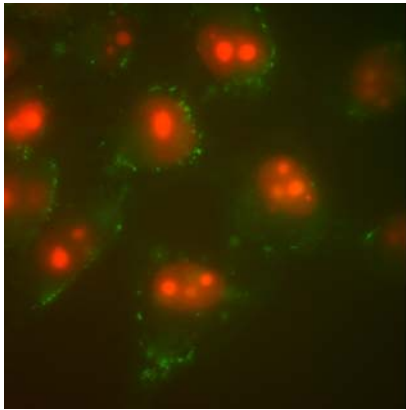


**Figure 5: Live cell imaging of GFP-tagged virions.** HeLa-DsRed2Nuc cells were infected with 60%-GFP-VP2-AAV ( $10^6$  capsids per cell). Cells were incubated for 20 min at 37°C and 5% CO<sub>2</sub>. Then live cell movies were obtained under physiological conditions. Still image obtained from the movie supplied in supplement (left panel). Heparin control (right).

### GFP-tagged virions within the cell are recognized by A20

To assess if the GFP signals within the cell are emitted from intact viral particles, cells were infected with 100%-GFP-AAV and fixed at 2, 4, 11 and 24 h p.i. Intact viral capsids were stained by A20 (A20 recognizes whole but not dissociated AAV capsids (Blecker *et al.*, 2005)) whereas an anti-lamin B antibody was used to visualize the nuclear membrane. Figure 6 shows one example obtained by confocal microscopy. GFP-tagged AAV particles recognized by A20 were detected within the cell and above the nuclear membrane. An almost 100% colocalization of the GFP-signals (upper left panel) with A20 reactive AAV capsids (upper right panel) was observed (merge: lower right panel). The few detectable non-colocalized signals were due to a very faint A20 signal which became visible after enhancing its excitation energy. Thus GFP signals visible within the cells emanate from intact virions.

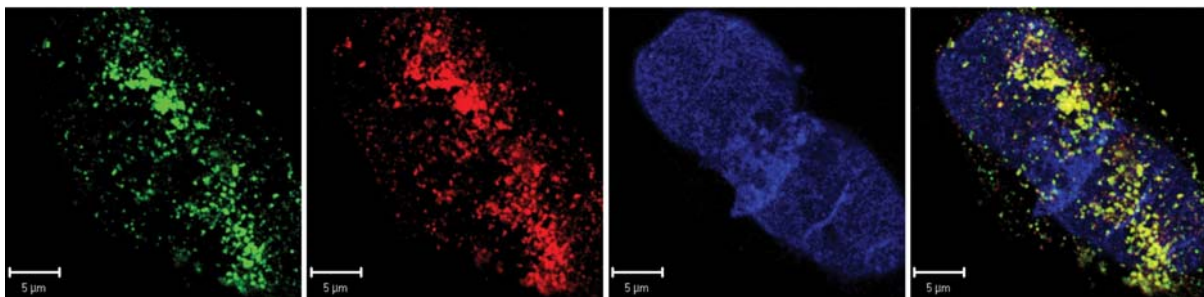


**Figure 6: Intact 100%-GFP-VP2-AAV particles within the cell.** HeLa cells were infected with 100%-GFP-VP2-AAV ( $10^6$  capsids per cell). 4 h p.i., cells were fixed and stained with A20 (recognizes intact AAV capsids; RRX conjugated secondary antibody) and anti-lamin B antibody (nuclear membrane; Cy5 conjugated secondary antibody). (upper left panel: GFP staining; upper right panel: A20 staining; lower left panel: anti-lamin B; lower right panel: merge). Analysis was performed by confocal microscopy.

### **Viral capsids do not enter the nucleus efficiently**

In order to analyze the time course of nuclear entry of AAV in more detail, HeLa cells were infected with 100%-GFP-VP2-AAV for 2, 4, 11 and 24 h with or without adenovirus type 5 coinfection (MOI 5), and confocal laser scanning images were obtained. For each image, a series of horizontal sections of 0.2  $\mu\text{m}$  was prepared (z-stack) and superimposed with the Leica confocal software. Figure 7B shows a typical image obtained 4 p.i. without adenovirus coinfection. Many GFP signals were visible in the nucleus of the infected cells (nuclear lamina stained in red by anti-lamin B antibody). This image leads to the assumption that GFP-tagged virions were efficiently transported into the nucleus within less than 4 hours, consistent with published results (Bartlett *et al.*, 2000). However, the Leica confocal software enables the vertical sectioning of the superimposed pictures and allows to visualize a certain image plane within this stack. The investigator can determine if a certain signal emanates within, above or below the image plane and this enables the investigator to localize the object of interest more precisely. Using this technique, we could determine that in the absence of helpervirus and up to 4 h p.i., the GFP signals (from the GFP-tagged virions) were localized above but not within the nucleus (upper row in Figure 7C). This is in contrast to results derived from the superimposed picture (Figure 7B) indicating its limitations. At 24 h p.i. isolated signals were visible inside the nucleus (arrows in upper row of Figure 7C).

Moreover, in the superimposed picture of cells coinfecting with adenovirus many GFP signals were observed in the nucleus 2 h p.i. Applying the new vertical sectioning method uncovered that most of the signals are localized above the nucleus (lower row in Figure 7C). With prolonged incubation time, the amount of coinfecting cells showing a GFP signal inside the nucleus slightly increased (e.g. 4 h p.i.), but still the majority of signals were found outside the nucleus. Even after prolonged incubation (up to 11 h, data not shown) more than 90% of the GFP signals remained outside the nucleus.

Interestingly, 24 h p.i. many coinfecting cells showed a diffused GFP distribution within the nucleus. This phenomenon was not observed in the absence of helpervirus coinfection even after prolonged observation times (48 h, data not shown). Since this image resembles the image obtained after transfection with pGFP-VP2 (Figure 7D), we analyzed the viral preparations used to infect the cells and the respective viral infected cells by PCR. These analyses revealed that GFP sequences were packaged into the viral capsid, although the plasmid used to express GFP-VP2 during the packaging process contained no AAV ITRs. It remains to be elucidated whether this is attributed to recombination or other events.

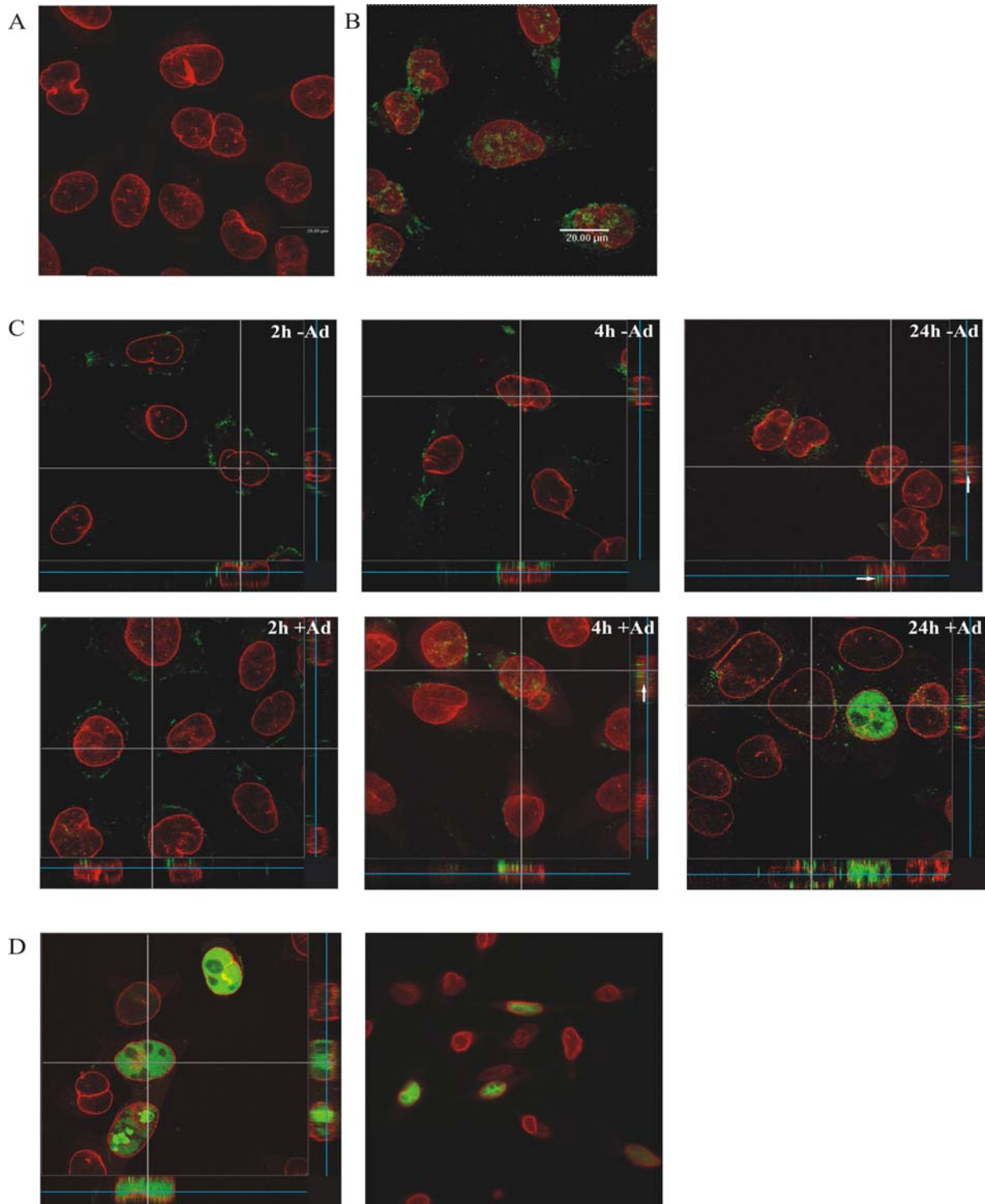
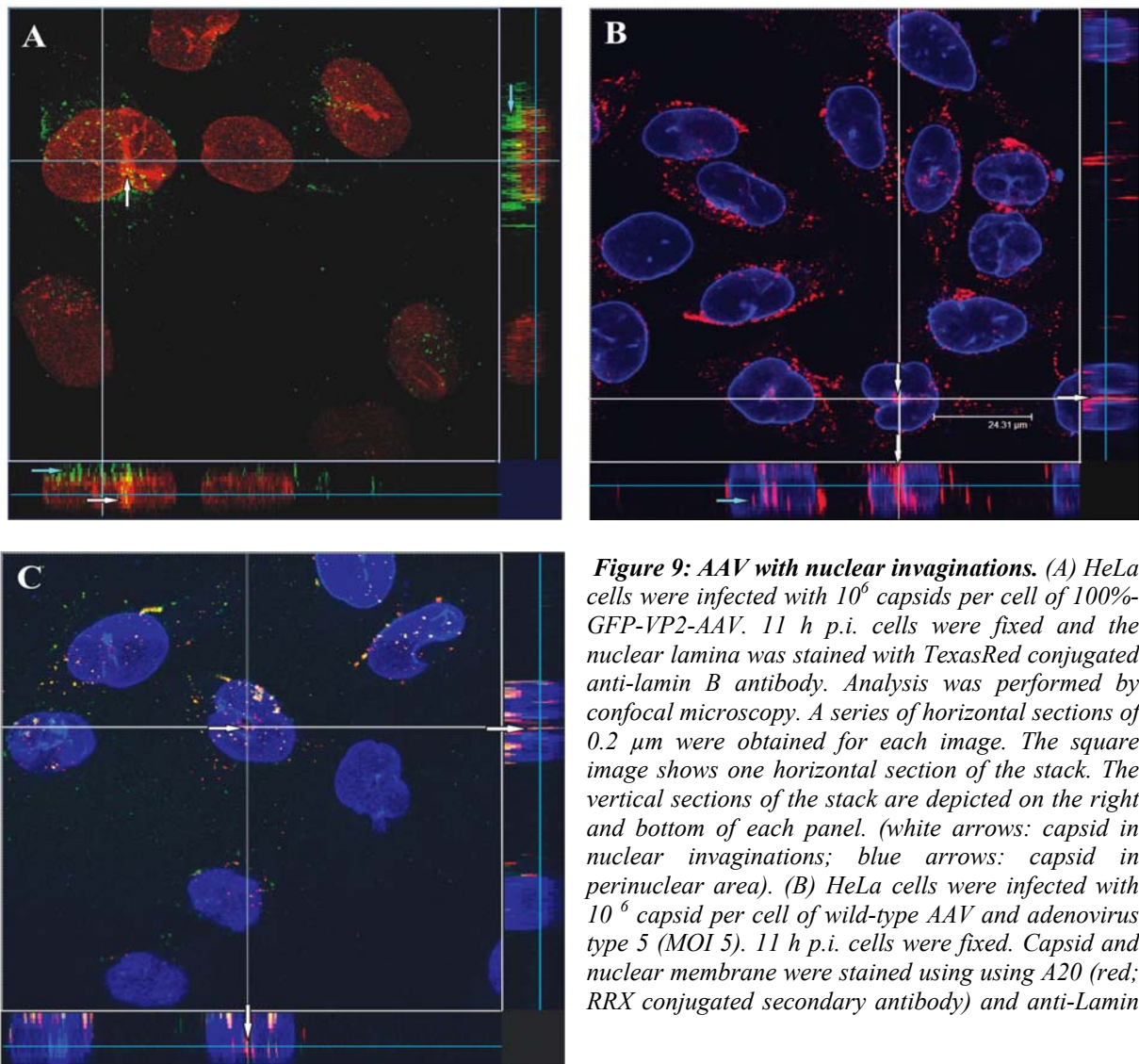


**Figure 7: Time course of AAV infection visualized by GFP-tagged AAV virions.** HeLa cells were infected with  $10^6$  capsids per cell of 100%-GFP-VP2-AAV with or without adenovirus type 5 (MOI 5) coinfection. In addition a heparin control was included (A). 2, 4 and 24 h p.i. cells were fixed and the nuclear lamina was stained with TexasRed conjugated anti-lamin B antibody. A series of horizontal sections of  $0.2 \mu\text{m}$  were obtained for each image. With Leica confocal software all images of a series were superimposed. (B) Superimposed image of a series of sections 4 h p.i. in the absence of adenoviral coinfection. (C) Time course of infection with and without adenovirus (Ad5) coinfection. The square image shows one horizontal section of the stack. The vertical sections of the stack are depicted on the right and bottom of each panel. Arrows show GFP signals detected within the nucleus. (D) Comparison of images obtained 24 h p.i. in the presence of adenovirus (left panel) and after transfection of pGFP-VP2 (right panel).

To exclude that the observed results are due to inefficient nuclear transport of the GFP-tagged virions, the same experiments were performed with wild-type AAV in Ad5 coinfecting cells. For detection of viral capsids and viral capsid proteins A20- and B1- antibodies were used, respectively. A20 recognizes intact but not dissociated AAV capsids whereas B1 binds to amino acid 726-733 at the C-terminus of all 3 capsid proteins (Blecker *et al.*, 2005). At 2, 4 and 11 h p.i. almost no B1 staining was detectable, in marked contrast to A20 staining (data not shown). At 4 and 11 h p.i., no difference was observed when comparing GFP-tagged with wild-type virions (Figure 9B shows one example 11 h p.i.). At these time points only isolated intact capsids (recognized by A20) were found within the nucleus and the majority (over 90%) of the virions were visible outside the nucleus (Figure 9B). At 24 h p.i. both antibodies were able to recognize their targets and resulted mainly in a nuclear staining (data not shown). This suggests that at this time point, new viral capsid proteins have been synthesized in the Ad5 coinfecting cells and new capsids have been formed.



*B antibody (blue: Cy5 conjugated secondary antibody), respectively. Microscopical analyses were performed as described in (A). Under these conditions isolated signals of intact capsid were detectable inside the nucleus (blue arrow). In addition, viral capsid within nuclear invaginations have been observed (white arrow). (C) HeLa cells were infected with  $10^6$  capsid per cell of 100%-GFP-VP2-AAV and coinfecting with adenovirus type 5 (MOI 5). 2 h p.i. cells were fixed. Capsids and nuclear membrane were stained using A20 (red; RRX conjugated secondary antibody) and anti-Lamin B antibody (blue: Cy5 conjugated secondary antibody), respectively. Microscopical analyses were performed as described in (A). GFP-tagged virions in nuclear invaginations were recognized by A20 (white arrow).*

From this we propose that an adenoviral function augments the nuclear translocation of viral capsids. However, the low level of GFP or A20 signals detected within the nucleus suggests a very inefficient nuclear translocation. Thus, uncoating seems to occur before or during nuclear entry.

To further investigate this hypothesis, HeLa cells were infected by wild-type AAV using 10x less virions per cell. Infections were performed with and without helpervirus. Since viral replication in adenovirus coinfecting cells is reported to start between 8 and 12 h p.i. (Mouw and Pintel, 2000; Xiao *et al.*, 2002), infections were stopped at 2, 4, and 11 h p.i. To visualize viral genomes FISH hybridization was performed. In addition, viral capsids and the nuclear lamina were stained by antibodies (Fig. 8A and 8B). Viral genomes were detectable outside and within the nucleus at 11 p.i. (Figure 8A and arrows in Figure 8B). No colocalization of viral genomes and intact viral capsids was observed within the nucleus, whereas colocalizations were detectable in the perinuclear area and within the cytoplasm (A20: red signals in the upper right panel of Figure 8A and merge). In addition empty capsids (no colocalization) were visible in the perinuclear area. Some of the FISH signals in the perinuclear area showed no colocalization with A20 and therefore with intact capsids. It has yet to be investigated if these signals emanate from free viral genomes or if they colocalize with one of the three VP proteins. The same image was obtained using a comparable amount of viral genomes in the absence of helpervirus, revealing that the observed viral genomes originate from incoming virions and are not the result of viral replication. Furthermore, it allows the assumption that a nearly comparable nuclear transport of viral genomes occurs with or without helpervirus. Interestingly, viral genomes within the nucleus are already detectable at earlier time points (2 and 4 h p.i.) both in the presence and absence of Ad5 although 10x less virions per cell were used than for the capsid studies (Figure 6, 7 and 9). Under these conditions ( $10^5$  instead of  $10^6$  capsids per cell) viral capsids are detected within the cell, but none of these localize within the nucleus as shown as an example in Figure 8B.

All these observations strongly support the hypothesis that uncoating of AAV occurs during or before nuclear entry. However, at the current state it can not be excluded that viral genomes within the nucleus are associated with one of the three viral capsid proteins.

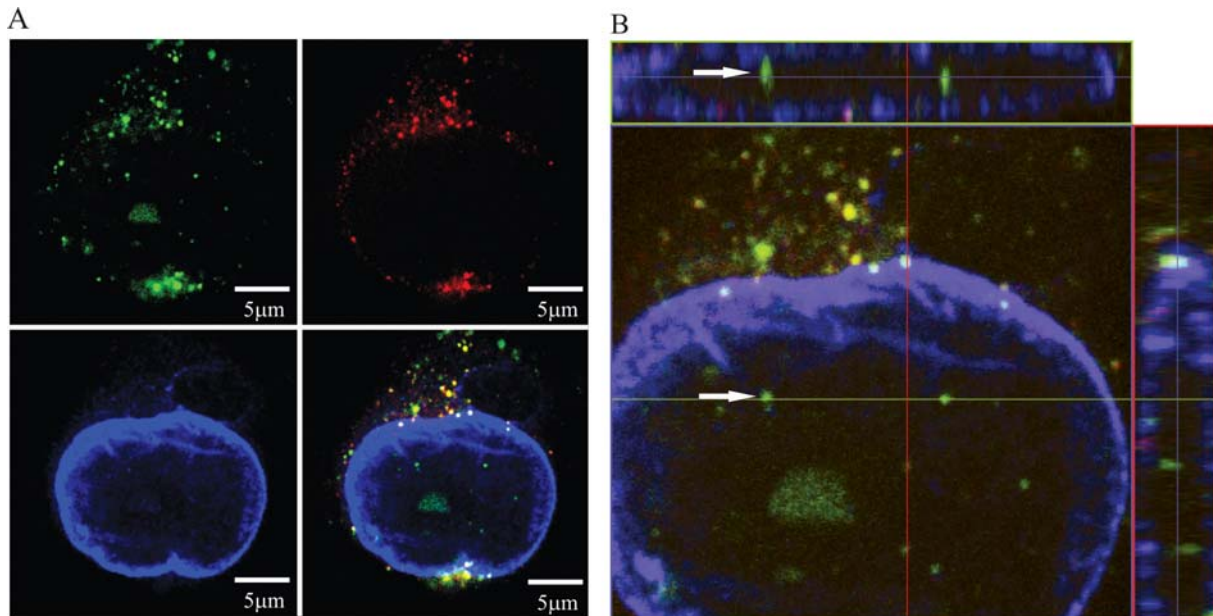


**Figure 8: Visualization of viral genomes by FISH hybridization.** (A) HeLa cells were infected with wild-type AAV ( $10^5$  capsids per cell = 8700 genomic particles per cell) and adenovirus type 5 (MOI 5). Cells were fixed 11 h p.i. FISH hybridization (green, Oregon green labelled DNA probe) was performed to visualize viral genomes, whereas intact capsids and nuclear membrane were stained using A20 (red; RRX conjugated secondary antibody) and anti-Lamin B antibody (blue: Cy5 conjugated secondary antibody), respectively. Analyses were performed by confocal microscopy and one image plane out of a z-stack is shown (upper left panel: FISH hybridization; upper right panel: A20; lower left panel: anti-Lamin B; lower right panel: merge). (B) Enlargement and vertical sectioning of merge shown in (A). The arrows show one example of a viral genome localized within the nucleus.

(viral genome: green, Oregon green labelled DNA probe; intact capsid: red, A20 recognized by RRX conjugated secondary antibody, nuclear membrane: blue: anti-Lamin B recognized by Cy5 conjugated secondary antibody)

### AAV is found in nuclear invaginations

Single particles have been shown to reach the nuclear area within seconds (Seisenberger *et al.*, 2001) and a perinuclear accumulation of AAV was described to occur within 1-2 h p.i. (Bartlett *et al.*, 2000; Xiao *et al.*, 2002). Interestingly, we observed in addition AAV particles within tubular channels, which extend deeply into the nucleoplasm (Figure 9). This could first be assumed from SVT analysis. Within our SVT studies we had observed that AAV moved very quickly on certain “pathways” through the nuclear area and we hypothesized that these “pathways” might be nuclear invaginations, which are tubular structures derived from the

nuclear envelope. The enclosed core is continuous with the cytoplasm and may function to bring larger proportions of the nucleoplasm close to a nuclear pore (Fricker *et al.*, 1997). In addition, a function of these nuclear channels in transport processes has been proposed (Dupuy-Coin *et al.*, 1986). Within our current analysis, we observed AAV particles within nuclear invaginations (visualized by nuclear lamina staining), which verify our former assumptions (Seisenberger *et al.*, 2001). These pictures were obtained for both, the GFP-tagged virions (Figure 9A and 9C) and wild-type AAV (Figure 9B). The capsids were recognized in both cases by A20 revealing that intact viral capsids were detected within the nuclear invaginations. Although the significance of this colocalization has to be clarified, it explains the directed motion along defined pathways through the nuclear area observed by SVT.

## Discussion

To track the intracellular trafficking of AAV and derived vectors in infected cells, we have tagged virions by incorporation of GFP-VP2 into the viral capsid. In a first step chimeric virions containing VP1, VP2, GFP-VP2 and VP3 were produced. GFP-tagged AAV particles could also be generated without the addition of wild-type VP2. This observation is in contrast to Yang *et al.* (1998), who showed that the AAV capsid is not able to tolerate large insertions at the N-terminus of VP2 without the simultaneous addition of wild-type VP2. This discrepancy might be due to differences in the production and purification method: Yang *et al.* expressed the different VP proteins from three different plasmids controlled by the CMV promoter, and used a CsCl density gradient for purification. In addition, remaining helpervirus was inactivated by heat. Using the natural AAV viral promoters and a helpervirus-free production method allowed to efficiently generate particles with N-terminal VP2-fusions of different size (Loiler *et al.*, 2003; Shi *et al.*, 2001; Warrington *et al.*, 2004; Wu *et al.*, 2000). The largest insertion described so far is the 30 kDa GFP protein used by Warrington *et al.* and in our study. Interestingly, although Warrington and colleagues used the same amino acid position (aa 138) for the VP2 fusion, the genomic particle-to-infectivity ratio reported by Warrington *et al.* was remarkably higher (up to 130 fold less infectious) than ratios obtained for our GFP-tagged virions (Warrington *et al.*, 2004). In addition an up to 30 fold higher amount of empty capsids was detected within their study. We observed a genomic particle-to-infectivity ratio between 84 and 195 for 60%-GFP-VP2-AAV, and between 208 and 2288 for

the 100%-GFP-VP2-AAV, which is higher than ratios obtained for the wild-type AAV within our study (29 and 62), but still in the range described for wild-type preparations (Ried *et al.*, 2002). Furthermore, no increase in the amount of empty capsids was detected. Since we used the same amino acid position for the fusion (aa 138), the differences observed must have been caused by other factors. One main difference could be the choice of the promoter responsible for the transcription of VP2. Warrington *et al.* used the natural p40 promoter, and translation was initiated from a modified and therefore stronger start codon (ATG instead of ACG), which resulted in a more efficient VP2 and in the inhibition of VP3 initiation from this template. In our case, the viral CMV promoter was used to control the transcription of the fusion protein and the VP2 translation start codon was deleted. Warrington and colleagues performed a Western blot of their GFP-tagged virions. When comparing their Western blot results with the results obtained for our GFP-tagged virions packaged in the presence of pGFP-VP2 (Figure 3) the most obvious difference was the amount of VP1 detected in the GFP-tagged virion preparations. While the preparations of Warrington and colleagues showed a clear reduction for the VP1 signal, the amount of VP1 in our preparations was comparable to wild-type AAV. It is known that VP1 - possibly because of its phospholipase activity - is essential for AAV infectivity (Blecker *et al.*, 2005; Girod *et al.*, 2002; Warrington *et al.*, 2004; Wu *et al.*, 2000). Therefore the reduced amount of VP1 within the preparations of Warrington *et al.* might be a reasonable explanation for the lower infectivity of the vectors produced by Warrington and colleagues and the discrepancy to our results. It remains unknown if the modification of the VP2 translation start codon as carried out by Warrington and colleagues or other factors are responsible for the VP1 reduction. However, our preparations yielded an up to 130 fold increased viral infectivity in comparison to Warrington *et al.* with an infectious titer of  $10^9$  per ml. These GFP-tagged virions were comparable to wild-type AAV. This assumption is based on our direct comparison with wild-type AAV and on antibody colocalization studies (Figure 6, 9).

According to the current model of AAV infection, AAV enters host cells by receptor-mediated endocytosis, which is a very fast process that occurs in approximately 60 ms (Seisenberger *et al.*, 2001). Within the first 10 minutes, two-thirds of membrane bound virus particles are internalized (Bartlett *et al.*, 2000). The endocytotic process and the subsequent trafficking steps are still poorly understood and may differ substantially in different, and in some cases even in the same cell types (Duan *et al.*, 2000; Hansen, Qing and Srivastava, 2001). The release of AAV from the endosomes is believed to take place at the late

endosomal stage and requires a low endosomal pH (Bartlett *et al.*, 2000). Thereafter, the destiny of AAV remains unclear. Some studies have observed perinuclear accumulation within 1-2 h p.i., which persisted in the absence of adenovirus coinfection for at least 16 h (Warrington *et al.*, 2004, Xiao *et al.*, 2002). In contrast, using laser scanning confocal microscopy, Bartlett observed AAV particles within the nucleus of infected cells already 2 h p.i. despite the absence of helpervirus (Bartlett *et al.*, 2000).

In this study, we observed that intracellular trafficking of GFP-tagged virions occurs quickly at least in HeLa cells. This is in agreement with results obtained with SVT. This sensitive method allows the observation of single particles in a living cell. Due to this high sensitivity it was possible for us to detect at least one AAV particle in the nuclear area of 50% of the cells 15 minutes p.i. In some cases AAV reached the nuclear area within seconds (Seisenberger *et al.*, 2001). In contrast to this, the nuclear entry of intact AAV capsids is comparably slow. Although many virions were already accumulated in the perinuclear area before 2 h p.i. we observed in the absence of helpervirus coinfection only isolated GFP signals from the GFP-VP2-AAV particles within the nucleus of cells at 11 and 24 h p.i. (no signal at 2 or 4 h p.i.). This result clearly contradicts results described by Bartlett *et al.*, who observed in the absence of helpervirus AAV particles inside the nucleus 2 h p.i. (Bartlett *et al.*, 2000). This can be explained by the limited microscopic possibilities available at that time.

In adenovirus coinfecting cells, already 2 h p.i. (earliest time point observed) GFP signals were observed within the nucleus, revealing that adenovirus is able to augment nuclear entry of AAV capsids. These results confirm previous observations that described intact viral particles within the nucleus of coinfecting cells in less than 1 h p.i. (Warrington *et al.*, 2004, Xiao *et al.*, 2002). However, the amount of AAV capsids we observed by applying the new vertical sectioning method for data analysis was much lower than described by e.g. Xiao *et al.* (Xiao *et al.*, 2002). In all conditions and at all time points analyzed during this study, only very few GFP signals provided by the GFP-VP2-AAV particles could be detected within the nucleus. This was not due to the GFP-VP2-AAV virions used to analyze this step of the infectious biology, since the same image was obtained with wild-type AAV visualized by A20 (Figure 9).

We assume that the transport of intact viral capsids into the nucleus of infected cells is a very inefficient process, and that viral uncoating takes place before or during nuclear entry independent of helpervirus coinfection. The very low amount of intact particles observed in the nucleus of cells infected with  $10^6$  viral capsids per cell could be due to unspecific events

and is likely to be not necessary for viral replication. This model is suggested by the comparison of the amount of viral genomes with the amount of capsids detected within the nucleus at different time points of the infection in the presence and absence of helpervirus: Neither in the presence nor in the absence of helpervirus intact viral capsids were detected within the nucleus of cells infected with  $10^5$  instead of  $10^6$  viral capsids per cell. In contrast, under the same condition already 2 h p.i. viral genomes were detected within the nucleus with a slight increase in signals with prolonged observation times. This argues for an uncoating of AAV before or during nuclear entry independent of helpervirus coinfection.

## Acknowledgements

This work was supported by the Deutsche Forschungsgemeinschaft (SFB 455 (M.H., L.P., J. E., D.G., S.F., H.B.) and SP 658/2-1 (K.L., H.B.)), the Promotionsstudiengang Molekulare Medizin (N.G.) and the Bayerische Forschungstiftung (M.H., H.B.). Furthermore, we would like to thank Prof. Dr. Richard Jude Samulski (University of North Carolina at Chapel Hill, USA) for kindly providing pXX6 and PD Dr. Jürgen Kleinschmidt (DKFZ Heidelberg, Germany) for kindly providing us with the A20 and B1 antibodies.

# **Chapter VII**

## Conclusion and Outlook

Refinement of procedures for the generation of neutralization resistant virions will contribute to the success of AAV as vector for human gene therapy.

Immune-evading variants of a successful vector have to meet two requirements. On one hand the antibody-mediated neutralization should be significantly reduced, while on the other the targeting ability should not be affected. As of yet, the generated mutants are still neutralized by serum concentrations inferior to the situation found *in vivo*. However, the successful selection of enhanced second-generation mutants and the established technologies such as *error prone* PCR, DNA shuffling and *evolution monitoring* suggest the potential for further improvement of the immune-evading phenotype by additional directed evolution. It has been shown that different epitopes are recognized by individual sera (Huttner *et al.*, 2003). Accordingly, clones containing an accumulation of mutations, which affect the most relevant immunogenic epitopes should reduce the observed serum-dependent variations of the immune-escaping effectivity. Selections using a large number of different sera and DNA shuffling of thereof derived successful mutants should yield novel vectors which retain infectivity in presence of most human sera. It is further planned to test the mutants in pre-immunized animals to allow an evaluation under *in vivo* conditions.

In addition to the problem of vector neutralization by serum antibodies, directed evolution holds the potential to address other challenges in gene therapy. However, the best results will likely be achieved by a combination of different successful approaches. One of the major problems for safe and efficient AAV-based gene therapy is the lack of tissue-specific targeting vectors. Although effective targeting to AAV non-permissive cells has been achieved by insertion of appropriated ligands in the wt capsid or direct selection from insertional targeting libraries (Girod *et al.*, 1999; Perabo *et al.*, 2003; Muller *et al.*, 2003), these method mostly generated vectors with extended tropism that, however, lacked selectivity (Perabo *et al.*, 2003). This was due to targeting of widely expressed receptors and because of the existence of important receptor binding domains on the capsid, which remain functional despite the insertions. The generation of efficient and specific vectors will therefore require a combination of retargeting to specific receptors and detargeting from the natural tropism. For this purpose a targeting library with a randomized peptide insertion at position 587 (VP1 numbering) has been subjected to *error prone* PCR creating a combined library (Fig. 1).

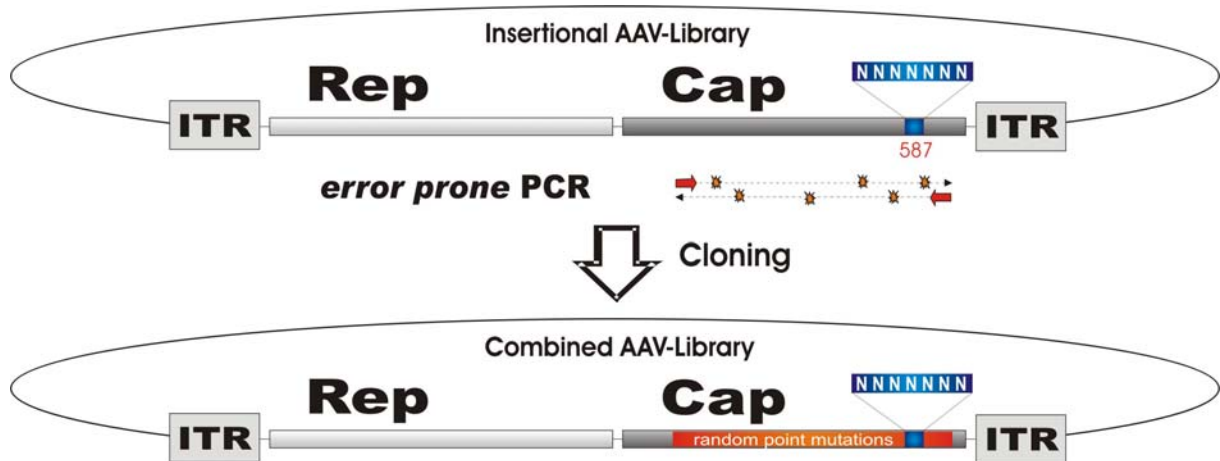


**Figure 1. Generation of a combined library.** Insertional mutagenesis is combined with random point mutations scattered throughout the viral capsid. For this goal, a region of the cap gene of an AAV library carrying a 7 aa long random insertion at the 587 position is further randomized by error prone PCR thus yielding a combined library.

This library can be screened by alternating rounds of positive selection steps on target cells and negative selections on non-target cells (noise cells) (Fig. 2A). 48 hrs post infection the replicated virions can be harvested from the target cells and incubated on noise cells. Mutants with reduced ability to bind noise cells can be harvested with the supernatant and used for a subsequent selection cycle. This process should result in the identification of clones with targeting efficiency provided by the selected insertion and selectivity provided by natural tropism-abolishing mutations.

Similar results can be achieved by the establishment of *in vivo* selection protocols (Fig 2B). The library can be administered intravenously to an animal and specific variants can be isolated from target tissue, e.g. a specific organ, tissue or previously introduced tumoral cells. As before, re-iteration should yield virions, which exhibit a high infectivity for the tissue of interest but a reduced ability to infect other cell types.

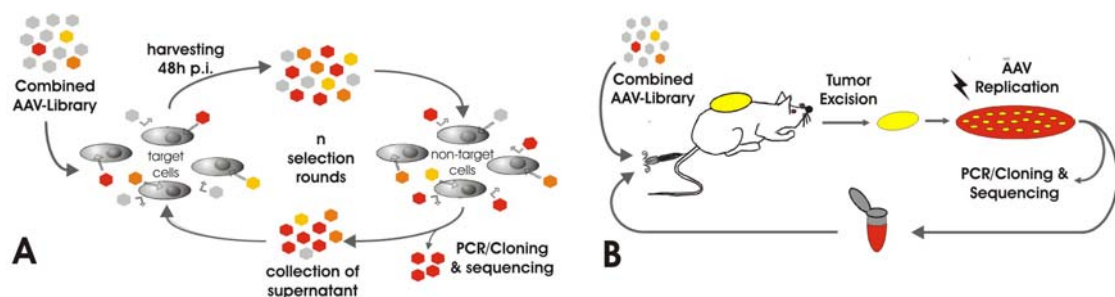


**Figure 2. Example of protocols for selection of efficient and specific mutants using a combined library.** A) Target cells are infected with the library. 48 hrs p.i. the harvest is briefly incubated on non-target cells to eliminate unspecific virions by infection. The supernatant is collected and used for additional cycles. B) *in vivo* biopanning protocol. After intravenous injection viral progeny is collected from the target tissue (e.g. induced tumor). Re-iteration after amplification of virions leads to selection of tissue-specific vectors.

Moreover, previously described targeting mutants could be optimized applying *error prone* PCR, DNA shuffling and selection protocols.

We anticipate that *error prone* PCR-based libraries, DNA shuffling and *evolution monitoring* could also be applied to engineer viral vector families other than AAV to obtain clones with improved phenotypes.

---

## Bibliography

- Acland, G. M., Aguirre, G. D., Ray, J., Zhang, Q., Aleman, T. S., Cideciyan, A. V., Pearce-Kelling, S. E., Anand, V., Zeng, Y., Maguire, A. M., Jacobson, S. G., Hauswirth, W. W., and Bennett, J.** (2001). Gene therapy restores vision in a canine model of childhood blindness. *Nat Genet* **28**(1), 92-5.
- Agbandje, M., Kajigaya, S., McKenna, R., Young, N. S., and Rossmann, M. G.** (1994). The structure of human parvovirus B19 at 8 Å resolution. *Virology* **203**(1), 106-15.
- Agbandje-McKenna, M., Llamas-Saiz, A. L., Wang, F., Tattersall, P., and Rossmann, M. G.** (1998). Functional implications of the structure of the murine parvovirus, minute virus of mice. *Structure* **6**(11), 1369-81.
- Allen, J. M., Halbert, C. L., and Miller, A. D.** (2000). Improved adeno-associated virus vector production with transfection of a single helper adenovirus gene, E4orf6. *Mol Ther* **1**(1), 88-95.
- Anderson, R., Macdonald, I., Corbett, T., Whiteway, A., and Prentice, H. G.** (2000). A method for the preparation of highly purified adeno-associated virus using affinity column chromatography, protease digestion and solvent extraction. *J Virol Methods* **85**(1-2), 23-34.
- Atchison, R. W., Casto, B. C., and Hammon, W. M.** (1965). Adenovirus-associated defective virus particles. *Science* **149**, 754-756.
- Auricchio, A., Hildinger, M., O'Connor, E., Gao, G. P., and Wilson, J. M.** (2001). Isolation of highly infectious and pure adeno-associated virus type 2 vectors with a single-step gravity-flow column. *Hum Gene Ther* **12**(1), 71-6.
- Awedikian, R., Francois, A., Guilbaud, M., Moullier, P., and Salvetti, A.** (2005). Intracellular route and biological activity of exogenously delivered Rep proteins from the adeno-associated virus type 2. *Virology* **335**(2), 252-63.
- Bantel-Schaal, U., Delius, H., Schmidt, R., and zur Hausen, H.** (1999). Human adeno-associated virus type 5 is only distantly related to other known primate helper-dependent parvoviruses. *J Virol* **73**(2), 939-47.
- Baranowski, E., Ruiz-Jarabo, C. M., and Domingo, E.** (2001). Evolution of cell recognition by viruses. *Science* **292**(5519), 1102-5.

- Bartlett, J. S., Kleinschmidt, J., Boucher, R. C., and Samulski, R. J.** (1999). Targeted adeno-associated virus vector transduction of nonpermissive cells mediated by a bispecific F(ab' $\gamma$ )<sub>2</sub> antibody. *Nat Biotechnol* **17**(2), 181-6.
- Bartlett, J. S., Wilcher, R., and Samulski, R. J.** (2000a). Infectious entry pathway of adeno-associated virus and adeno-associated virus vectors. *J Virol* **74**(6), 2777-85.
- Bartlett, J. S., Wilcher, R., and Samulski, R. J.** (2000b). Infectious entry pathway of adeno-associated virus and adeno-associated virus vectors. *J Virol* **74**(6), 2777-85.
- Becerra, S. P., Koczot, F., Fabisch, P., and Rose, J. A.** (1988). Synthesis of adeno-associated virus structural proteins requires both alternative mRNA splicing and alternative initiations from a single transcript. *J Virol* **62**(8), 2745-54.
- Becerra, S. P., Rose, J. A., Hardy, M., Baroudy, B. M., and Anderson, C. W.** (1985). Direct mapping of adeno-associated virus capsid proteins B and C: a possible ACG initiation codon. *Proc Natl Acad Sci U S A* **82**(23), 7919-23.
- Berns, K. I.** (1990). Parvovirus replication. *Microbiol Rev* **54**(3), 316-29.
- Berns, K. I., and Linden, R. M.** (1995). The cryptic life style of adeno-associated virus. *Bioessays* **17**(3), 237-45.
- Berns, K. I., Pinkerton, T. C., Thomas, G. F., and Hoggan, M. D.** (1975). Detection of adeno-associated virus (AAV)-specific nucleotide sequences in DNA isolated from latently infected Detroit 6 cells. *Virology* **68**(2), 556-60.
- Blacklow, N. R.** (1988a). Adeno-associated virus in humans. *Parvovirus and Human disease*, 165-174.
- Blacklow, N. R.** (1988b). Adeno-associated virus of humans. In "Parvoviruses and human disease" (J. Pattison, Ed.), pp. 165-174. CRC Press, Boca Raton, FL.
- Blacklow, N. R., Hoggan, M. D., Kapikian, A. Z., Austin, J. B., and Rowe, W. P.** (1968). Epidemiology of adenovirus-associated virus infection in a nursery population. *Am J Epidemiol* **88**(3), 368-78.
- Blacklow, N. R., Hoggan, M. D., and Rowe, W. P.** (1968). Serologic evidence for human infection with adenovirus-associated viruses. *J Natl Cancer Inst* **40**(2), 319-27.
- Blacklow, N. R., Hoggan, M. D., Sereno, M. S., Brandt, C. D., Kim, H. W., Parrott, R. H., and Chanock, R. M.** (1971). A seroepidemiologic study of adenovirus-associated virus infection in infants and children. *Am J Epidemiol* **94**(4), 359-66.
- Brockstedt, D. G., Podsakoff, G. M., Fong, L., Kurtzman, G., Mueller-Ruchholtz, W., and Engleman, E. G.** (1999). Induction of immunity to antigens expressed by

- recombinant adeno-associated virus depends on the route of administration. *Clin Immunol* **92**(1), 67-75.
- Buning, H., Ried, M. U., Perabo, L., Gerner, F. M., Huttner, N. A., Enssle, J., and Hallek, M.** (2003a). Receptor targeting of adeno-associated virus vectors. *Gene Ther* **10**(14), 1142-51.
- Buning, H., Nicklin, S. A., Perabo, L., Hallek, M., and Baker, A. H.** (2003b). AAV-based gene transfer. *Curr Opin Mol Ther* **5**(4), 367-75.
- Burguete, T., Rabreau, M., Fontanges-Darriet, M., Roset, E., Hager, H. D., Koppel, A., Bischof, P., and Schlehofer, J. R.** (1999). Evidence for infection of the human embryo with adeno-associated virus in pregnancy. *Hum Reprod* **14**(9), 2396-401.
- Carter, P. J., and Samulski, R. J.** (2000). Adeno-associated viral vectors as gene delivery vehicles. *Int J Mol Med* **6**(1), 17-27.
- Chalfie, M., Tu, Y., Euskirchen, G., Ward, W. W., and Prasher, D. C.** (1994). Green fluorescent protein as a marker for gene expression. *Science* **263**(5148), 802-5.
- Chang, S. F., Sgro, J. Y., and Parrish, C. R.** (1992). Multiple amino acids in the capsid structure of canine parvovirus coordinately determine the canine host range and specific antigenic and hemagglutination properties. *J Virol* **66**(12), 6858-67.
- Chao, H., Liu, Y., Rabinowitz, J., Li, C., Samulski, R. J., and Walsh, C. E.** (2000). Several log increase in therapeutic transgene delivery by distinct adeno-associated viral serotype vectors. *Mol Ther* **2**(6), 619-23.
- Chapman, M. S., and Rossmann, M. G.** (1993). Structure, sequence, and function correlations among parvoviruses. *Virology* **194**(2), 491-508.
- Chejanovsky, N., and Carter, B. J.** (1989). Replication of a human parvovirus nonsense mutant in mammalian cells containing an inducible amber suppressor. *Virology* **171**(1), 239-47.
- Cheung, A. K., Hoggan, M. D., Hauswirth, W. W., and Berns, K. I.** (1980). Integration of the adeno-associated virus genome into cellular DNA in latently infected human Detroit 6 cells. *J Virol* **33**(2), 739-48.
- Chipman, P. R., Agbandje-McKenna, M., Kajigaya, S., Brown, K. E., Young, N. S., Baker, T. S., and Rossmann, M. G.** (1996). Cryo-electron microscopy studies of empty capsids of human parvovirus B19 complexed with its cellular receptor. *Proc Natl Acad Sci U S A* **93**(15), 7502-6.

- Chirmule, N., Propert, K., Magosin, S., Qian, Y., Qian, R., and Wilson, J.** (1999). Immune responses to adenovirus and adeno-associated virus in humans. *Gene Ther* **6**(9), 1574-83.
- Chirmule, N., Xiao, W., Truneh, A., Schnell, M. A., Hughes, J. V., Zoltick, P., and Wilson, J. M.** (2000). Humoral immunity to adeno-associated virus type 2 vectors following administration to murine and nonhuman primate muscle. *J Virol* **74**(5), 2420-5.
- Christians, F. C., Scapozza, L., Cramer, A., Folkers, G., and Stemmer, W. P.** (1999). Directed evolution of thymidine kinase for AZT phosphorylation using DNA family shuffling. *Nat Biotechnol* **17**(3), 259-64.
- Collaco, R. F., Cao, X., and Trempe, J. P.** (1999). A helper virus-free packaging system for recombinant adeno-associated virus vectors. *Gene* **238**(2), 397-405.
- Cramer, A., Cwirla, S., and Stemmer, W. P.** (1996). Construction and evolution of antibody-phage libraries by DNA shuffling. *Nat Med* **2**(1), 100-2.
- Cramer, A., Raillard, S. A., Bermudez, E., and Stemmer, W. P.** (1998). DNA shuffling of a family of genes from diverse species accelerates directed evolution. *Nature* **391**(6664), 288-91.
- Cramer, A., Whitehorn, E. A., Tate, E., and Stemmer, W. P.** (1996). Improved green fluorescent protein by molecular evolution using DNA shuffling. *Nat Biotechnol* **14**(3), 315-9.
- Crystal, R. G., Sondhi, D., Hackett, N. R., Kaminsky, S. M., Worgall, S., Stieg, P., Souweidane, M., Hosain, S., Heier, L., Ballon, D., Dinner, M., Wisniewski, K., Kaplitt, M., Greenwald, B. M., Howell, J. D., Strybing, K., Dyke, J., and Voss, H.** (2004). Clinical protocol. Administration of a replication-deficient adeno-associated virus gene transfer vector expressing the human CLN2 cDNA to the brain of children with late infantile neuronal ceroid lipofuscinosis. *Hum Gene Ther* **15**(11), 1131-54.
- Culver, K. W., Anderson, W. F., and Blaese, R. M.** (1991). Lymphocyte gene therapy. *Hum Gene Ther* **2**(2), 107-9.
- de la Maza, L. M., and Carter, B. J.** (1981). Inhibition of adenovirus oncogenicity in hamsters by adeno-associated virus DNA. *J Natl Cancer Inst* **67**(6), 1323-6.
- Desai, P., and Person, S.** (1998). Incorporation of the green fluorescent protein into the herpes simplex virus type 1 capsid. *J Virol* **72**(9), 7563-8.
- Dong, J. Y., Fan, P. D., and Frizzell, R. A.** (1996). Quantitative analysis of the packaging capacity of recombinant adeno-associated virus. *Hum Gene Ther* **7**(17), 2101-12.

- Douar, A. M., Poulard, K., Stockholm, D., and Danos, O.** (2001). Intracellular trafficking of adeno-associated virus vectors: routing to the late endosomal compartment and proteasome degradation. *J Virol* **75**(4), 1824-33.
- Duan, D., Li, Q., Kao, A. W., Yue, Y., Pessin, J. E., and Engelhardt, J. F.** (1999). Dynamin is required for recombinant adeno-associated virus type 2 infection. *J Virol* **73**(12), 10371-6.
- Duan, D., Yue, Y., Yan, Z., Yang, J., and Engelhardt, J. F.** (2000). Endosomal processing limits gene transfer to polarized airway epithelia by adeno-associated virus. *J Clin Invest* **105**(11), 1573-87.
- Dubielzig, R., King, J. A., Weger, S., Kern, A., and Kleinschmidt, J. A.** (1999). Adeno-associated virus type 2 protein interactions: formation of pre-encapsidation complexes. *J Virol* **73**(11), 8989-98.
- Dupuy-Coin, A. M., Moens, P., and Bouteille, M.** (1986). Three-dimensional analysis of given cell structures: nucleolus, nucleoskeleton and nuclear inclusions. *Methods Achiev Exp Pathol* **12**, 1-25.
- Elliott, G., and O'Hare, P.** (1999). Live-cell analysis of a green fluorescent protein-tagged herpes simplex virus infection. *J Virol* **73**(5), 4110-9.
- Erles, K., Sebokova, P., and Schlehofer, J. R.** (1999). Update on the prevalence of serum antibodies (IgG and IgM) to adeno-associated virus (AAV). *J Med Virol* **59**(3), 406-11.
- Fisher, K. J., Jooss, K., Alston, J., Yang, Y., Haecker, S. E., High, K., Pathak, R., Raper, S. E., and Wilson, J. M.** (1997). Recombinant adeno-associated virus for muscle directed gene therapy. *Nat Med* **3**(3), 306-12.
- Fisher-Adams, G., Wong, K. K., Jr., Podsakoff, G., Forman, S. J., and Chatterjee, S.** (1996). Integration of adeno-associated virus vectors in CD34+ human hematopoietic progenitor cells after transduction. *Blood* **88**(2), 492-504.
- Flannery, J. G., Zolotukhin, S., Vaquero, M. I., LaVail, M. M., Muzyczka, N., and Hauswirth, W. W.** (1997). Efficient photoreceptor-targeted gene expression in vivo by recombinant adeno-associated virus. *Proc Natl Acad Sci U S A* **94**(13), 6916-21.
- Flotte, T. R.** (2005). Adeno-associated virus-based gene therapy for inherited disorders. *Pediatr Res* **58**(6), 1143-7.
- Flotte, T. R., Afione, S. A., Conrad, C., McGrath, S. A., Solow, R., Oka, H., Zeitlin, P. L., Guggino, W. B., and Carter, B. J.** (1993). Stable in vivo expression of the cystic

- fibrosis transmembrane conductance regulator with an adeno-associated virus vector. *Proc Natl Acad Sci U S A* **90**(22), 10613-7.
- Fricke, M., Hollinshead, M., White, N., and Vaux, D.** (1997). Interphase nuclei of many mammalian cell types contain deep, dynamic, tubular membrane-bound invaginations of the nuclear envelope. *J Cell Biol* **136**(3), 531-44.
- Fry, E. E., Lea, S. M., Jackson, T., Newman, J. W., Ellard, F. M., Blakemore, W. E., Abu-Ghazaleh, R., Samuel, A., King, A. M., and Stuart, D. I.** (1999). The structure and function of a foot-and-mouth disease virus-oligosaccharide receptor complex. *Embo J* **18**(3), 543-54.
- Gao, G., Qu, G., Burnham, M. S., Huang, J., Chirmule, N., Joshi, B., Yu, Q. C., Marsh, J. A., Conceicao, C. M., and Wilson, J. M.** (2000). Purification of recombinant adeno-associated virus vectors by column chromatography and its performance in vivo. *Hum Gene Ther* **11**(15), 2079-91.
- Gao, G., Vandenberghe, L. H., Alvira, M. R., Lu, Y., Calcedo, R., Zhou, X., and Wilson, J. M.** (2004). Clades of Adeno-associated viruses are widely disseminated in human tissues. *J Virol* **78**(12), 6381-8.
- Gao, G. P., Alvira, M. R., Wang, L., Calcedo, R., Johnston, J., and Wilson, J. M.** (2002). Novel adeno-associated viruses from rhesus monkeys as vectors for human gene therapy. *Proc Natl Acad Sci U S A* **99**(18), 11854-9.
- Girod, A., Ried, M., Wobus, C., Lahm, H., Leike, K., Kleinschmidt, J., Deleage, G., and Hallek, M.** (1999a). Genetic capsid modifications allow efficient re-targeting of adeno-associated virus type 2. *Nat Med* **5**(9), 1052-6.
- Girod, A., Ried, M., Wobus, C., Lahm, H., Leike, K., Kleinschmidt, J., Deleage, G., and Hallek, M.** (1999b). Genetic capsid modifications allow efficient re-targeting of adeno-associated virus type 2. *Nat Med* **5**(9), 1052-6.
- Girod, A., Wobus, C. E., Zadori, Z., Ried, M., Leike, K., Tijssen, P., Kleinschmidt, J. A., and Hallek, M.** (2002). The VP1 capsid protein of adeno-associated virus type 2 is carrying a phospholipase A2 domain required for virus infectivity. *J Gen Virol* **83**(Pt 5), 973-8.
- Glotzer, J. B., Michou, A. I., Baker, A., Saltik, M., and Cotten, M.** (2001). Microtubule-independent motility and nuclear targeting of adenoviruses with fluorescently labeled genomes. *J Virol* **75**(5), 2421-34.
- Griesenbach, U., Ferrari, S., Geddes, D. M., and Alton, E. W.** (2002). Gene therapy progress and prospects: cystic fibrosis. *Gene Ther* **9**(20), 1344-50.

- Grifman, M., Trepel, M., Speece, P., Gilbert, L. B., Arap, W., Pasqualini, R., and Weitzman, M. D.** (2001). Incorporation of tumor-targeting peptides into recombinant adeno-associated virus capsids. *Mol Ther* **3**(6), 964-75.
- Grimm, D., and Kay, M. A.** (2003). From virus evolution to vector revolution: use of naturally occurring serotypes of adeno-associated virus (AAV) as novel vectors for human gene therapy. *Curr Gene Ther* **3**(4), 281-304.
- Grimm, D., Kern, A., Pawlita, M., Ferrari, F., Samulski, R., and Kleinschmidt, J.** (1999). Titration of AAV-2 particles via a novel capsid ELISA: packaging of genomes can limit production of recombinant AAV-2. *Gene Ther* **6**(7), 1322-30.
- Grimm, D., and Kleinschmidt, J. A.** (1999). Progress in adeno-associated virus type 2 vector production: promises and prospects for clinical use. *Hum Gene Ther* **10**(15), 2445-50.
- Hacker, U. T., Gerner, F. M., Buning, H., Hutter, M., Reichenspurner, H., Stangl, M., and Hallek, M.** (2001). Standard heparin, low molecular weight heparin, low molecular weight heparinoid, and recombinant hirudin differ in their ability to inhibit transduction by recombinant adeno-associated virus type 2 vectors. *Gene Ther* **8**(12), 966-8.
- Halbert, C. L., Allen, J. M., and Miller, A. D.** (2001). Adeno-associated virus type 6 (AAV6) vectors mediate efficient transduction of airway epithelial cells in mouse lungs compared to that of AAV2 vectors. *J Virol* **75**(14), 6615-24.
- Halbert, C. L., Standaert, T. A., Wilson, C. B., and Miller, A. D.** (1998). Successful readministration of adeno-associated virus vectors to the mouse lung requires transient immunosuppression during the initial exposure. *J Virol* **72**(12), 9795-805.
- Hallek, M., and Wendtner, C. M.** (1996). Recombinant adeno-associated virus (rAAV) vectors for somatic gene therapy: recent advances and potential clinical applications. *Cytokines Mol Ther* **2**(2), 69-79.
- Hansen, J., Qing, K., and Srivastava, A.** (2001a). Adeno-associated virus type 2-mediated gene transfer: altered endocytic processing enhances transduction efficiency in murine fibroblasts. *J Virol* **75**(9), 4080-90.
- Hansen, J., Qing, K., and Srivastava, A.** (2001b). Infection of purified nuclei by adeno-associated virus 2. *Mol Ther* **4**(4), 289-96.
- Hermonat, P. L.** (1989). The adeno-associated virus Rep78 gene inhibits cellular transformation induced by bovine papillomavirus. *Virology* **172**(1), 253-61.

- Hernandez, Y. J., Wang, J., Kearns, W. G., Loiler, S., Poirier, A., and Flotte, T. R.** (1999). Latent adeno-associated virus infection elicits humoral but not cell-mediated immune responses in a nonhuman primate model. *J Virol* **73**(10), 8549-58.
- High, K. A.** (2004). Clinical gene transfer studies for hemophilia B. *Semin Thromb Hemost* **30**(2), 257-67.
- Hinshaw, J. E.** (2000). Dynamin and its role in membrane fission. *Annu Rev Cell Dev Biol* **16**, 483-519.
- Hinshaw, J. E., and Schmid, S. L.** (1995). Dynamin self-assembles into rings suggesting a mechanism for coated vesicle budding. *Nature* **374**(6518), 190-2.
- Hoggan, M. D., Blacklow, N. R., and Rowe, W. P.** (1966). Studies of small DNA viruses found in various adenovirus preparations: physical, biological, and immunological characteristics. *Proc Natl Acad Sci U S A* **55**(6), 1467-74.
- Hoque, M., Ishizu, K., Matsumoto, A., Han, S. I., Arisaka, F., Takayama, M., Suzuki, K., Kato, K., Kanda, T., Watanabe, H., and Handa, H.** (1999a). Nuclear transport of the major capsid protein is essential for adeno-associated virus capsid formation. *J Virol* **73**(9), 7912-5.
- Hoque, M., Ishizu, K., Matsumoto, A., Han, S. I., Arisaka, F., Takayama, M., Suzuki, K., Kato, K., Kanda, T., Watanabe, H., and Handa, H.** (1999b). Nuclear transport of the major capsid protein is essential for adeno-associated virus capsid formation. *J Virol* **73**(9), 7912-5.
- Hueffer, K., Parker, J. S., Weichert, W. S., Geisel, R. E., Sgro, J. Y., and Parrish, C. R.** (2003). The natural host range shift and subsequent evolution of canine parvovirus resulted from virus-specific binding to the canine transferrin receptor. *J Virol* **77**(3), 1718-26.
- Hueffer, K., and Parrish, C. R.** (2003). Parvovirus host range, cell tropism and evolution. *Curr Opin Microbiol* **6**(4), 392-8.
- Hughes, S. M., Moussavi-Harami, F., Sauter, S. L., and Davidson, B. L.** (2002). Viral-mediated gene transfer to mouse primary neural progenitor cells. *Mol Ther* **5**(1), 16-24.
- Huttner, N. A., Girod, A., Perabo, L., Edbauer, D., Kleinschmidt, J. A., Buning, H., and Hallek, M.** (2003a). Genetic modifications of the adeno-associated virus type 2 capsid reduce the affinity and the neutralizing effects of human serum antibodies. *Gene Ther* **10**(26), 2139-47.

- Huttner, N. A., Girod, A., Schnittger, S., Schoch, C., Hallek, M., and Buning, H.** (2003b). Analysis of site-specific transgene integration following co-transduction with recombinant adeno-associated virus and a rep encoding plasmid. *J Gene Med* **5**(2), 120-9.
- Im, D. S., and Muzyczka, N.** (1990). The AAV origin binding protein Rep68 is an ATP-dependent site-specific endonuclease with DNA helicase activity. *Cell* **61**(3), 447-57.
- Inoue, N., and Russell, D. W.** (1998). Packaging cells based on inducible gene amplification for the production of adeno-associated virus vectors. *J Virol* **72**(9), 7024-31.
- Jooss, K., Yang, Y., Fisher, K. J., and Wilson, J. M.** (1998). Transduction of dendritic cells by DNA viral vectors directs the immune response to transgene products in muscle fibers. *J Virol* **72**(5), 4212-23.
- Kaludov, N., Brown, K. E., Walters, R. W., Zabner, J., and Chiorini, J. A.** (2001). Adeno-associated virus serotype 4 (AAV4) and AAV5 both require sialic acid binding for hemagglutination and efficient transduction but differ in sialic acid linkage specificity. *J Virol* **75**(15), 6884-93.
- Kaplitt, M. G., Leone, P., Samulski, R. J., Xiao, X., Pfaff, D. W., O'Malley, K. L., and During, M. J.** (1994). Long-term gene expression and phenotypic correction using adeno-associated virus vectors in the mammalian brain. *Nat Genet* **8**(2), 148-54.
- Kashiwakura, Y., Tamayose, K., Iwabuchi, K., Hirai, Y., Shimada, T., Matsumoto, K., Nakamura, T., Watanabe, M., Oshimi, K., and Daida, H.** (2005). Hepatocyte growth factor receptor is a coreceptor for adeno-associated virus type 2 infection. *J Virol* **79**(1), 609-14.
- Kay, M. A., Glorioso, J. C., and Naldini, L.** (2001). Viral vectors for gene therapy: the art of turning infectious agents into vehicles of therapeutics. *Nat Med* **7**(1), 33-40.
- Kay, M. A., Manno, C. S., Ragni, M. V., Larson, P. J., Couto, L. B., McClelland, A., Glader, B., Chew, A. J., Tai, S. J., Herzog, R. W., Arruda, V., Johnson, F., Scallan, C., Skarsgard, E., Flake, A. W., and High, K. A.** (2000). Evidence for gene transfer and expression of factor IX in haemophilia B patients treated with an AAV vector. *Nat Genet* **24**(3), 257-61.
- Kern, A., Schmidt, K., Leder, C., Muller, O. J., Wobus, C. E., Bettinger, K., Von der Lieth, C. W., King, J. A., and Kleinschmidt, J. A.** (2003). Identification of a heparin-binding motif on adeno-associated virus type 2 capsids. *J Virol* **77**(20), 11072-81.

- King, J. A., Dubielzig, R., Grimm, D., and Kleinschmidt, J. A.** (2001). DNA helicase-mediated packaging of adeno-associated virus type 2 genomes into preformed capsids. *Embo J* **20**(12), 3282-91.
- Kolkman, J. A., and Stemmer, W. P.** (2001). Directed evolution of proteins by exon shuffling. *Nat Biotechnol* **19**(5), 423-8.
- Kotin, R. M.** (1994). Prospects for the use of adeno-associated virus as a vector for human gene therapy. *Hum Gene Ther* **5**(7), 793-801.
- Kotin, R. M., Menninger, J. C., Ward, D. C., and Berns, K. I.** (1991). Mapping and direct visualization of a region-specific viral DNA integration site on chromosome 19q13-pter. *Genomics* **10**(3), 831-4.
- Kotin, R. M., Siniscalco, M., Samulski, R. J., Zhu, X. D., Hunter, L., Laughlin, C. A., McLaughlin, S., Muzyczka, N., Rocchi, M., and Berns, K. I.** (1990). Site-specific integration by adeno-associated virus. *Proc Natl Acad Sci U S A* **87**(6), 2211-5.
- Kronenberg, S., Bottcher, B., von der Lieth, C. W., Bleker, S., and Kleinschmidt, J. A.** (2005). A conformational change in the adeno-associated virus type 2 capsid leads to the exposure of hidden VP1 N termini. *J Virol* **79**(9), 5296-303.
- Kronenberg, S., Kleinschmidt, J. A., and Bottcher, B.** (2001). Electron cryo-microscopy and image reconstruction of adeno-associated virus type 2 empty capsids. *EMBO Rep* **2**(11), 997-1002.
- Kyostio, S. R., Owens, R. A., Weitzman, M. D., Antoni, B. A., Chejanovsky, N., and Carter, B. J.** (1994). Analysis of adeno-associated virus (AAV) wild-type and mutant Rep proteins for their abilities to negatively regulate AAV p5 and p19 mRNA levels. *J Virol* **68**(5), 2947-57.
- Labow, M. A., and Berns, K. I.** (1988). The adeno-associated virus rep gene inhibits replication of an adeno-associated virus/simian virus 40 hybrid genome in cos-7 cells. *J Virol* **62**(5), 1705-12.
- Laughlin, C. A., Myers, M. W., Risin, D. L., and Carter, B. J.** (1979). Defective-interfering particles of the human parvovirus adeno-associated virus. *Virology* **94**(1), 162-74.
- Laughlin, C. A., Tratschin, J. D., Coon, H., and Carter, B. J.** (1983). Cloning of infectious adeno-associated virus genomes in bacterial plasmids. *Gene* **23**(1), 65-73.
- Linden, R. M., Ward, P., Giraud, C., Winocour, E., and Berns, K. I.** (1996). Site-specific integration by adeno-associated virus. *Proc Natl Acad Sci U S A* **93**(21), 11288-94.

- Linden, R. M., Winocour, E., and Berns, K. I.** (1996). The recombination signals for adeno-associated virus site-specific integration. *Proc Natl Acad Sci U S A* **93**(15), 7966-72.
- Lochrie, M. A., Tatsuno, G. P., Christie, B., McDonnell, J. W., Zhou, S., Surosky, R., Pierce, G. F., and Colosi, P.** (2006). Mutations on the external surfaces of adeno-associated virus type 2 capsids that affect transduction and neutralization. *J Virol* **80**(2), 821-34.
- Loiler, S. A., Conlon, T. J., Song, S., Tang, Q., Warrington, K. H., Agarwal, A., Kaptureczak, M., Li, C., Ricordi, C., Atkinson, M. A., Muzyczka, N., and Flotte, T. R.** (2003). Targeting recombinant adeno-associated virus vectors to enhance gene transfer to pancreatic islets and liver. *Gene Ther* **10**(18), 1551-8.
- Lukashov, V. V., and Goudsmit, J.** (2001). Evolutionary relationships among parvoviruses: virus-host coevolution among autonomous primate parvoviruses and links between adeno-associated and avian parvoviruses. *J Virol* **75**(6), 2729-40.
- Lusby, E. W., and Berns, K. I.** (1982). Mapping of the 5' termini of two adeno-associated virus 2 RNAs in the left half of the genome. *J Virol* **41**(2), 518-26.
- Lux, K., Goerlitz, N., Schlemminger, S., Perabo, L., Goldnau, D., Endell, J., Leike, K., Kofler, D. M., Finke, S., Hallek, M., and Buning, H.** (2005). Green fluorescent protein-tagged adeno-associated virus particles allow the study of cytosolic and nuclear trafficking. *J Virol* **79**(18), 11776-87.
- Maheshri, N., Koerber, J. T., Kaspar, B. K., and Schaffer, D. V.** (2006). Directed evolution of adeno-associated virus yields enhanced gene delivery vectors. *Nat Biotechnol* **24**(2), 198-204.
- Mandel, R. J., and Burger, C.** (2004). Clinical trials in neurological disorders using AAV vectors: promises and challenges. *Curr Opin Mol Ther* **6**(5), 482-90.
- Manning, W. C., Paliard, X., Zhou, S., Pat Bland, M., Lee, A. Y., Hong, K., Walker, C. M., Escobedo, J. A., and Dwarki, V.** (1997). Genetic immunization with adeno-associated virus vectors expressing herpes simplex virus type 2 glycoproteins B and D. *J Virol* **71**(10), 7960-2.
- Manning, W. C., Zhou, S., Bland, M. P., Escobedo, J. A., and Dwarki, V.** (1998). Transient immunosuppression allows transgene expression following readministration of adeno-associated viral vectors. *Hum Gene Ther* **9**(4), 477-85.
- Marcus, C. J., Laughlin, C. A., and Carter, B. J.** (1981). Adeno-associated virus RNA transcription in vivo. *Eur J Biochem* **121**(1), 147-54.

- Margalit, H., Fischer, N., and Ben-Sasson, S. A.** (1993). Comparative analysis of structurally defined heparin binding sequences reveals a distinct spatial distribution of basic residues. *J Biol Chem* **268**(26), 19228-31.
- Mayor, H. D., Houlditch, G. S., and Mumford, D. M.** (1973). Influence of adeno-associated satellite virus on adenovirus-induced tumours in hamsters. *Nat New Biol* **241**(106), 44-6.
- McCarty, D. M., Pereira, D. J., Zolotukhin, I., Zhou, X., Ryan, J. H., and Muzyczka, N.** (1994). Identification of linear DNA sequences that specifically bind the adeno-associated virus Rep protein. *J Virol* **68**(8), 4988-97.
- McDonald, D., Vodicka, M. A., Lucero, G., Svitkina, T. M., Borisy, G. G., Emerman, M., and Hope, T. J.** (2002). Visualization of the intracellular behavior of HIV in living cells. *J Cell Biol* **159**(3), 441-52.
- McKenna, R., Olson, N. H., Chipman, P. R., Baker, T. S., Booth, T. F., Christensen, J., Aasted, B., Fox, J. M., Bloom, M. E., Wolfinbarger, J. B., and Agbandje-McKenna, M.** (1999). Three-dimensional structure of Aleutian mink disease parvovirus: implications for disease pathogenicity. *J Virol* **73**(8), 6882-91.
- McLaughlin, S. K., Collis, P., Hermonat, P. L., and Muzyczka, N.** (1988). Adeno-associated virus general transduction vectors: analysis of proviral structures. *J Virol* **62**(6), 1963-73.
- McPherson, R. A., Rosenthal, L. J., and Rose, J. A.** (1985). Human cytomegalovirus completely helps adeno-associated virus replication. *Virology* **147**(1), 217-22.
- Mizukami, H., Young, N. S., and Brown, K. E.** (1996). Adeno-associated virus type 2 binds to a 150-kilodalton cell membrane glycoprotein. *Virology* **217**(1), 124-30.
- Monahan, P. E., and Samulski, R. J.** (2000a). AAV vectors: is clinical success on the horizon? *Gene Ther* **7**(1), 24-30.
- Monahan, P. E., and Samulski, R. J.** (2000b). Adeno-associated virus vectors for gene therapy: more pros than cons? *Mol Med Today* **6**(11), 433-40.
- Moore, J. C., Jin, H. M., Kuchner, O., and Arnold, F. H.** (1997). Strategies for the in vitro evolution of protein function: enzyme evolution by random recombination of improved sequences. *J Mol Biol* **272**(3), 336-47.
- Mori, S., Wang, L., Takeuchi, T., and Kanda, T.** (2004). Two novel adeno-associated viruses from cynomolgus monkey: pseudotyping characterization of capsid protein. *Virology* **330**(2), 375-83.

- Moskalenko, M., Chen, L., van Roey, M., Donahue, B. A., Snyder, R. O., McArthur, J. G., and Patel, S. D.** (2000). Epitope mapping of human anti-adenovirus type 2 neutralizing antibodies: implications for gene therapy and virus structure. *J Virol* **74**(4), 1761-6.
- Mouw, M. B., and Pintel, D. J.** (2000). Adeno-associated virus RNAs appear in a temporal order and their splicing is stimulated during coinfection with adenovirus. *J Virol* **74**(21), 9878-88.
- Muller, O. J., Kaul, F., Weitzman, M. D., Pasqualini, R., Arap, W., Kleinschmidt, J. A., and Trepel, M.** (2003). Random peptide libraries displayed on adeno-associated virus to select for targeted gene therapy vectors. *Nat Biotechnol* **21**(9), 1040-6.
- Nakai, H., Storm, T. A., and Kay, M. A.** (2000). Increasing the size of rAAV-mediated expression cassettes in vivo by intermolecular joining of two complementary vectors. *Nat Biotechnol* **18**(5), 527-32.
- Neylon, C.** (2004). Chemical and biochemical strategies for the randomization of protein encoding DNA sequences: library construction methods for directed evolution. *Nucleic Acids Res* **32**(4), 1448-59.
- Nicklin, S. A., Buening, H., Dishart, K. L., de Alwis, M., Girod, A., Hacker, U., Thrasher, A. J., Ali, R. R., Hallek, M., and Baker, A. H.** (2001). Efficient and selective AAV2-mediated gene transfer directed to human vascular endothelial cells. *Mol Ther* **4**(3), 174-81.
- Opie, S. R., Warrington, K. H., Jr., Agbandje-McKenna, M., Zolotukhin, S., and Muzyczka, N.** (2003). Identification of amino acid residues in the capsid proteins of adeno-associated virus type 2 that contribute to heparan sulfate proteoglycan binding. *J Virol* **77**(12), 6995-7006.
- Owens, R. A.** (2002). Second generation adeno-associated virus type 2-based gene therapy systems with the potential for preferential integration into AAVS1. *Curr Gene Ther* **2**(2), 145-59.
- Padron, E., Bowman, V., Kaludov, N., Govindasamy, L., Levy, H., Nick, P., McKenna, R., Muzyczka, N., Chiorini, J. A., Baker, T. S., and Agbandje-McKenna, M.** (2005). Structure of adeno-associated virus type 4. *J Virol* **79**(8), 5047-58.
- Pajusola, K., Gruchala, M., Joch, H., Luscher, T. F., Yla-Herttuala, S., and Bueler, H.** (2002). Cell-type-specific characteristics modulate the transduction efficiency of adeno-associated virus type 2 and restrain infection of endothelial cells. *J Virol* **76**(22), 11530-40.

- Perabo, L., Buning, H., Kofler, D. M., Ried, M. U., Girod, A., Wendtner, C. M., Enssle, J., and Hallek, M.** (2003). In vitro selection of viral vectors with modified tropism: the adeno-associated virus display. *Mol Ther* **8**(1), 151-7.
- Perabo, L., Endell, J., King, S., Lux, K., Goldnau, D., Hallek, M., and Buning, H.** (2006). Combinatorial engineering of a gene therapy vector: directed evolution of adeno-associated virus. *J Gene Med* **8**(2), 155-62.
- Pfeifer, A., and Verma, I. M.** (2001). Gene therapy: promises and problems. *Annu Rev Genomics Hum Genet* **2**, 177-211.
- Philpott, N. J., Gomos, J., Berns, K. I., and Falck-Pedersen, E.** (2002). A p5 integration efficiency element mediates Rep-dependent integration into AAVS1 at chromosome 19. *Proc Natl Acad Sci U S A* **99**(19), 12381-5.
- Ponnazhagan, S., Erikson, D., Kearns, W. G., Zhou, S. Z., Nahreini, P., Wang, X. S., and Srivastava, A.** (1997). Lack of site-specific integration of the recombinant adeno-associated virus 2 genomes in human cells. *Hum Gene Ther* **8**(3), 275-84.
- Powell, S. K., Kaloss, M. A., Pinkstaff, A., McKee, R., Burimski, I., Pensiero, M., Otto, E., Stemmer, W. P., and Soong, N. W.** (2000). Breeding of retroviruses by DNA shuffling for improved stability and processing yields. *Nat Biotechnol* **18**(12), 1279-82.
- Qing, K., Mah, C., Hansen, J., Zhou, S., Dwarki, V., and Srivastava, A.** (1999). Human fibroblast growth factor receptor 1 is a co-receptor for infection by adeno-associated virus 2. *Nat Med* **5**(1), 71-7.
- Qiu, J., and Brown, K. E.** (1999). A 110-kDa nuclear shuttle protein, nucleolin, specifically binds to adeno-associated virus type 2 (AAV-2) capsid. *Virology* **257**(2), 373-82.
- Rabinowitz, J. E., Xiao, W., and Samulski, R. J.** (1999). Insertional mutagenesis of AAV2 capsid and the production of recombinant virus. *Virology* **265**(2), 274-85.
- Raj, K., Ogston, P., and Beard, P.** (2001). Virus-mediated killing of cells that lack p53 activity. *Nature* **412**(6850), 914-7.
- Ried, M. U., Girod, A., Leike, K., Buning, H., and Hallek, M.** (2002). Adeno-associated virus capsids displaying immunoglobulin-binding domains permit antibody-mediated vector retargeting to specific cell surface receptors. *J Virol* **76**(9), 4559-66.
- Rohde, V., Erles, K., Sattler, H. P., Derouet, H., Wullich, B., and Schlehofer, J. R.** (1999). Detection of adeno-associated virus in human semen: does viral infection play a role in the pathogenesis of male infertility? *Fertil Steril* **72**(5), 814-6.

- Rolling, F., and Samulski, R. J.** (1995). AAV as a viral vector for human gene therapy. Generation of recombinant virus. *Mol Biotechnol* **3**(1), 9-15.
- Root, C. N., Wills, E. G., McNair, L. L., and Whittaker, G. R.** (2000). Entry of influenza viruses into cells is inhibited by a highly specific protein kinase C inhibitor. *J Gen Virol* **81**(Pt 11), 2697-705.
- Sampaio, K. L., Cavignac, Y., Stierhof, Y. D., and Sinzger, C.** (2005). Human cytomegalovirus labeled with green fluorescent protein for live analysis of intracellular particle movements. *J Virol* **79**(5), 2754-67.
- Samulski, R. J., Berns, K. I., Tan, M., and Muzyczka, N.** (1982). Cloning of adeno-associated virus into pBR322: rescue of intact virus from the recombinant plasmid in human cells. *Proc Natl Acad Sci U S A* **79**(6), 2077-81.
- Samulski, R. J., Chang, L. S., and Shenk, T.** (1987). A recombinant plasmid from which an infectious adeno-associated virus genome can be excised in vitro and its use to study viral replication. *J Virol* **61**(10), 3096-101.
- Samulski, R. J., Zhu, X., Xiao, X., Brook, J. D., Housman, D. E., Epstein, N., and Hunter, L. A.** (1991). Targeted integration of adeno-associated virus (AAV) into human chromosome 19. *Embo J* **10**(12), 3941-50.
- Sanlioglu, S., Benson, P. K., Yang, J., Atkinson, E. M., Reynolds, T., and Engelhardt, J. F.** (2000). Endocytosis and nuclear trafficking of adeno-associated virus type 2 are controlled by rac1 and phosphatidylinositol-3 kinase activation. *J Virol* **74**(19), 9184-96.
- Sanlioglu, S., Duan, D., and Engelhardt, J. F.** (1999). Two independent molecular pathways for recombinant adeno-associated virus genome conversion occur after UV-C and E4orf6 augmentation of transduction. *Hum Gene Ther* **10**(4), 591-602.
- Sarukhan, A., Camugli, S., Gjata, B., von Boehmer, H., Danos, O., and Jooss, K.** (2001). Successful interference with cellular immune responses to immunogenic proteins encoded by recombinant viral vectors. *J Virol* **75**(1), 269-77.
- Schlehofer, J. R., Ehrbar, M., and zur Hausen, H.** (1986). Vaccinia virus, herpes simplex virus, and carcinogens induce DNA amplification in a human cell line and support replication of a helpervirus dependent parvovirus. *Virology* **152**(1), 110-7.
- Seisenberger, G., Ried, M. U., Endress, T., Buning, H., Hallek, M., and Brauchle, C.** (2001). Real-time single-molecule imaging of the infection pathway of an adeno-associated virus. *Science* **294**(5548), 1929-32.

- Sever, S., Damke, H., and Schmid, S. L.** (2000). Dynamin:GTP controls the formation of constricted coated pits, the rate limiting step in clathrin-mediated endocytosis. *J Cell Biol* **150**(5), 1137-48.
- Shi, W., Arnold, G. S., and Bartlett, J. S.** (2001). Insertional mutagenesis of the adeno-associated virus type 2 (AAV2) capsid gene and generation of AAV2 vectors targeted to alternative cell-surface receptors. *Hum Gene Ther* **12**(14), 1697-711.
- Siegl, G., Bates, R. C., Berns, K. I., Carter, B. J., Kelly, D. C., Kurstak, E., and Tattersall, P.** (1985). Characteristics and taxonomy of Parvoviridae. *Intervirology* **23**(2), 61-73.
- Smith, R. H., and Kotin, R. M.** (1998). The Rep52 gene product of adeno-associated virus is a DNA helicase with 3'-to-5' polarity. *J Virol* **72**(6), 4874-81.
- Smith-Arica, J. R., Thomson, A. J., Ansell, R., Chiorini, J., Davidson, B., and McWhir, J.** (2003). Infection efficiency of human and mouse embryonic stem cells using adenoviral and adeno-associated viral vectors. *Cloning Stem Cells* **5**(1), 51-62.
- Snyder, R. O., Im, D. S., and Muzyczka, N.** (1990). Evidence for covalent attachment of the adeno-associated virus (AAV) rep protein to the ends of the AAV genome. *J Virol* **64**(12), 6204-13.
- Snyder, R. O., Im, D. S., Ni, T., Xiao, X., Samulski, R. J., and Muzyczka, N.** (1993). Features of the adeno-associated virus origin involved in substrate recognition by the viral Rep protein. *J Virol* **67**(10), 6096-104.
- Snyder, R. O., Miao, C. H., Patijn, G. A., Spratt, S. K., Danos, O., Nagy, D., Gown, A. M., Winther, B., Meuse, L., Cohen, L. K., Thompson, A. R., and Kay, M. A.** (1997). Persistent and therapeutic concentrations of human factor IX in mice after hepatic gene transfer of recombinant AAV vectors. *Nat Genet* **16**(3), 270-6.
- Somia, N., and Verma, I. M.** (2000). Gene therapy: trials and tribulations. *Nat Rev Genet* **1**(2), 91-9.
- Soong, N. W., Nomura, L., Pekrun, K., Reed, M., Sheppard, L., Dawes, G., and Stemmer, W. P.** (2000). Molecular breeding of viruses. *Nat Genet* **25**(4), 436-9.
- Stemmer, W. P.** (1994). Rapid evolution of a protein in vitro by DNA shuffling. *Nature* **370**(6488), 389-91.
- Strassheim, M. L., Gruenberg, A., Veijalainen, P., Sgro, J. Y., and Parrish, C. R.** (1994). Two dominant neutralizing antigenic determinants of canine parvovirus are found on the threefold spike of the virus capsid. *Virology* **198**(1), 175-84.

- Summerford, C., Bartlett, J. S., and Samulski, R. J.** (1999). AlphaVbeta5 integrin: a co-receptor for adeno-associated virus type 2 infection. *Nat Med* **5**(1), 78-82.
- Summerford, C., and Samulski, R. J.** (1998). Membrane-associated heparan sulfate proteoglycan is a receptor for adeno-associated virus type 2 virions. *J Virol* **72**(2), 1438-45.
- Sun, L., Li, J., and Xiao, X.** (2000). Overcoming adeno-associated virus vector size limitation through viral DNA heterodimerization. *Nat Med* **6**(5), 599-602.
- Suomalainen, M., Nakano, M. Y., Keller, S., Boucke, K., Stidwill, R. P., and Greber, U. F.** (1999). Microtubule-dependent plus- and minus end-directed motilities are competing processes for nuclear targeting of adenovirus. *J Cell Biol* **144**(4), 657-72.
- Tal, J.** (2000). Adeno-associated virus-based vectors in gene therapy. *J Biomed Sci* **7**(4), 279-91.
- Tamayose, K., Hirai, Y., and Shimada, T.** (1996). A new strategy for large-scale preparation of high-titer recombinant adeno-associated virus vectors by using packaging cell lines and sulfonated cellulose column chromatography. *Hum Gene Ther* **7**(4), 507-13.
- Theiss, H. D., Kofler, D. M., Buning, H., Aldenhoff, A. L., Kaess, B., Decker, T., Baumert, J., Hallek, M., and Wendtner, C. M.** (2003). Enhancement of gene transfer with recombinant adeno-associated virus (rAAV) vectors into primary B-cell chronic lymphocytic leukemia cells by CpG-oligodeoxynucleotides. *Exp Hematol* **31**(12), 1223-9.
- Thomas, C. E., Ehrhardt, A., and Kay, M. A.** (2003). Progress and problems with the use of viral vectors for gene therapy. *Nat Rev Genet* **4**(5), 346-58.
- Thomson, B. J., Weindler, F. W., Gray, D., Schwaab, V., and Heilbronn, R.** (1994). Human herpesvirus 6 (HHV-6) is a helper virus for adeno-associated virus type 2 (AAV-2) and the AAV-2 rep gene homologue in HHV-6 can mediate AAV-2 DNA replication and regulate gene expression. *Virology* **204**(1), 304-11.
- Tsao, J., Chapman, M. S., Agbandje, M., Keller, W., Smith, K., Wu, H., Luo, M., Smith, T. J., Rossmann, M. G., Compans, R. W., and et al.** (1991). The three-dimensional structure of canine parvovirus and its functional implications. *Science* **251**(5000), 1456-64.
- Vafaie, J., and Schwartz, R. A.** (2004). Parvovirus B19 infections. *Int J Dermatol* **43**(10), 747-9.

- Vincent, K. A., Piraino, S. T., and Wadsworth, S. C. (1997). Analysis of recombinant adeno-associated virus packaging and requirements for rep and cap gene products. *J Virol* **71**(3), 1897-905.
- Wagner, J. A., Nepomuceno, I. B., Messner, A. H., Moran, M. L., Batson, E. P., Dimiceli, S., Brown, B. W., Desch, J. K., Norbash, A. M., Conrad, C. K., Guggino, W. B., Flotte, T. R., Wine, J. J., Carter, B. J., Reynolds, T. C., Moss, R. B., and Gardner, P. (2002). A phase II, double-blind, randomized, placebo-controlled clinical trial of tgAAVCF using maxillary sinus delivery in patients with cystic fibrosis with antrostomies. *Hum Gene Ther* **13**(11), 1349-59.
- Walters, R. W., Agbandje-McKenna, M., Bowman, V. D., Moninger, T. O., Olson, N. H., Seiler, M., Chiorini, J. A., Baker, T. S., and Zabner, J. (2004). Structure of adeno-associated virus serotype 5. *J Virol* **78**(7), 3361-71.
- Walz, C., Deprez, A., Dupressoir, T., Durst, M., Rabreau, M., and Schlehofer, J. R. (1997). Interaction of human papillomavirus type 16 and adeno-associated virus type 2 co-infecting human cervical epithelium. *J Gen Virol* **78** ( Pt 6), 1441-52.
- Wang, K., Huang, S., Kapoor-Munshi, A., and Nemerow, G. (1998). Adenovirus internalization and infection require dynamin. *J Virol* **72**(4), 3455-8.
- Ward, B. M. (2004). Pox, dyes, and videotape: making movies of GFP-labeled vaccinia virus. *Methods Mol Biol* **269**, 205-18.
- Warrington, K. H., Jr., Gorbatyuk, O. S., Harrison, J. K., Opie, S. R., Zolotukhin, S., and Muzyczka, N. (2004). Adeno-associated virus type 2 VP2 capsid protein is nonessential and can tolerate large peptide insertions at its N terminus. *J Virol* **78**(12), 6595-609.
- Weitzman, M. D., Kyostio, S. R., Kotin, R. M., and Owens, R. A. (1994). Adeno-associated virus (AAV) Rep proteins mediate complex formation between AAV DNA and its integration site in human DNA. *Proc Natl Acad Sci U S A* **91**(13), 5808-12.
- Wendtner, C. M., Kofler, D. M., Theiss, H. D., Kurzeder, C., Buhmann, R., Schweighofer, C., Perabo, L., Danhauser-Riedl, S., Baumert, J., Hiddemann, W., Hallek, M., and Buning, H. (2002). Efficient gene transfer of CD40 ligand into primary B-CLL cells using recombinant adeno-associated virus (rAAV) vectors. *Blood* **100**(5), 1655-61.
- White, S. J., Nicklin, S. A., Buning, H., Brosnan, M. J., Leike, K., Papadakis, E. D., Hallek, M., and Baker, A. H. (2004). Targeted gene delivery to vascular tissue in vivo by tropism-modified adeno-associated virus vectors. *Circulation* **109**(4), 513-9.

- Wistuba, A., Kern, A., Weger, S., Grimm, D., and Kleinschmidt, J. A.** (1997). Subcellular compartmentalization of adeno-associated virus type 2 assembly. *J Virol* **71**(2), 1341-52.
- Wobus, C. E., Hugle-Dorr, B., Girod, A., Petersen, G., Hallek, M., and Kleinschmidt, J. A.** (2000). Monoclonal antibodies against the adeno-associated virus type 2 (AAV-2) capsid: epitope mapping and identification of capsid domains involved in AAV-2-cell interaction and neutralization of AAV-2 infection. *J Virol* **74**(19), 9281-93.
- Work, L. M., Nicklin, S. A., Brain, N. J., Dishart, K. L., Von Seggern, D. J., Hallek, M., Buning, H., and Baker, A. H.** (2004). Development of efficient viral vectors selective for vascular smooth muscle cells. *Mol Ther* **9**(2), 198-208.
- Wu, P., Xiao, W., Conlon, T., Hughes, J., Agbandje-McKenna, M., Ferkol, T., Flotte, T., and Muzyczka, N.** (2000). Mutational analysis of the adeno-associated virus type 2 (AAV2) capsid gene and construction of AAV2 vectors with altered tropism. *J Virol* **74**(18), 8635-47.
- Xiao, W., Chirmule, N., Berta, S. C., McCullough, B., Gao, G., and Wilson, J. M.** (1999). Gene therapy vectors based on adeno-associated virus type 1. *J Virol* **73**(5), 3994-4003.
- Xiao, W., Chirmule, N., Schnell, M. A., Tazelaar, J., Hughes, J. V., and Wilson, J. M.** (2000). Route of administration determines induction of T-cell-independent humoral responses to adeno-associated virus vectors. *Mol Ther* **1**(4), 323-9.
- Xiao, W., Warrington, K. H., Jr., Hearing, P., Hughes, J., and Muzyczka, N.** (2002). Adenovirus-facilitated nuclear translocation of adeno-associated virus type 2. *J Virol* **76**(22), 11505-17.
- Xiao, X., Li, J., and Samulski, R. J.** (1996). Efficient long-term gene transfer into muscle tissue of immunocompetent mice by adeno-associated virus vector. *J Virol* **70**(11), 8098-108.
- Xiao, X., Li, J., and Samulski, R. J.** (1998). Production of high-titer recombinant adeno-associated virus vectors in the absence of helper adenovirus. *J Virol* **72**(3), 2224-32.
- Xie, Q., Bu, W., Bhatia, S., Hare, J., Somasundaram, T., Azzi, A., and Chapman, M. S.** (2002). The atomic structure of adeno-associated virus (AAV-2), a vector for human gene therapy. *Proc Natl Acad Sci U S A* **99**(16), 10405-10.
- Yakobson, B., Hrynko, T. A., Peak, M. J., and Winocour, E.** (1989). Replication of adeno-associated virus in cells irradiated with UV light at 254 nm. *J Virol* **63**(3), 1023-30.

- Yalkinoglu, A. O., Heilbronn, R., Burkle, A., Schlehofer, J. R., and zur Hausen, H.** (1988). DNA amplification of adeno-associated virus as a response to cellular genotoxic stress. *Cancer Res* **48**(11), 3123-9.
- Yan, Z., Zhang, Y., Duan, D., and Engelhardt, J. F.** (2000). Trans-splicing vectors expand the utility of adeno-associated virus for gene therapy. *Proc Natl Acad Sci U S A* **97**(12), 6716-21.
- Yang, Q., Mamounas, M., Yu, G., Kennedy, S., Leaker, B., Merson, J., Wong-Staal, F., Yu, M., and Barber, J. R.** (1998). Development of novel cell surface CD34-targeted recombinant adenoassociated virus vectors for gene therapy. *Hum Gene Ther* **9**(13), 1929-37.
- Young, S. M., Jr., McCarty, D. M., Degtyareva, N., and Samulski, R. J.** (2000). Roles of adeno-associated virus Rep protein and human chromosome 19 in site-specific recombination. *J Virol* **74**(9), 3953-66.
- Young, S. M., Jr., and Samulski, R. J.** (2001). Adeno-associated virus (AAV) site-specific recombination does not require a Rep-dependent origin of replication within the AAV terminal repeat. *Proc Natl Acad Sci U S A* **98**(24), 13525-30.
- Young, S. M., Jr., Xiao, W., and Samulski, R. J.** (2000). Site-specific targeting of DNA plasmids to chromosome 19 using AAV cis and trans sequences. *Methods Mol Biol* **133**, 111-26.
- Zadori, Z., Szelei, J., Lacoste, M. C., Li, Y., Gariepy, S., Raymond, P., Allaire, M., Nabi, I. R., and Tijssen, P.** (2001). A viral phospholipase A2 is required for parvovirus infectivity. *Dev Cell* **1**(2), 291-302.
- Zaiss, A. K., Liu, Q., Bowen, G. P., Wong, N. C., Bartlett, J. S., and Muruve, D. A.** (2002). Differential activation of innate immune responses by adenovirus and adeno-associated virus vectors. *J Virol* **76**(9), 4580-90.
- Zhang, J. H., Dawes, G., and Stemmer, W. P.** (1997). Directed evolution of a fucosidase from a galactosidase by DNA shuffling and screening. *Proc Natl Acad Sci U S A* **94**(9), 4504-9.
- Zhao, H., and Arnold, F. H.** (1997). Optimization of DNA shuffling for high fidelity recombination. *Nucleic Acids Res* **25**(6), 1307-8.
- Zolotukhin, S., Byrne, B. J., Mason, E., Zolotukhin, I., Potter, M., Chesnut, K., Summerford, C., Samulski, R. J., and Muzyczka, N.** (1999). Recombinant adeno-associated virus purification using novel methods improves infectious titer and yield. *Gene Ther* **6**(6), 973-85

## Abbreviations

|                     |  |            |  |
|---------------------|--|------------|--|
| aa                  | amino acid   | ADV        | Aleutian mink disease virus                |
| AAV                 | adeno-associated virus, specifically                       | B-AAV-pool | Heparin binders                            |
| AAV-2               | adeno-associated virus type 2                              | B19        | B19 human parvovirus                       |
| AAVS1               | AAV integration site 1<br>(located in human chromosome 19) | bp         | base pair                                  |
| Ab                  | antibody   | BSA        | bovine serum albumin                       |
| Ad                  | adenovirus   | Cap        | capsid protein                             |
|                     |  | cDNA       | complementary DNA                          |
|                     |  | ch         | chromosome                                 |
|                     |  | CMV        | cytomegalovirus                            |
|                     |  | CNS        | central nervous system                     |
|                     |  | CPV        | canine parvovirus                          |
|                     |  | Cryo-EM    | cryo-electron microscopy                   |
|                     |  | CTL        | cytotoxic T-lymphocyte                     |
|                     |  | Cy3, Cy5   | indocarbocyanine dyes                      |
|                     |  | Da         | Dalton                                     |
|                     |  | DMEM       | Dulbecco's Modified Eagle                  |
|                     |  | Medium     |  |
|                     |  | EGFP       | enhanced GFP                               |
|                     |  | e.g.       | for example (Lat.: <i>exempli gratia</i> ) |
|                     |  | ELISA      | enzyme-linked immunosorbent                |
|                     |  | assay      |  |
|                     |  | EP-PCR     | <i>error prone</i> PCR                     |
|                     |  | FACS       | fluorescence-activated cell sorting        |
|                     |  | FCS        | fetal calf serum                           |
|                     |  | FGFR       | fibroblast growth factor receptor 1        |
|                     |  | Fig.       | figure                                     |
|                     |  | FISH       | fluorescence <i>in situ</i> hybridization  |
|                     |  | FITC       | fluorescein isothiocyanate                 |
|                     |  | FPV        | feline panleukopenia virus                 |
|                     |  | GFP        | green fluorescence protein                 |
|                     |  | Gy         | Gray                                       |
|                     |  | h          | hour                                       |
|                     |  | HA         | hemagglutinin                              |
|                     |  | HSPG       | heparan sulfate proteoglycan               |
|                     |  | i.e.       | that is (Lat.: <i>id est</i> )             |
|                     |  | i.m.       | intra muscular                             |
| <u>Amino acids:</u> |  |            |  |
| A (Ala)             | alanine  |            |  |
| C (Cys)             | cysteine   |            |  |
| D (Asp)             | aspartate  |            |  |
| E (Glu)             | glutamate  |            |  |
| F (Phe)             | phenylalanine  |            |  |
| G (Gly)             | glycine  |            |  |
| H (His)             | histidine  |            |  |
| I (Ile)             | isoleucine   |            |  |
| K (Lys)             | lysine   |            |  |
| L (Leu)             | leucine  |            |  |
| M (Met)             | methionine   |            |  |
| N (Asn)             | asparagine   |            |  |
| P (Pro)             | proline  |            |  |
| Q (Gln)             | glutamine  |            |  |
| R (Arg)             | arginine   |            |  |
| S (Ser)             | serine   |            |  |
| T (Thr)             | threonine  |            |  |
| V (Val)             | valine   |            |  |
| W (Trp)             | tryptophan   |            |  |
| Y (Tyr)             | tyrosine   |            |  |
| <u>Bases:</u>       |  |            |  |
| A                   | adenin   |            |  |
| C                   | cytosin  |            |  |
| G                   | guanin   |            |  |
| T                   | thymin   |            |  |

---

|                |                                  |       |                                    |
|----------------|----------------------------------|-------|------------------------------------|
| ITR            | inverted terminal repeat         | p.i.  | post infection                     |
| kb             | kilobases                        | PIK-3 | phosphatidylinositol-3-kinase      |
| K <sub>d</sub> | dissociation constant            | PLA2  | phospholipase A2                   |
| LC-PCR         | light cycler PCR                 | PNRE  | perinuclear recycling endosome     |
| mAb            | monoclonal antibody              | rAAV  | recombinant AAV                    |
| MHC            | major histocompatibility complex | RBS   | Rep binding site                   |
| min            | minute                           | Rep   | viral regulatory protein           |
| MOI            | multiplicity of infection        | rpm   | rounds per minute                  |
| MT             | microtubule                      | RT    | room temperature                   |
| MVM            | minute virus of mice             | SDS   | sodium dodecyl sulfate             |
| NB-AAV-pool    | Heparin non-binders              | sFv   | single chain antibody              |
| NLS            | nuclear localisation sequence    | Stav  | streptavidin                       |
| NPC            | nuclear pore complex             | SVT   | single virus tracing               |
| nt             | nucleotide                       | TRS   | terminal resolution site           |
| ori            | origin of replication            | U     | units                              |
| ORF            | open reading frame               | VP    | viral protein (AAV capsid protein) |
| PFA            | paraform aldehyde                | wtAAV | wild-type AAV                      |

---

## CURRICULUM VITAE

### Persönliche Daten

---

Jan Christof Endell  
Partnachstr. 6  
81373 München  
geboren am 24. September 1976 in Oberhausen  
ledig  
Staatsangehörigkeit: deutsch

### Schulbildung

---

1987 - 1996                      Otto-Hahn Gymnasium in Dinslaken  
Abschluß: Allgemeine Hochschulreife

### Hochschulausbildung

---

1997 - 2002                      Studium der Chemie an der  
Westfälischen Wilhelms-Universität Münster  
  
bis Dez. 2001                      Abschluss der mündlichen Diplomprüfungen  
bis Aug. 2002                      Diplomarbeit  
Aug. 2002                          Abschluss des Studiums als Diplom-Chemiker

### Promotion

---

seit Januar 2003                      Promotion am Institut für Biochemie der LMU München in der  
Arbeitsgruppe von Prof. Dr. Michael Hallek  
Thema: Generation of enhanced gene delivery vectors by  
directed evolution of adeno-associated virus